

156
114
**ENHANCED ENERGY MANEUVERABILITY FOR ATTACK HELICOPTERS
USING CONTINUOUS, VARIABLE ROTOR SPEED CONTROL**

by

Carl George Schaefer, Jr.

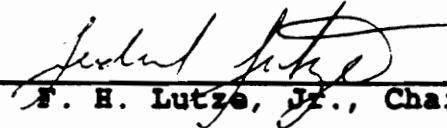
**Major Paper submitted to the Faculty of the
Virginia Polytechnic Institute and State University
in partial fulfillment of the requirements for the degree of**

Master of Engineering

in

Systems Engineering

APPROVED:



F. H. Lutze, Jr., Chairman



B. S. Blanchard, Jr.



A. A. Trani



M. P. Deisenroth

July, 1990

Blacksburg, Virginia

2

LD
5655
V851
1990
S352
C.2

DEDICATION

To my wife, Deborah Ann, for her love, support, and understanding in this endeavor. And to my son, Geoffrey, for all the hours we did not have together.

ACKNOWLEDGEMENTS

As in all major endeavors, there are many who ultimately contribute to the success of the final result; this modest project and report is no exception.

The author wishes to thank the Naval Aviation Executive Institute, the Naval Air Systems Command, and the Virginia Tech College of Engineering for the endowment of the Senator John W. Warner Fellowship for Systems Engineering, without which this opportunity for advanced study would not have been possible. Many thanks also go to Ben Blanchard, Assistant Dean of Engineering, whose support and guidance was invaluable to me during my stay at Virginia Tech.

The author also wishes to acknowledge the following people for their support and professional advice in the preparation of this report: At the Naval Air Systems Command, Mr. Adolph Ragghianti, Mr. Mike McMahon, Mr. Mike Dubberly, Mr. John McKeown, and Captain Mike O'Bar, USN. Also at the Naval Air Systems Command, Mr. Steve Wood for his help and explanations regarding energy maneuverability concepts as used by the U.S. Navy and Marine Corps. At the U.S. Naval Test

Pilot School, Patuxent River, MD, Mr. Jim J. McCue for his help, encouragement, and answers to my many questions. At the McDonnell Douglas Helicopter Company, Mr. Charles A. (Cap) Parlier for his help and words of encouragement. And last, but certainly not least, Dr. Fred Lutze, my committee chairman, who realized only too late what he was getting himself into. Without his expert help, guidance, and dry sense of humor, this project would not have been possible.

TABLE OF CONTENTS

DEDICATION	ii
ACKNOWLEDGEMENTS	iii
TABLE OF CONTENTS	v
LIST OF FIGURES	vii
LIST OF TABLES	x
1.0 INTRODUCTION	1
2.0 PROBLEM STATEMENT	6
3.0 LITERATURE REVIEW	
3.1 Energy Maneuverability Concepts	12
3.2 Rotor Speed Control	
3.3 Tactical Implications of Decelerating Turns ...	39
4.0 SIMULATION MODEL DEVELOPMENT	
4.1 Power Required Model	42
4.1.1 Induced Power Required	43
4.1.2 Profile Drag Power Required	50
4.1.3 Fuselage Parasite Drag Power Required ..	53
4.1.4 Compressibility and Stall Effects	55
4.1.5 Total Power Required	57
4.2 AH-1G Power Available Model	64
4.3 Point-Mass Simulation Model	66
5.0 THE OPTIMAL CONTROL PROBLEM	
5.1 Introduction and Approach	72

v

TABLE OF CONTENTS
(continued)

5.2	DTURN5 Rotor Speed Control Laws	75
5.3	DT5-DNCONF Parameterization	84
5.4	Maneuver Load Factor Control	90
6.0	RESULTS AND DISCUSSION	
6.1	Power Required Model Correlation	97
6.2	Point-Mass Model Validation	101
6.3	Sub-optimal Control Laws and Data Presentation	103
6.4	Operational Feasibility	112
7.0	RECOMMENDATIONS FOR FUTURE RESEARCH	147
8.0	CONCLUSIONS	150
9.0	BIBLIOGRAPHY	152
10.0	APPENDICES	
10.1	POWER3 Program Listing	158
10.2	DTURN5 Program Listing	160
10.3	DT5 Program Listing	165

LIST OF FIGURES

Figure 1 - Plot of Constant Energy Lines	29
Figure 2 - P_g versus Altitude and Airspeed	30
Figure 3 - Turn Rate versus Airspeed	31
Figure 4 - Energy Maneuverability Diagram	32
Figure 5 - Example Power Polar	60
Figure 6 - AH-1G Specific Excess Power, 90% RPM	61
Figure 7 - AH-1G Specific Excess Power, 100% RPM	62
Figure 8 - AH-1G Specific Excess Power, 120% RPM	63
Figure 9 - AH-1G Power Available Flight Test Data	65
Figure 10 - Proposed Rotor Speed Control Laws	76
Figure 11 - Proposed Rotor Speed Control Laws	77
Figure 12 - Proposed Rotor Speed Control Laws	78
Figure 13 - Proposed Rotor Speed Control Laws	79
Figure 14 - Proposed Rotor Speed Control Laws	80
Figure 15 - Proposed Rotor Speed Control Laws	81
Figure 16 - Proposed Rotor Speed Control Laws	82
Figure 17 - Rotor Speed Control Law Used in DT5 Parametric Optimization	89
Figure 18 - AH-1G Level Flight Performance (Calculate vs. Flight Test)	116
Figure 19 - AH-1G Level Flight Performance (Calculated vs. Flight Test)	117
Figure 20 - AH-1G Turn Performance, Flight Test	118
Figure 21 - AH-1G Turn Performance, Calculated (Wood and Wells)	119

LIST OF FIGURES
(continued)

Figure 22 - AH-1G Max Performance Turn, Wood's Methodology	120
Figure 23 - AH-1G Max Performance Turn, Wood's Methodology	121
Figure 24 - AH-1G Max Performance Turn, Wood's Methodology	122
Figure 25 - AH-1G Max Performance Turn RCDR Control, Power 4, 115% RPM	123
Figure 26 - AH-1G Max Performance Turn RCDR Control, Power 4, 115% RPM	124
Figure 27 - AH-1G Max Performance Turn RCDR Control, Power 4, 115% RPM	125
Figure 28 - AH-1G Max Performance Turn RCR Control, Power 4, 110% RPM	126
Figure 29 - AH-1G Max Performance Turn RCR Control, Power 4, 110% RPM	127
Figure 30 - AH-1G Max Performance Turn RCR Control, Power 4, 110% RPM	128
Figure 31 - AH-1G Max Performance Turn RCDR Control, Power 3, 110% RPM	129
Figure 32 - AH-1G Max Performance Turn RCDR Control, Power 3, 110% RPM	130
Figure 33 - AH-1G Max Performance Turn RCDR Control, Power 3, 110% RPM	131
Figure 34 - AH-1G Max Performance Turn TRC Control, Power 1, 120% RPM	132
Figure 35 - AH-1G Max Performance Turn TRC Control, Power 1, 120% RPM	133
Figure 36 - AH-1G Max Performance Turn TRC Control, Power 1, 120% RPM	134

LIST OF FIGURES
(continued)

Figure 37 - AH-1G Max Performance Turn TRC Control, Power 2, 120% RPM	135
Figure 38 - AH-1G Max Performance Turn TRC Control, Power 2, 120% RPM	136
Figure 39 - AH-1G Max Performance Turn TRC Control, Power 2, 120% RPM	137
Figure 40 - AH-1G Max Performance Turn T(RC) Control, Power 4, 120% RPM	138
Figure 41 - AH-1G Max Performance Turn T(RC) Control, Power 4, 120% RPM	139
Figure 42 - AH-1G Max Performance Turn T(RC) Control, Power 4, 120% RPM	140
Figure 43 - AH-1G Max Performance Turn RCDR Control, Power 3, 110% RPM 125, 105, 80 Velocity Breakpoints	141
Figure 44 - AH-1G Max Performance Turn RCDR Control, Power 3, 110% RPM 125, 105, 80 Velocity Breakpoints	142
Figure 45 - AH-1G Max Performance Turn RCDR Control, Power 3, 110% RPM 125, 105, 80 Velocity Breakpoints	143
Figure 46 - AH-1G Max Performance Turn RCDR Control, Power 3, 115% RPM 125, 105, 80 Velocity Breakpoints	144
Figure 47 - AH-1G Max Performance Turn RCDR Control, Power 3, 115% RPM 125, 105, 80 Velocity Breakpoints	145
Figure 48 - AH-1G Max Performance Turn RCDR Control, Power 3, 115% RPM 125, 105, 80 Velocity Breakpoints	146

LIST OF TABLES

Table I	- AH-1G Characteristics	19
Table II	- Power Required Model, Empirical Constants	100
Table III	- Rotor Speed Control Laws, Maneuver Summary	115

1.0 INTRODUCTION

Although attack helicopter operational roles have in the past traditionally been limited to the anti-armor, air-to-ground, and close air support missions, the modern attack helicopter is now being promoted as a potential air-to-air machine, especially as counter-air helicopter threats, most notably those being developed by Warsaw Pact nations, are developed and deployed in ever larger numbers. The Soviet Union now has several helicopters that pose a threat to current NATO alliance attack helicopters; the aging, but highly lethal, Mi-24D/E HIND, the recently introduced Mi-28 HAVOC, and the much talked about, and recently revealed, Ka-34 HOKUM (rumored to be a dedicated air-to-air combat helicopter), [Anonymous, 1989]. In the interim, until a dedicated air combat helicopter exists, both the U.S. and other NATO alliance countries are now adapting, arming, and otherwise "converting" many existing attack and scout helicopters to address the counter-air helicopter threat.

The idea of helicopter air-to-air combat is certainly not without its critics. Indeed, many do not believe that the helicopter has either the weaponry, sophistication, or aerodynamic capability to be an effective counter-air deterrent. However, both NATO and Soviet doctrine acknowledge

that air-to-air combat involving helicopters is a foregone conclusion. McCue [McCue et al, 1984] notes that six countries already have deployed (or have in development) 10 potential air-to air helicopter platforms (the AH-1G/S, MD-500 series, AH-64, MBB BO-105, SA 341/342 Gazelle, WG13 Lynx, MIL Mi-24 HIND, LHX, PAH-2, and the A-129). Since that article was written several years ago, other potential candidates for the air-combat mission have appeared (the AH-1W, Mi-28, Ka-34, AUH-76, SA-365, and, possibly, the MV-22).

Both the NATO and Warsaw Alliances take very seriously the air-to-air helicopter threat. For instance, in the U.S., the Marine Corps founded (in 1978) the U.S. Marine Corps Aviation Weapons and Tactics Squadron One (MAWTS-1) which includes as part of its tactical training syllabus helicopter vs. helicopter (helo vs. helo) and helo vs. fixed-wing air combat training [Anonymous, 1986]. On the Soviet side, a Colonel M. Belov [Belov, 1981; Bodansky, 1989] is quoted as saying,

" ... it has become vital to get a weapon which could compete with the helicopter in respect of combat power, tactical possibilities, etc. Logic and history suggest that such a weapon is the helicopter itself. Just as tanks have always been the most effective weapon against tanks, helicopters are the most efficacious means of fighting

helicopters. Use of helicopters by both warring sides will inevitably lead to clashes between them ..."

Such was the case during the Iran-Iraq war just a few years ago. Several unclassified sources have revealed that during this conflict, an Iranian IAH-1J attack helicopter fired an anti-tank TOW missile at an Iraqi Mirage F-1 fixed wing fighter, which subsequently impacted, and destroyed, the aircraft [Parlier, 1989]. Other sources have documented similar incidents as having occurred during the Persian Gulf War. Bodansky notes, for instance, that at least one Iranian F-4 interceptor, and possibly more, were victims of air-to-air missiles fired from Soviet-built Mi-24 HINDs flown by the Iraqi's, [Bodansky, 1989].

These incidents and several others have resulted in numerous analyses, flight test programs, and fighter helicopter conferences, all seemingly established in an attempt to define the ideal counter-air helicopter. In the early to mid- 1980's, the U.S. Army, for example, initiated four exhaustive flight test programs at the U.S. Naval Air Test Center in order to document the maneuvering capabilities of several existing military and commercial helicopters. The Army's investigation, the Air-to-Air Combat Test (AACT I-IV), was conducted over a period of about five years and

generated substantial amounts of data which, even today, is still being analyzed, [Wolfrom, 1986; Drummond, 1988; Wolfrom and Fisher, 1985]. The U.S. Navy and Marine Corps also initiated several programs to evaluate the helicopter air combat concept, although their studies have concentrated predominantly on the effects of air combat on airframe strength and fatigue for their diverse inventory of attack, assault, and ASW (anti-submarine warfare) helicopters, [Trainer and Lamb, 1988; Lindsey et al, 1989; Schaefer, 1989].

These and other studies have shown, however, that as sophisticated as current inventory helicopters are, they nevertheless fall short in their ability to fulfill the counter-air helicopter role. Occhiato et al have noted that helicopter designers have traditionally focused only on weight, performance, and cost -- at the expense of the high maneuverability and agility required for the successful air combat machine, [Occhiato et al, 1989]. In addition, Schaefer notes that air combat maneuvering was never included (until very recently) in the mission statement or mission usage spectrum for any existing U.S. military helicopter - consequently, none of these helicopters were designed for air combat, although many are being used in this manner today, [Schaefer, 1989]. But the apparent disregard for

maneuverability and agility as design drivers has left unanswered numerous questions relative to the suitability of today's operational helicopters to the modern battlefield, particularly one where fighter helicopter threats are present. Unfortunately, several attempts by the U.S. and other NATO countries to answer these questions or develop a dedicated counter-air helicopter deterrent have met their demise through a combination of defense fiscal austerity and program mismanagement. Consequently, many programs are now looking at innovative ways to upgrade existing helicopter performance, maneuverability, and agility to acceptable standards. Although the present research is but one alternative in a field flooded with research and development, the author is confident that the concept presented here, when coupled with already existing technologies, will be one viable solution to a problem deserving so much attention.

2.0 PROBLEM STATEMENT

There have been, probably, as many definitions for maneuverability and agility as there have been papers published on the subject. In an attempt to break from tradition, the definitions for maneuverability and agility are taken from McCue, [McCue et al, 1985]. McCue defines maneuverability as the aircraft's ability to perform basic maneuvers that are primarily governed by performance variables, such as power available and power required. Agility, on the other hand, "implies quickness of movement - - maneuvers primarily governed by flying qualities variables such as damping and control power ... ". In other words, while maneuverability can be thought of as the aircraft's ability to change the direction and magnitude of the aircraft velocity vector, agility can be defined or thought of as the time rate of change of maneuverability. Since they can be related to instantaneous and sustained turn performance, both maneuverability and agility play a very important role in any design effort focused on improving the air combat capabilities of either fixed- or rotary-winged aircraft.

The air combat performance of most fixed-wing aircraft is primarily governed by excess thrust or power and wing

loading. In an analogous fashion, the helicopter also depends on these parameters for successful air combat maneuvering, although they are defined somewhat differently. Occhiato maintains that helicopter maneuverability and agility is really a function of many parameters, some of which include rotor speed, disk loading, blade loading, blade hinge offset, Lock Number, installed engine power, and tail rotor blade loading, [Occhiato, 1989]. Although all these factors are important in designing to a high level of maneuverability, their relative importance changes depending on the flight regime or airspeed at which maneuverability demands are placed. But Occhiato, however, notes that "success in producing high levels of maneuverability in all flight regions is directly related to the ability to produce high levels of rotor thrust". For the most part, rotor thrust capability is primarily a function of rotor geometry, blade airfoil shape, installed engine power, and rotor speed. Assuming for the moment that the first three are fixed variables in any existing helicopter design, the fourth, rotor speed, seems a likely candidate for investigating improvements to existing maneuverability and agility. Unfortunately, however, helicopter manufacturers are loath to change or vary rotor speed since it is often optimized for maximum cruise and hover efficiency. Furthermore, nothing shakes like a helicopter, and rotor speed is also chosen for

optimum placement between rigid and flexible airframe vibratory modes - varying rotor speed could result in a coalescence with known helicopter modal frequencies, causing both excessive vibrations and possible reductions in dynamic component fatigue lives. But recognizing that some problems would most likely exist if rotor speed were used as a variable in investigating maneuverability and agility, the present research was nevertheless conducted under the assumption that these problems would need to be addressed at some future point.

The primary goal of the current research, simply stated, is to determine the effects of continuous, variable rotor speed on the maneuverability of an attack helicopter, the AH-1G HueyCobra. Once these effects are established, the research is then directed toward the development of optimum rotor speed control laws such that several measures of combat effectiveness are optimized, the purpose being to improve the AH-1G's combat effectiveness in both ground attack and air combat missions. Two computer programs are developed to evaluate these control laws; a mainframe-based program which uses a commercially available optimization code to search for optimal control law parameters, and an IBM PC-based program that generates maneuver time histories for control law candidates being investigated. The mainframe-based program,

DT5, is written in FORTRAN 77 and uses the IMSL optimization routine DNCONF to search for and optimize various control law parameters. The IBM PC-based program, DTURN5, is written in Microsoft QuickBasic and allows rotor speed control laws to be investigated interactively. Both programs, which are described in detail later, generate maneuver time histories for an AH-1G executing a 180 degree, maximum performance decelerating turn. This particular maneuver was chosen not only for its tactical significance to both air-to-ground and air-to-air combat missions, but also because the decelerating turn has been used in the past as a benchmark in previous studies investigating helicopter maneuverability and agility.

The helicopter chosen as the candidate for this research, the AH-1G HueyCobra, is a Vietnam-era attack helicopter. It is a teeter rotor (two-bladed rotor with zero hinge offset), single engine helicopter that saw considerable service in Vietnam during the late 1960's and early 1970's, (see Table I for a list of AH-1G characteristics). The AH-1G was a first generation attack helicopter developed by Bell Helicopter as an armed escort helicopter to utility helicopters such as the UH-1B, but was also used by itself as a close air support and fire suppression helicopter. Although the AH-1G is somewhat outdated (it evolved into several U.S. Marine Corps and Army derivatives, the AH-1J,

AH-1S, AH-1T, and the AH-1W), it was nevertheless used for this study because vast amounts of published, public domain data exist for this helicopter. In addition, several researchers in the past have used the AH-1G as a test bed for their maneuverability and agility studies, making it an ideal vehicle with which to compare past and present research.

TABLE I

AH-1G Descriptive Data

Main Rotor

Number of Blades - 2
 Radius - 22 ft
 Chord - 2.25 ft
 Section - 9.33%,
 (Symmetrical Wortmann)
 Hub Type - Teetering
 Undersling - 4.5 in.
 Twist - -10 deg
 Shaft Tilt - Zero
 Design RPM
 314 - 324 (power on)
 294 - 339 (power off)
 Blade Flapping
 Inertia - 2842 slug-ft³

Tail Rotor

Number of Blades - 2
 Radius - 4.25 ft
 Chord - 0.701 ft
 Twist - Zero
 Gear Ratio - 5.123

Wing

Area - 27.8 ft²
 Aspect Ratio - 3.91
 Incidence - 14 deg
 Dihedral - 3.5 deg

Elevator (each side)

Area - 7.35 ft²
 Aspect Ratio - 1.49
 Incidence - Variable

Vertical Stabilizer

Area - 18.60 ft²
 Aspect Ratio - 1.56

Gross Weight Range

7500 - 9500 lbs (TOGW)

3.0 LITERATURE REVIEW

3.1 Energy Maneuverability Concepts

In March 1966, (then) U.S. Air Force Major John R. Boyd and Mr. T. P. Christie developed the energy maneuverability (E-M) concept to help explain both the U.S. Air Force's and U.S. Navy's low kill-to-loss ratios in Vietnam, [Thomas, 1987]. Despite state-of-the-art aircraft and well-trained pilots, the years 1965-68 saw the Navy's kill ratio at only 2.42 to 1 while the U.S. Air Force's was slightly lower at 2.25 to 1, [Cunningham, 1984]. Predictably, Major Boyd's study concentrated on comparisons between the U.S. F-4C and the North Vietnamese MiG-21C, in order to help the crews of the American aircraft regain tactical air superiority in an aircraft specifically designed for the long range interceptor role, rather than the close-in, short-range, air battles which had manifested themselves during the Vietnam conflict. The E-M concept enabled a direct performance comparison between these and other dissimilar aircraft by contrasting each aircraft's total energy available for maneuvering. In essence, by overlaying E-M charts for each aircraft, a tactician could theoretically predict which aircraft would retain superiority for various flight conditions or regimes.

Ironically, though, the U.S. Navy was the first to adopt the Air Force's new tool, and by 1972 the Navy's kill ratio had increased nearly four times to 12.0 to 1. This success eventually led to the organization of the Navy's premier Navy Fighter Weapons School, better known as "Top Gun", at the Miramar Naval Air Station in San Diego, CA, [Cunningham, 1984].

In 1970, the Bell Helicopter Company recognized E-M's unique capability and became the first to apply the use of energy methods in predicting the performance capabilities of their newly fielded attack and gunship helicopters (e.g., the AH-1G HueyCobra, the UH-1B Huey, etc.), [Wood and Livingston, 1971]. Unfortunately, as future studies would indicate, the disparity between helicopter and fixed-wing performance was too great to effectively apply fixed-wing tactics directly to the helicopter "across the board". In fact, while the tactical air superiority jet fighter had evolved steadily since the Korean War, helicopter air combat was still in its infancy, with helicopter performance, maneuverability, and agility, even today, closely paralleling those of late World War I fixed-wing fighters. Furthermore, the helicopter's hovering ability and low speed, uncoordinated maneuvering capabilities, (typical of all VTOL (Vertical Takeoff or Landing) aircraft), introduced analytical and tactical

complexities unique to helicopter maneuvering flight and the fixed-wing E-M methodology needed to be adjusted accordingly, [Lappos, 1984]. Recognizing that helicopter E-M methods needed to be refined further, Bell Helicopter put these problems aside, and began its studies by successfully adapting much of the fixed-wing E-M methodology, with generally good results, especially at the higher airspeeds, [Wood and Livingston, 1971]. However, before considering Bell Helicopter's methodology and its application to this research, it is perhaps instructive to digress and analyze the E-M methodology as proposed by Boyd and Christie, which has remained largely unchanged since 1966.

Performance analysis assumes the aircraft to be a point mass vehicle whose motion is described by Newton's Laws, where the force equals the mass times the acceleration. This approach assumes that the aircraft's velocity vector is slowly varying with time, that is to say that the acceleration vector can be neglected and the forces assumed to be in equilibrium. While this greatly simplifies the analysis, performance problems which deal with highly accelerated flight are not properly modeled. For these types of problems, the complete set of three force equations of motion must be used, along with the appropriate kinematic relations, to find the aircraft trajectory, [Hale, 1984].

The energy-state approximation (the basis for all E-M concepts), however, is a much simpler, though less accurate, technique for problems involving accelerated flight. This concept makes use of the vehicle's total energy, being defined as the sum of its potential and kinetic energy. Hence,

$$\text{Total Energy} = \text{Potential Energy} + \text{Kinetic Energy}$$

where, for an aircraft, the potential energy is related to the altitude of the vehicle and the kinetic energy to its velocity. By definition, the energy-state for a vehicle in flight is [Hale, 1984],

$$E = Wh + \frac{WV^2}{2g} \quad (1)$$

where E is the total energy, W is the weight of the aircraft, h is the true altitude above sea level, V is the aircraft's true airspeed, and g is the acceleration due to gravity

(32.17 ft/s²). If both sides of equation (1) are divided by the can be determined, allowing a more convenient comparison between aircraft of different weights. This new quantity is referred to as the specific energy (total energy per pound of aircraft weight) or the energy height, since the resulting units are expressed in feet. Hence,

$$E_s = \frac{E}{W} = h + \frac{V^2}{2g} \quad (2)$$

Figure 1 is a plot of lines of constant energy height as a function of altitude and airspeed. For any given constant energy height, it is apparent that numerous combinations of airspeed and altitude are possible. This implies that a pilot may tradeoff altitude for airspeed (or vice versa) and still remain at a given energy state. As an example, an aircraft at some initial airspeed and altitude combination corresponding to an energy height of 20,000 feet, could theoretically "zoom" to 20,000 feet, but only after arriving at that point with zero airspeed. On the other hand, a dive along the 20,000 feet constant energy line would result in an airspeed of 1135 feet per second as the aircraft impacted the ground, [Hale, 1984].

One rather interesting observation can be made about Figure 1, and that is that the plot is the same for all vehicles, regardless of vehicle characteristics. The utility of this figure, therefore, is of limited use when comparing different aircraft and their respective performance capabilities, [Shaw, 1985, and Thomas, 1987]. It is necessary, then, to define specific excess power, which is the time rate of change of specific energy. Specific excess power, or P_s , is defined as,

$$P_s = \frac{dE_s}{dt} = \frac{dh}{dt} + \frac{V}{g} \frac{dV}{dt} \quad (3)$$

Unlike E_s , P_s can be related to individual aircraft characteristics and flight parameters. As the name implies, P_s can be equated to the aircraft's excess power available for maneuvering, since the rate of change of energy, or power, must equal the power to move from one energy state to another. From the force equations of motion, [Hale, 1984],

$$P_s = \frac{(T - D)V}{W} \quad (4)$$

or, in a different, sometimes more useful form, (especially for helicopter analysis), [Wood and Wells, 1972],

$$P_s = \frac{(HP_{av} - HP_{req})550}{W} \quad (5)$$

where, T, is the aircraft thrust; D, the aircraft drag; V, the velocity; W, the aircraft weight; HP_{av}, the horsepower available from the aircraft's engines; HP_{req}, the horsepower required for the particular flight condition; and the constant 550 a unit conversion factor relating ft-lb/s (work per unit time) to shaft horsepower.

The particular value of specific excess power determines the aircraft's ability to maneuver. For instance, a positive value of P_s indicates that the aircraft has excess power to maneuver (i.e., to climb or accelerate), whereas a negative value of P_s indicates that the aircraft's available horsepower

is exceeded by the horsepower required, and subsequently, the aircraft will begin to lose energy (i.e., descend or decelerate), [Thomas, 1987]. As an example, a P_e value of 30 feet per second would enable an aircraft to either accelerate 4.2 knots per second or climb at 1800 feet per minute, [Wood and Livingston, 1971]. Although not readily apparent from the above equations, excess power can also be used to curve the flight path enabling the aircraft to pull higher normal load factors in sustained turns or pullouts, (this will be addressed in more detail in a later section).

The utility of specific excess power comparisons between two dissimilar aircraft is not fully realized unless the information is assembled in one of two forms. The first, the energy diagram, is obtained by plotting P_e contours as a function of altitude and airspeed, as shown in Figure 2. Although a review is beyond the scope of this discussion, these plots are useful in predicting maximum rates of climb or maximum-energy climb schedules. A more detailed discussion on energy diagrams can be found in Thomas, [Thomas, 1987]. The second form, the so-called E-M or maneuver diagram is arguably the most practical in contrasting dissimilar aircraft performance and, in addition, is most frequently used in comparing air-to-air combat

performance between two or more aircraft. The E-M diagram superimposes lines of constant energy rate over a "carpet plot" of bank angle and turn radius for a particular altitude; this, in turn, is plotted with P_g against turn rate and airspeed, (see Figures 3 and 4). Much useful information can be gained through an inspection of the E-M diagram. For instance, maximum turn rate can be found at the maximum of each energy rate (P_g) contour. Minimum turn radius exists at the "point of tangency between the constant energy rate contours and the lines of constant radius", [Wood and Livingston, 1971]. The $P_g = 0$ (or zero energy rate) contour represents the aircraft's sustained flight capability. Once again, operation outside of this envelope is possible, but only at the expense of altitude, airspeed, or both, [Wood and Livingston, 1971]. Although the utility of the E-M diagram is without question for fixed-wing aircraft, it unfortunately "breaks down" for certain regimes of VTOL flight, in particular, low airspeed, uncoordinated flight with heavy sideslip. This problem was one that Bell Helicopter became aware of early on in their studies of helicopter maneuverability and agility. The problem continues to be researched even today and new maneuverability and agility metrics are being sought for these unique flight regimes, [Occhiato, et al, 1989].

CONSTANT ENERGY LINES
STANDARD DAY

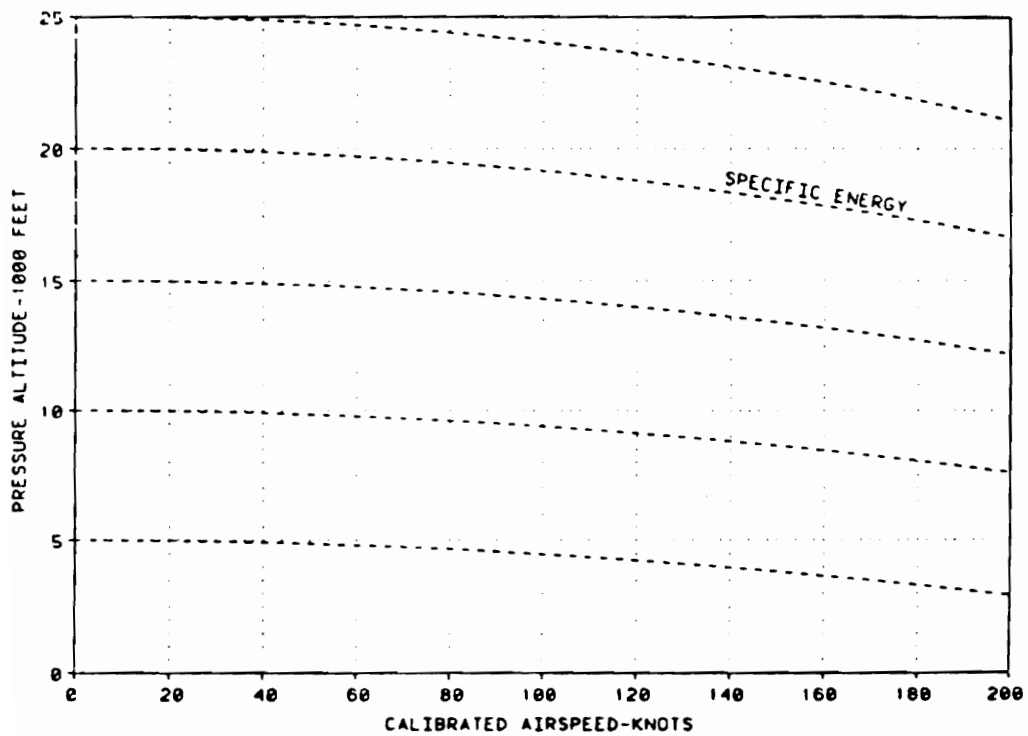


Figure 1
Plot of Constant Energy Lines

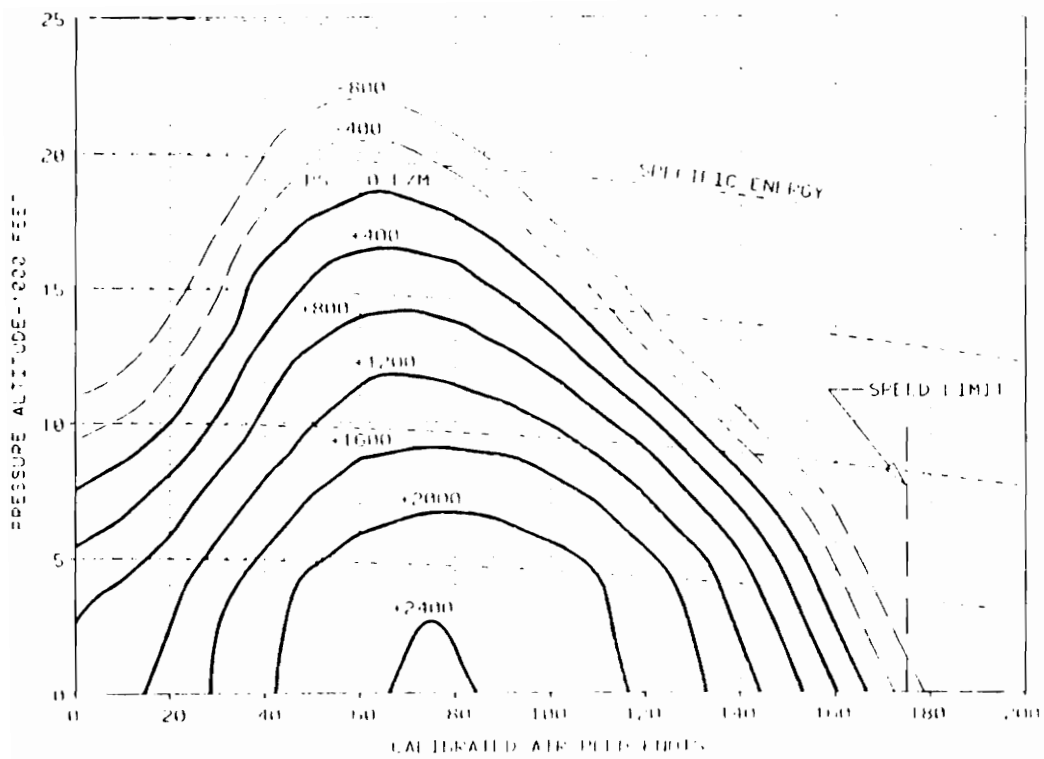


Figure 2
 P_s versus Altitude and Airspeed

E-M DIAGRAM
SEA LEVEL
STANDARD DAY

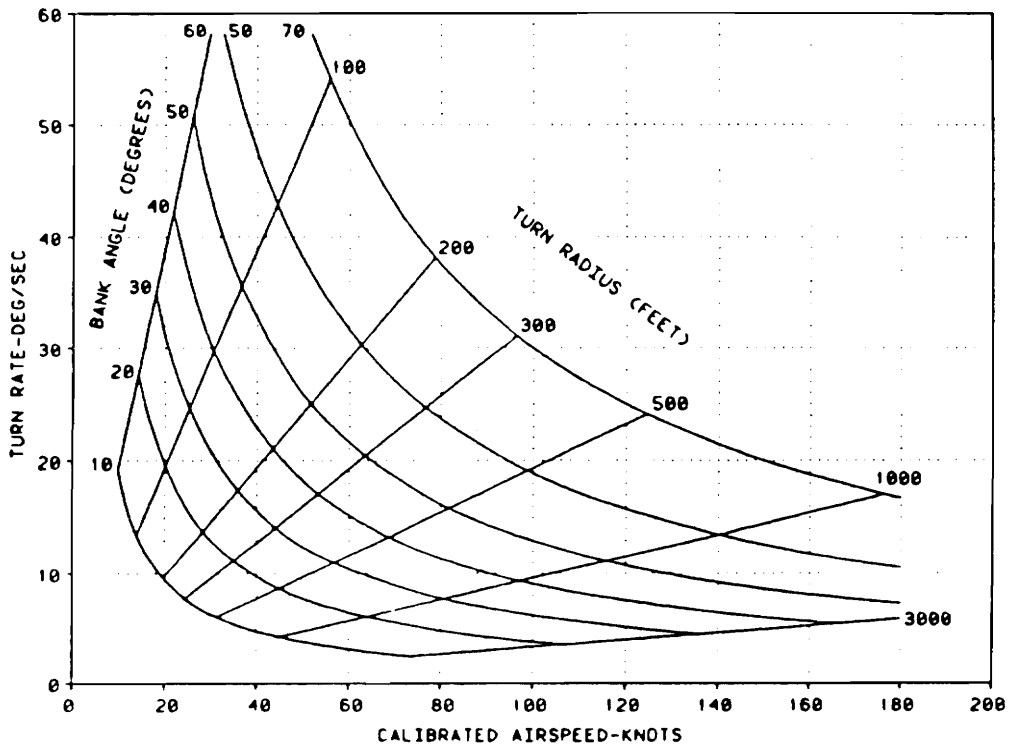


Figure 3
Turn Rate versus Airspeed

E-M DIAGRAM
SEA LEVEL
STANDARD DAY

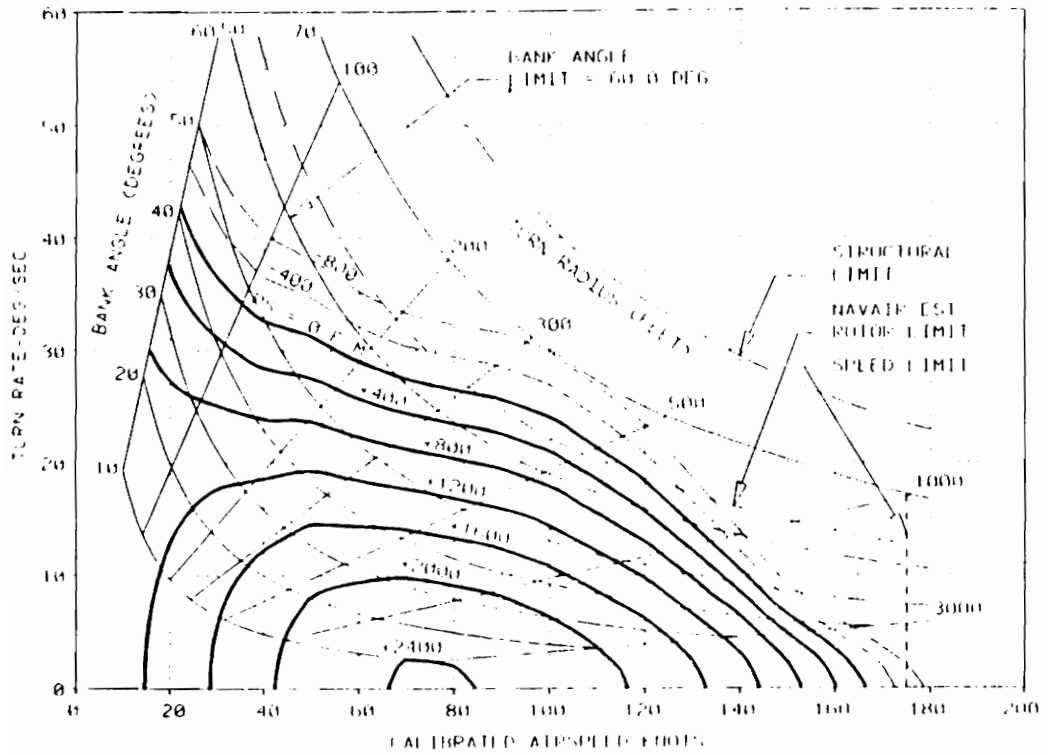


Figure 4

Energy Maneuverability (E-M) Diagram

3.2 Rotor Speed Control

Unlike its fixed-wing counter-part, the helicopter has an additional form of energy that can be used in air combat maneuvering; that is, the energy inherent in the helicopter rotor speed. For the helicopter, then, the specific energy can be redefined as follows,

$$E_s = h + \frac{V^2}{2g} + \frac{I_b \Omega^2}{2W} \quad (6)$$

where Ω is the helicopter rotor speed (in rad/sec), I_b is the rotor system moment of inertia (slug-ft³), and the other variables are as defined previously. Taking the first derivative with respect to time gives the energy rate or specific excess power,

$$P_s = \frac{dE_s}{dt} = \frac{dh}{dt} + \frac{V}{g} \frac{dV}{dt} + \frac{I_b \Omega}{W} \frac{d\Omega}{dt} \quad (7)$$

Using the concepts developed in the last few pages, it is readily apparent that changes in energy state may now be

accomplished through various combinations of, or tradeoffs between, altitude, airspeed, and rotor speed.

Although Bell Helicopter's early maneuverability research neglected the energy present in the rotor [Wood and Wells, 1972; Wood and Livingston, 1971], Bell initiated the High Energy Rotor System (HERS) program some years later [Wood, 1976]; its primary focus was to investigate energy recovery from transient rotor speed droop (rotor speed decay) in order to increase autorotation performance and transient maneuverability. The HERS flight test results were very promising and indicated that, among other things, bleed RPM could be used to increase vertical rate of climb in hover bob-up maneuvers and decrease total time to accelerate in longitudinal, constant altitude, acceleration maneuvers. Even though this and other Bell Helicopter maneuverability programs were extremely successful [Wood and Waak, 1979], rotor speed (in these studies) was allowed to droop through slack engine and rotor speed governing rather than allowing the rotor speed to be directly and accurately controlled.

In 1984, Sikorsky Aircraft hinted at the possible use of direct rotor speed control to increase the helicopters maneuverability during air combat encounters, [Lappos, 1984]. Although continuous, variable rotor speed control in the

strictest sense was not investigated, the beneficial effects of re-indexing rotor speed to a higher, constant value, was duly noted. In fact, a study by Sikorsky Aircraft and Chandler Evans, Inc., [Howlett et al, 1984], indicated that re-indexing rotor speed during flight not only resulted in enhanced maneuverability for certain transient maneuvers, but could decrease fuel consumption during cruise flight as well. Lappos noted that "design attention [could] be focused on a mission adaptive control system which [would] temporarily increase N_r [rotor speed] to store energy during low power maneuvers. During transient high power demands, the energy stored in the rotor [could] be recovered, with [a] dramatic increase in short term maneuverability", [Lappos, 1984]. He noted, however, that several problems needed to be addressed; i.e., higher blade centrifugal loads, rotor instabilities, and higher rotor control loads. Sikorsky, however, continued its research and published a series of papers on adaptive fuel control for helicopters, a technology that uses digital electronic control (DEC) to closely govern rotor speed and engine performance parameters, [Howlett et al, 1984; Sweet, 1989; Greenberg, 1989; Walsh, 1989]. Proper rotor speed control has always been a concern for rotorcraft engineers since thrust and power demands during maneuvering flight usually result in a loss of engine and rotor speed if not

properly governed; for maximum efficiency, the helicopter rotor system is designed for constant speed operation. Typically, rotor speed is limited on the high side by engine power available and compressibility effects on the advancing blade, and limited on the low end by high vibration levels, rotor blade stall (especially on the retreating blade side), reverse flow, and the loss of safe autorotation characteristics, [Occhiato et al, 1989; Anonymous, 1974]. Consequently, proper power management requires an engine control system that not only senses rapid changes in power required but also responds quickly to compensate for either rotor speed transient droop or rotor overspeed conditions. Sikorsky Aircraft research has recently focused on replacing traditional hydro-mechanical (HMU) fuel controls with full authority digital electronic fuel control (FADEC) that "respond repeatively [isochronously] to the feedback state of the engine ... [and] evaluate and adjust its internal software to correct for changing internal engine as well as external ambient conditions that [could] affect overall powerplant [and aircraft] performance", [Sweet, 1989]. Several studies by Sikorsky and the manufacturer of the FADEC, Chandler Evans, Inc., [Walsh, 1989; Howlett et al, 1984], investigated the effects of a fully integrated FADEC controller on the mission effectiveness of an S-76A helicopter performing simulated ground attack and air combat

maneuvers; their preliminary results showed that, on average, ground targets could be acquired 13% faster with an 18% increase in target tracking accuracy. These results were based primarily on the FADEC's ability to provide not only a more stable, more responsive weapons platform, but also increased pilot confidence in aircraft capabilities, and a general reduction in pilot workload. The most significant of Walsh's results, and the most germane to the present research, was a feature called Load Factor Enhancement (LFE). This innovation, which is unique to FADEC control and probably not practical for traditional HMU engine control, allows rotor speed to be re-indexed according to maneuver load factor schedules or thresholds. If the helicopter is in a tight turn, for example, and load factor is increased above a pre-defined threshold value, the rotor speed reference is reset by the FADEC to a higher value, where it remains until the load factor decreases below some lower threshold trip. The increase in rotor speed during the maneuver provides several advantages, namely an increase in the incipient stall boundary, increased control power and responsiveness, lower vibration levels, and additional rotor thrust, which can be used to maneuver more aggressively.

An examination of Howlett and Walsh's research suggests that rotor speed could be continuously or variably reset to

adapt to different flight regimes or demands. In fact, FADEC flight test data indicated that the superb handling qualities and target tracking (in both air-to-ground and air-to-air modes) could be enhanced even further if the LFE FADEC feature was active over the entire airspeed range, [Sweet, 1989]. Although not addressed in any depth or detail, Sweet noted that target tracking through high performance turns could be enhanced even further by "scheduling an increase in rotor speed rapidly at the onset of load factor buildup and gradually decreasing rotor speed [upon] completion of the maneuver", [Sweet, 1989]. The intent of the scheduling, however, was to "reduce adverse yaw excursions during roll-out for the targeting maneuvers", (helicopter rotor speed and directional control are highly coupled, especially for large power or torque demands), rather than using LFE to reduce time to turn, turn radius, or enhance other performance factors. By 1986, however, the U.S. Army Air-to-Air Combat Test (AACT) flight test program had demonstrated that helicopters with inferior maneuverability could enhance their maneuvering capability by allowing rotor speed to passively increase during the maneuver, using this advantage to turn inside an opponent with a nominally superior turn radius, [Wolf from, 1986].

3.3 Tactical Implications of Decelerating Turns

The evasive, maximum performance quick turn and the return-to-target maneuver are integral elements of the attack helicopter mission; their successful implementation is critical to the helicopter's survivability, lethality, and probability of mission success. These were two maneuvers flown in the Sikorsky S-76A flight test program and were chosen because of the severe demands placed on the helicopter's performance, maneuverability, and agility capabilities.

The evasive quick turn is usually initiated between 80-150 knots of airspeed with the purpose of changing direction as quickly as possible, usually 180 degrees from the initial heading angle. This maneuver is particularly severe since it is usually performed at nap-of-the-earth (NOE) or contour flight altitudes in order to avoid both ground-based and air-based threats present at altitudes greater than 150-300 feet above the battlefield, [Howlett, 1984; Anonymous, 1986]. The return-to-target maneuver is similar to the evasive quick turn except that it is typically used in the ground attack mission and is distinguished by an initial firing pass over the target followed by a quick turn and a subsequent re-attack in the shortest possible time, [Prouty, 1986]. The

importance of the maximum performance turn to helicopter lethality and survivability has long been recognized and several studies have used the maximum performance, decelerating turn as a tool in understanding the effects of various performance parameters on helicopter maneuverability and agility. The Bell Helicopter research of the early 1970's, as noted at the beginning of this section, was really the first of its kind and laid the groundwork for many of the future studies in high performance helicopter flight, [Wood and Livingston, 1971; Wood and Wells, 1972; Wood and Waak, 1979]. In 1985, the Naval Air Development Center (NADC) considered presenting maximum performance, decelerating turn charts for NATO and Warsaw Pact helicopters as a supplement to tactical plots already present in the Marine Corps AH-1 Tactical Manual (TACMAN). Their research concentrated on the development of a program called DECEL that calculated ground tracks for helicopters performing decelerating turns at various entry airspeeds, [Woods, 1985]. Eventually, though, the idea of incorporating these charts into the AH-1 TACMAN was dropped because of the uncertainties involved in extrapolating flight test performance data to high rotor thrust coefficients and, also, the difficulty in obtaining information to accurately model adversary helicopters with which to make direct comparisons to charts generated for friendly helicopters. The NADC and Bell Helicopter computer

programs (DECEL and MCEP, respectively) nevertheless remain valid tools for investigating performance related parameters, hence, the present research uses both the energy maneuverability approach and the decelerating turn methodologies developed by Bell (albeit, slightly improved), to investigate the use of continuous, variable rotor speed control.

4.0 SIMULATION MODEL DEVELOPMENT

4.1 Power Required Model

Regardless of the type of aircraft being studied, both fixed-wing and helicopter performance analyses require an accurate accounting of power required and power available for the flight regimes being studied. Once these quantities are known, many important aircraft performance parameters such as climb rate, absolute ceiling, endurance, range, maximum speed, and load factor capability can be determined. It comes as no surprise, then, that rotorcraft performance simulation programs, even relatively simple ones such as DTURNS, must base their calculations on fairly accurate power required and power available models in order to be of any use to the analyst and engineer.

The power required for a helicopter to sustain forward flight is the sum of the powers required to overcome fuselage parasite drag, the rotor lift-induced drag, and the rotor profile or torque drag, [Wood, 1973; Prouty, 1986; Layton, 1984; Johnson, 1980]. In maneuvering flight, there are additional contributions to each of these three components associated with the demands for increased rotor thrust during the maneuver. In addition, high speed and maneuvering flight

will result in additional power demands required to overcome compressibility effects on the advancing blade, blade stall on the retreating blade, or a combination of both. Therefore, the total power required to sustain level and accelerated flight is the sum of five specific components; they are the fuselage parasite drag, rotor lift or thrust-induced drag, rotor blade profile drag, advancing blade compressibility or wave drag, and the drag associated with stalled and/or reversed flow on the retreating blade, [Wood, 1973].

4.1.1 Induced Power Required

Power required for helicopter flight is usually determined using two approaches, the first being the momentum theory and the second blade element theory, [Prouty, 1986; Bramwell, 1976; Johnson, 1980]. Momentum theory is often referred to as the energy balance method since its basic premise allows rotor thrust to be predicted based on the conservation of momentum and energy of the air mass accelerated by the rotor disk. Although the blade element method is a more accurate means of calculating rotorcraft performance, Johnson states that "... the energy method is fast and reasonably accurate, and hence it is well suited for

preliminary design use", [Johnson, 1980]. The momentum theory has enjoyed widespread use for quite some time and its predictive capabilities and deficiencies have been improved over the years through the application of empirical and semi-empirical data gathered from various wind tunnel and flight tests.

The blade element theory, on the other hand, is more refined and is used extensively by many helicopter manufacturers in performance prediction and flight simulation, (examples include Sikorsky Aircraft's GENHEL, Bell Helicopter's C81, and Boeing Helicopters' CAMRAD). Rotor forces and moments are calculated by performing a force balance on individual 2-dimensional blade elements; these forces and moments are then integrated along spanwise and azimuthal directions with respect to time, forming time varying, periodic functions which must be balanced for each helicopter trim state. Conceptually, the blade element theory is easier to understand, but it is computationally intense and is difficult to apply beyond the realm of quasi-steady maneuvers. The current research does not require or warrant the complexity of the blade element method; however, what follows is a compromise, as the power required model employed by DTURN5 is a combination of both blade element and momentum theories.

Momentum theory uses the principles of momentum theory and energy conservation to predict rotor thrust and the resulting downwash velocities necessary for the calculation of induced power required. To simplify the analysis, momentum theory makes several assumptions relative to the flow state and the rotor geometry, [Layton, 1984]:

- (1) The rotor consists of an infinite number of blades which act as an "actuator disk" to uniformly accelerate air through the rotor,
- (2) Flow through the actuator disk is uniform and steady,
- (3) The rotor imparts no swirl or rotational components to the rotor downwash, and,
- (4) Energy is imparted to the air by a pressure jump across the rotor disk.

These assumptions, along with continuity relationships, allow rotor thrust to be defined as a function of the pressure change across the actuator disk. In practical applications, though, determination of this incremental pressure jump is difficult at best, and much of the theory is based on the development of rotor thrust as a function of the induced

velocity. Induced velocity is the localized increase in velocity due to the generation of lift or thrust from the rotor blades and can be related by Bernoulli's equation to the pressure jump which occurs at the rotor disk. In hovering flight, the induced velocity is a direct function of the thrust required to hover, whereas in climbing and forward flight there are additional velocity components contributing to the rotor inflow or air flux, the magnitude of which is a function of the forward airspeed and the rate of climb or descent. Prouty gives the induced velocity as a function of airspeed,

$$v_1 = \sqrt{\frac{-V^2}{2} + \sqrt{\left(\frac{V^2}{2}\right)^2 + \left(\frac{T}{2\rho A}\right)^2}} \quad (8)$$

where v_1 is the induced velocity, V is the forward airspeed, ρ is the local air density, T is the rotor thrust, and A is the rotor disk area defined by πR^2 , where R is the rotor radius. It is easily shown that in hovering flight, the above equation reduces to,

$$v_1 = \sqrt{\frac{T}{2\rho A}} \quad (9)$$

The induced drag of the ideal rotor in forward flight can be defined as follows, [Prouty, 1986],

$$D_{ind} = \frac{Tv_i}{V} \quad (10)$$

The horsepower required to overcome the induced power then becomes,

$$hp_{ind} = \frac{D_{ind}V}{550} \quad (11)$$

where 550 is a unit conversion factor relating ft-lbs/s (work per unit time) to horsepower required. It is interesting to note that induced power requirements actually decrease with forward speed, this being a result of the rotor having to accelerate less fluid through the rotor disk for a given thrust level as the forward velocity of the helicopter increases, [Prouty, 1986].

Since momentum theory imposes the condition of uniform downwash velocity cross the face of the rotor disk, practical application of equation (10) requires an empirical correction factor to compensate for losses due to rotor swirl or

vorticity, blade tip losses, and the fact that the rotor disk actually contains a finite rather than an infinite number of blades. Prouty notes that the ideal rotor is analogous to the ideal wing with an elliptical lift distribution. With the possible exception of the British Spitfire of World War II, most wings do not have an ideal elliptical lift distribution, and the Oswald efficiency factor, e , is used to account for flow non-uniformities. Prouty proposes a similar concept, the rotor efficiency factor, to compensate for the non-ideal rotor. He states, however, that this efficiency factor is only applicable when momentum theory is used to calculate rotor induced drag since the use of the more accurate blade element theory would automatically compensate for these problems. (Although blade element theory is a more accurate analytical approach to helicopter performance and rotor limit estimation, this research uses momentum theory to predict induced horsepower required primarily because of the difficulties associated with integrating time dependent rotor blade forces and moments over the blade span and the disk azimuth and in predicting the non-uniform induced velocities required for an accurate assessment of those forces). The rotor efficiency factor is taken in most research as a constant, but in reality the rotor efficiency factor is a complex function of rotor thrust, forward airspeed, blade twist, and rotor tip path plane angle of attack, [Prouty,

1986]. Past research, however, has shown that, given the accuracy of the assumptions which exist for momentum theory calculations, a constant value can usually be assumed, with typical values for e ranging from 0.7 to 1.0, [Wood, 1971]. Since the rotor efficiency factor strongly depends upon rotor geometry blade characteristics and forward velocity, the appropriate value used will vary depending on the specific helicopter being analyzed. Wood showed that the rotor efficiency factor for the AH-1G attack helicopter varied linearly from 0.77 at hover to 1.0 at 110 knots, where it remained constant for airspeeds greater than 110 knots, [Wood, 1971]. Wood's model for rotor induced power was essentially the same as that adapted to this research with the exception that his model used a more complicated, semi-empirical expression for velocity inflow to the rotor disk, rather than the expression for induced velocity given by Prouty above. Because of this small difference, it was found that good correlation with AH-1G flight test data using Prouty's expression for induced velocity could be achieved by assuming a rotor efficiency factor of 0.69, constant over the entire airspeed range. Regardless of this slight departure from Wood's methodology, excellent correlation with AH-1G power required flight test data was obtained. Model correlation and validation with AH-1G flight test data will be discussed in a later section.

4.1.2 Rotor Blade Profile Drag Power Required

When helicopter rotor blades cease to create lift, induced power requirements due to lift generation approach zero but power nevertheless is still required to compensate for rotor blade parasite or skin friction (viscous) drag and pressure or form drag. This contribution to the total power required for flight is known as the profile power and is derived using a combination of simple blade element theory and empirical results gathered through years of testing. The blade element theory assumes that each helicopter rotor blade is composed of numerous 2-dimensional blade elements or airfoils each contributing to the total performance of the rotor disk. The lift, drag, and pitching moment of each element is integrated both over the span of each blade and in the azimuthal direction to obtain time dependent rotor disk forces and moments acting about the rotor hub. Several factors contribute to the total power required to overcome parasite drag: Rotor torque due to the drag component normal to the blade leading edge, (about 65% of the total), drag due to the radial component of flow, that is flow along the blade span (about 22%), drag due to yawed flow (10%), and the contribution due to reverse flow on the retreating side of the rotor disk, (about 3%), [Johnson, 1980]. After

integration, the blade element theory gives the expression for the total rotor profile power required as, [Wood, 1971],

$$hp_p = \frac{C_{\bar{d}}}{8} \rho b c R (\Omega R)^3 \frac{(1 + 4.6 \mu^2)}{550} \quad (12)$$

where $C_{\bar{d}}$ is the mean or averaged profile drag coefficient, b is the number of rotor blades, ρ the local air density, R the rotor radius, Ω the rotor speed, and the μ is the rotor advance ratio defined as $\mu = \frac{V}{\Omega R}$ for small rotor disk angles of attack. The constant 4.6 is an empirical constant applied by Bennet, [Bennett, 1940]. Bennet assumed that this factor remained constant over the airspeed range, in direct contrast to the more accurate method derived by Glauert which indicated that this constant actually ranged from 4.50 in a hover to 6.13 in high speed flight, [Johnson, 1980]. Johnson and Wood, however, note that Bennett's approximation is more widely used since the additional accuracy of Glauert's expression may not be warranted given the assumptions used in the blade element theory.

In Wood's methodology, an attempt was made to more accurately represent the average or mean profile drag

coefficient and the method proposed by Bailey [Bailey, 1941], was adopted. Specifically, the drag coefficient can be represented by a quadratic function of the mean rotor angle of attack as the blade rotates through one revolution,

$$\bar{C}_d = \delta_0 + \delta_1 \bar{\alpha} + \delta_2 \bar{\alpha}^2 \quad (13)$$

where δ_0 , δ_1 , δ_2 are correlation constants and $\bar{\alpha}$ is defined as the mean rotor blade angle of attack. Wood showed an empirical expression for $\bar{\alpha}$ based on AH-1G flight test data,

$$\bar{\alpha} = 3.5 \frac{t_c}{2\pi} \quad (14)$$

where t_c is the blade loading coefficient defined as,

$$t_c = \frac{N_z W}{1/2 \rho (\Omega R)^2 (bcR)} \quad (15)$$

where N_z is the maneuvering load factor, W is the gross weight

of the helicopter, and the other variables are as defined before. The complete expression for profile power required, as employed by DTURN5, remains unchanged from Wood's basic methodology and those presented in classic texts on rotorcraft performance,

$$hp_p = \frac{(\delta_o + \delta_1 \times \bar{\alpha} + \delta_2 \times \bar{\alpha}^2)}{8} \rho b c R (\Omega R)^3 \frac{(1 + 4.6 \mu^2)}{550} \quad (16)$$

4.1.3 Fuselage Parasite Drag Power Required

The remainder of the forward flight power required to overcome drag not formed by rotor lift is that due to fuselage parasite drag. Parasite drag, in general, is caused by skin friction and pressure (or form) drag on the various components of the helicopter fuselage; these include the fuselage itself, engine nacelles, main rotor hub and shaft, landing gear, external ordnance, guns, etc., [Prouty, 1986; AMCP, 1974]. The power required to overcome the drag of these different components is,

$$hp_f = \frac{D_f V}{550} \quad (17)$$

where D_f is the parasite drag defined as,

$$D_f = C_d q S \quad (18)$$

where C_d is the drag coefficient, q the dynamic pressure, and S , is some reference area, (normally taken as the rotor disk area). Prouty, however, states that it is inappropriate to use the rotor disk area as the reference area for fuselage parasite drag calculations and he proposes instead that this drag be defined in terms of an equivalent flat plate area, f , which is just the fuselage drag divided by the dynamic pressure. That is,

$$f = \frac{D_f}{q} \quad (19)$$

The equivalent flat plate area is the "frontal area of a flat plate with a drag coefficient of 1, which has the same drag

as the object whose drag is being estimated", [Prouty, 1986]. Typical values of equivalent frontal flat plate area for helicopters normally range from 5 ft² to about 60 ft² [Prouty, 1986]. Flight tests have shown that the AH-1G, fully loaded with air-to-ground rocket pods, has an equivalent flat plate area of 19.3 ft², [Wood, 1971]. The expression for total fuselage parasite drag used in the DTURN5 model is,

$$hp_f = \frac{D_f V}{550} = \frac{f_p V^3}{1100} \quad (20)$$

4.1.4 Compressibility and Stall Effects

The induced and profile power required equations derived above do not take into account those losses incurred as a result of wave drag on the advancing side of the rotor disk at high forward speeds or those losses incurred as a result of retreating blade stall. Retreating blade stall, which occurs at high forward airspeeds and/or high thrust coefficients, is not addressed here since the maneuver controller routine of DTURN5 will not allow the rotor to enter into deep rotor stall. Subsequently, the power required to compensate for any stall losses is assumed to be

zero. The maneuver controller, however, does not account for compressibility losses and an empirical relationship arrived at by Wood through an examination of relevant AH-1G flight test data was used to model these losses. It is believed, however, that the DTURN5 program never referred to this part of the power required routine because high airspeeds at which these effects occur were not investigated. For both completeness sake and added versatility of DTURN5, the empirical correction was nevertheless allowed to remain in the power required subroutine. According to Wood, the AH-1G empirical correction for compressibility is,

$$hp_c = \frac{\rho A (QR)^3}{550} \Delta M^3 (0.0033 - \Delta M (0.022 - 0.11 \Delta M)) \quad (21)$$

where ΔM is defined as follows,

$$\Delta M = \frac{QR(1+\mu)}{V_s} - M_{cr} + 0.75 t_c \quad (22)$$

where the first term of equation (22) is the tip Mach number of the advancing blade, V_s (in the same expression) is the

speed of sound at that particular "point-in-the-sky", M_{cr} is the critical Mach number above which wave drag divergence of the rotor blade occurs, and the other variables are as defined before. M_{cr} is usually determined from flight test or wind tunnel test results. In practice, if the tip Mach number is above the critical or divergence Mach number, equation (21) will predict the horsepower required to overcome these effects. On the other hand, if the rotor blade tip Mach number on the advancing side is less than the critical Mach number, ΔM will be zero and equation (21) would predict zero power required for compressibility effects, [Wood, 1971].

4.1.5 Total Power Required

As mentioned previously, the total power required for level or maneuvering flight is the sum of the power required to overcome the individual contributors to rotor and airframe drag. When the various components of power required are summed together over the helicopter's airspeed range, a power polar, similar to Figure 5, may be constructed. A more useful form of the power polar is obtained by overlaying

power available engine data as a function of airspeed since the difference between power available and power required indicates the amount of excess power available for maneuvering. Figure 5 indicates that both hover and high speed forward flight place the heaviest power demands on the engines. The bucket speed is defined as the airspeed for which power required is a minimum and it is particularly important to the present research since it is the region of maximum maneuverability and the greatest excess power. The recent U.S. Army air-to-air combat flight testing emphasized that helicopter pilots will either accelerate or decelerate to the power bucket speed, which is usually 60-80 knots, in order to use the power advantage to out-turn, out-maneuver, or out-climb their opponent. According to Wolfrom, "the aircraft with the lowest bucket speed or the best deceleration capabilities has an advantage in that it can force its opponent below its bucket speed, where it will require more power, and therefore will have less excess power to use for maneuvering", [Wolfrom, 1986]. In other words, the aircraft with the lower bucket speed forces the opponent or adversary to fight and maneuver on the "backside" of its power curve where its maneuvering or load factor capabilities are slightly degraded. If the adversary were to fly at its bucket speed for maximum maneuvering capability, the slower aircraft can offset the faster aircraft's speed advantage by

out-turning the adversary during the maneuver.

One final and extremely interesting observation can be made with regard to the helicopter's specific excess power and that is the unique form of the P_s plots which arise for helicopters which use variable rotor speed control. Traditional P_s plots are functions of both altitude and airspeed, regardless of whether the aircraft is a helicopter or fixed-wing, high performance jet fighter. However, it is interesting to note that helicopters using variable rotor speed control extend the domain of the specific excess power plots into a third dimension, that is, P_s plots become 3-dimensional surfaces that are functions of altitude, airspeed, and rotor speed. (Imagine the AH-1G P_s plots given for different rotor speeds in Figures 6, 7, and 8, as being one graph with three orthogonal axes, defined as airspeed, altitude, and rotor speed). Although this brings up several very interesting questions with regards to calculating optimal flight trajectories, the current research makes the simplifying assumption of constant altitude flight in the horizontal plane. The problem addressed therefore reverts back to a consideration of the 2-dimensional P_s plot, only now the problem is a function of airspeed and rotor speed rather than the more traditional airspeed and altitude.

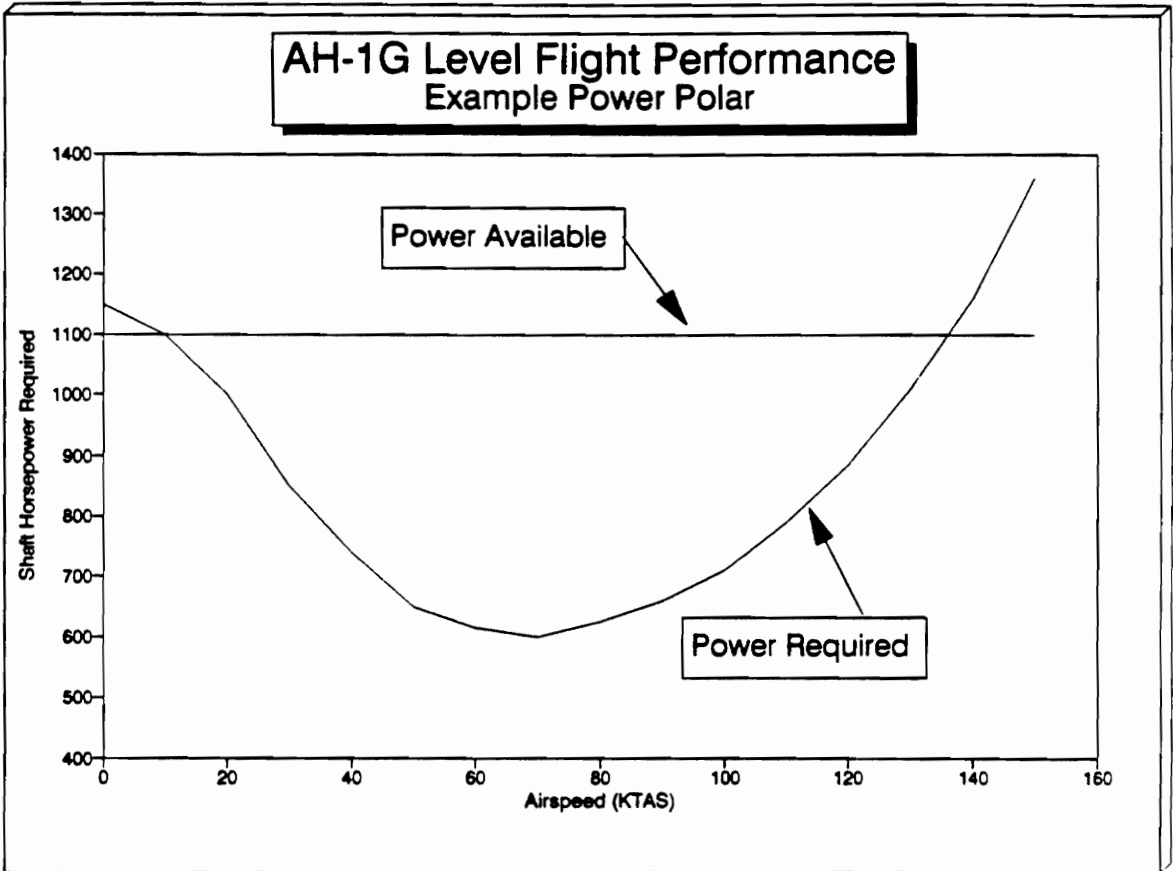


Figure 5
Power Polar, "Hot/High Day"

**Specific Excess Power
AH-1G Attack Helicopter - 90% RPM**

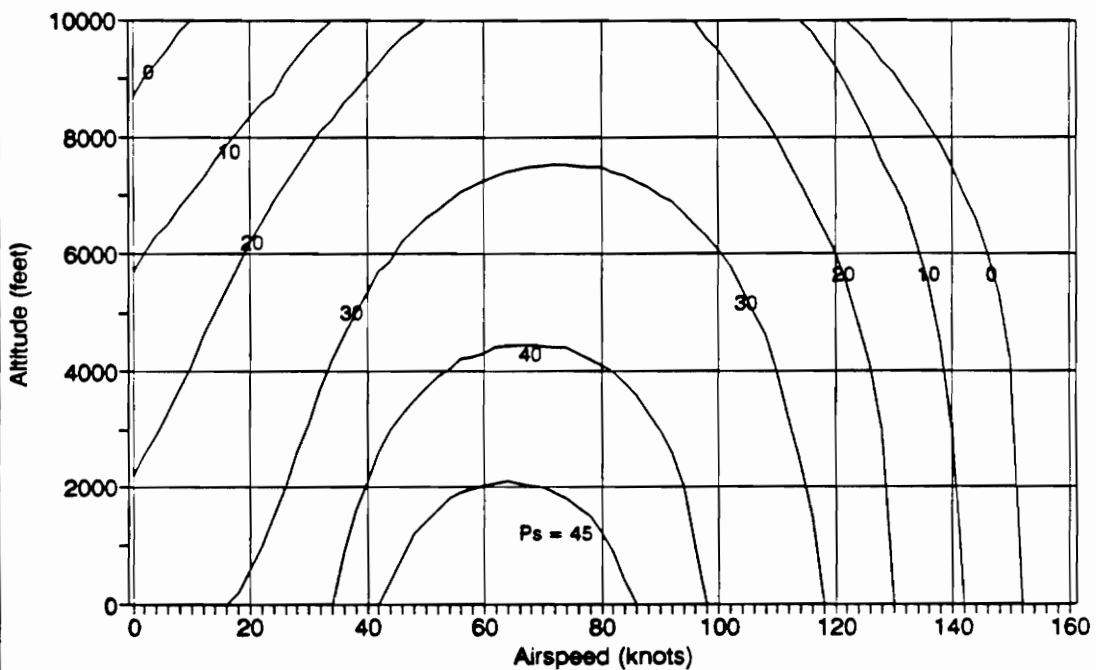


Figure 6

AH-1G Specific Excess Power - 90% RPM

**Specific Excess Power
AH-1G Attack Helicopter - 100% RPM**

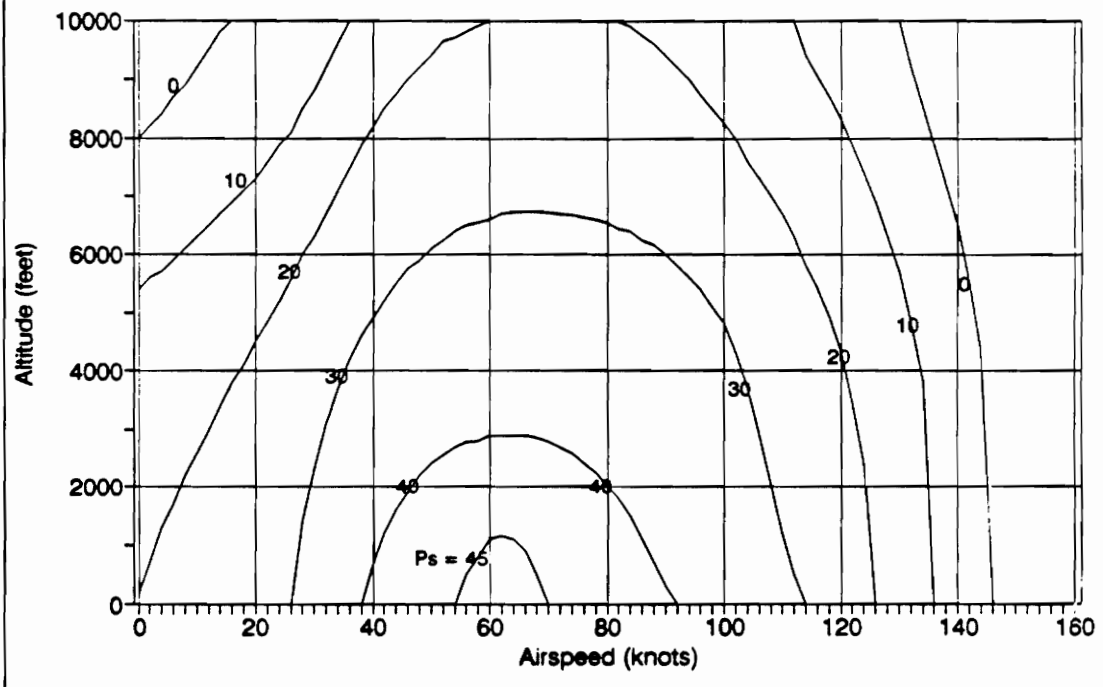


Figure 7

AH-1G Specific Excess Power - 100% RPM

**Specific Excess Power
AH-1G Attack Helicopter - 120% RPM**

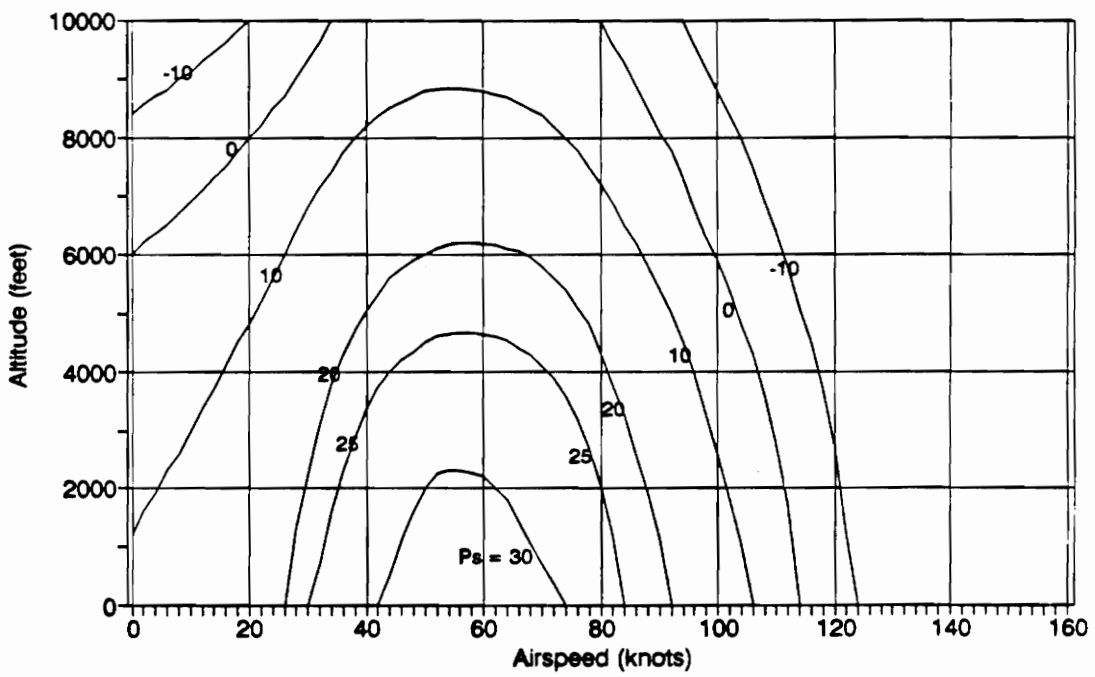


Figure 8

AH-1G Specific Excess Power - 120% RPM

4.2 AH-1G Power Available Model

The DTURN5 program uses a power available model derived from flight test data of the AH-1G Lycoming T53-L-13 gas turbine engine. A copy of the original flight test data is reproduced in Figure 9, [Finnestead et al, 1970]. Clearly, the horsepower available is a function of both altitude and outside air temperature, with horsepower varying inversely with these two parameters. Unfortunately, however, the AH-1G is transmission limited, which means that the torque limit of the main rotor transmission limits power output to the rotor at the high end of the power spectrum. As shown in Figure 9, this limit corresponds to the equivalent of 1100 engine shaft horsepower, (ESHP). As the AH-1G matured in later years, however, Bell Helicopter eventually increased the transmission limit to 1135 ESHP even though the rest of the horsepower data remained unchanged. It is this higher limit which is used in the present study, [Wood and Waak, 1976]. The 1135 ESHP corresponds to 100% military limit shaft horsepower at an altitude of 2400 feet, the altitude assumed as a constant in the DTURN5 model.

FIGURE NO. 114
 MILITARY LIMIT SHAFT HORSEPOWER AVAILABLE

AH-1G T53-L-13

HOVERING

- NOTES: 1. ENGINE PARTICLE SEPARATOR INSTALLED
 2. DATA BASED ON LYCOMING T53-L-13 ENGINE
 MODEL SPECIFICATION NO. 104-33
 3. ENGINE INLET CHARACTERISTICS BASED ON
 FIGURE 113 APP. VII
 4. GENERATOR ELECTRICAL LOAD = ZERO
 5. PERCENT AIR BLEED (W_{B1}/W_{B2}) = 0.67%
 6. ENGINE OIL COOLER DRIVEN BY ENGINE BLEED AIR
 7. ROTOR SPEED = 324 RPM

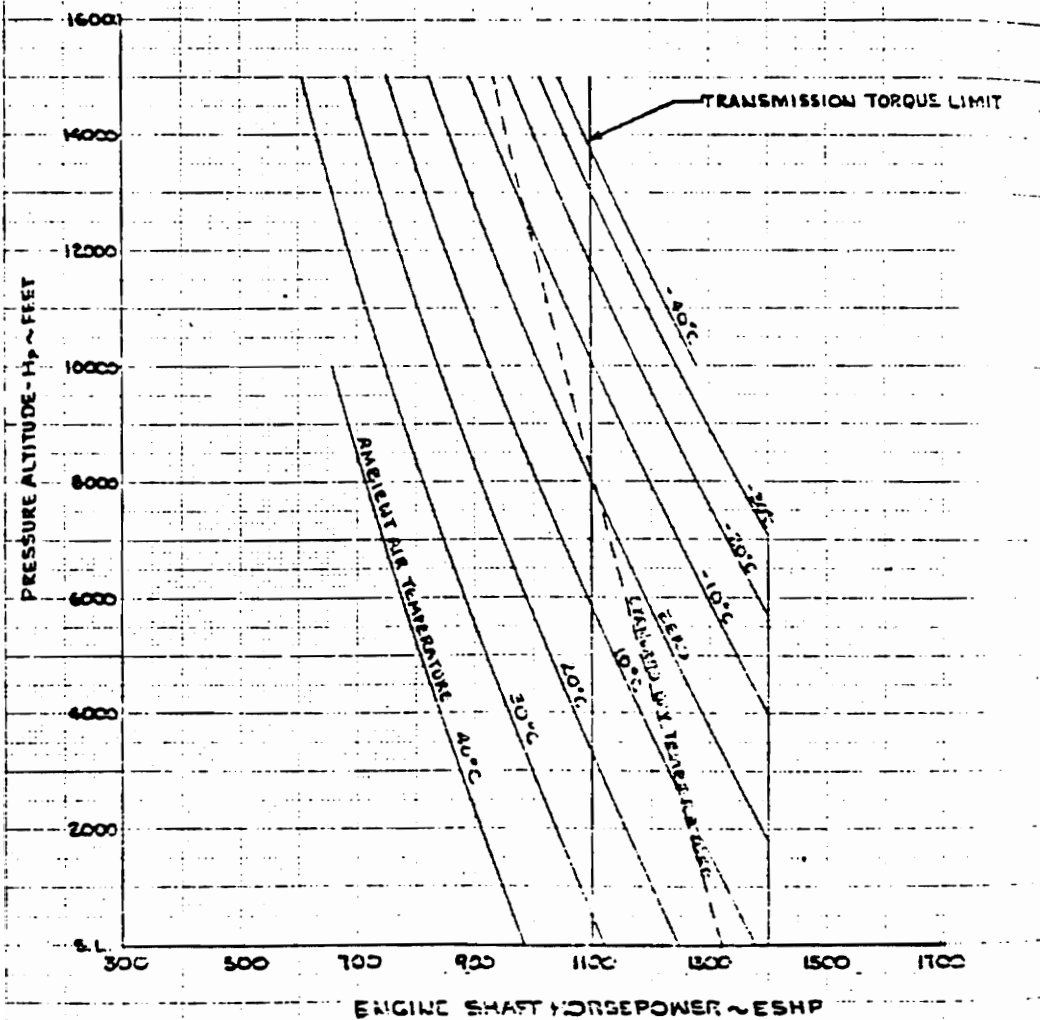


Figure 9

AH-1G Power Available - Flight Test Data
 (Finnestad et al, 1970)

4.3 Point-Mass Simulation Model

Hale notes that there are two "basic and fundamental modes of aircraft behavior", the translational mode, in which the aircraft is treated as a point mass with three translational degrees of freedom, and the rotational mode in which the aircraft acquires three additional degrees of freedom by considering angular motion about three mutually orthogonal axes whose origin is located at the aircraft center of gravity, [Hale, 1984]. In general, most performance books treat the aircraft as a point-mass body whose behavior may be described using only the three force equations of motion; the three moment equations are only needed or introduced if the problem must consider rigid body rotation -- classic stability and control problems, for instance, require these additional degrees of freedom.

The equations of motion (written in wind axes) and kinematic relationships for turning, accelerated flight in the horizontal plane only (i.e., constant altitude) are defined as follows, [Hale, 1984; Johnson, 1980],

$$\frac{W}{g} \frac{dV}{dt} = -H - W(\cos\alpha_{HP})\theta \quad (23)$$

$$T\sin\phi - \frac{W}{g} V\dot{X} = 0 \quad (24)$$

$$T\cos\phi - W = 0 \quad (25)$$

$$\frac{dX}{dt} = \dot{X} = V\cos X \quad (26)$$

$$\frac{dY}{dt} = \dot{Y} = V\sin X \quad (27)$$

where T is the rotor thrust, α_{HP} is the angle the rotor tip path plane makes with respect to an earth-fixed horizontal plane, θ is the fuselage body pitch attitude, ϕ is the fuselage body roll attitude, \dot{X} is the turn rate, X is the heading angle, V is the velocity vector along the tangential axis (x-wind axis), W is the aircraft weight, H is the H-force (defined as the rotor drag in the plane of the rotor), and X and Y are ground (earth-fixed) track coordinates of the aircraft flight path during the turn.

Equation (23) above is not in a convenient form for use in the DTURN5 model since the tip path plane angle is difficult to calculate without a full six degree of freedom (DOF) model, i.e., one using both force and moment equations of motion. This equation is necessary, however, since it contains the time rate of change of velocity needed for the problem's solution. Alternately, equation (7), derived in an earlier section, may be used to determine the helicopter acceleration or deceleration. This form is more convenient since acceleration/deceleration may be solved in terms of specific excess power, rotor speed, gross weight, rotor disk inertia, and altitude -- all known or easily obtained variables. Assuming constant altitude, (i.e., $dh/dt = 0$),

Equation (7) can be rearranged as follows,

$$\frac{dV}{dt} = \dot{V} = \frac{g}{V} \left(P_s - \frac{I_b \Omega}{W} \frac{d\Omega}{dt} \right) \quad (28)$$

In a maximum performance turn in which power required demands are greater than engine power available from the helicopters engines, P_s will be negative. If the turn places severe demands on power required, the negative P_s term will dominate equation (28) and the helicopter will decelerate at a rate commensurate with the negative magnitude of equation (28).

During an accelerating or decelerating turn, turn radius, turn rate, and heading angle are constantly changing with time. Turn rate can be obtained in a convenient form by dividing equation (24) by equation (25). The result of that operation, after simplification, yields,

$$\frac{dX}{dt} = \dot{X} = \frac{g \tan \phi}{V} = \frac{g \sqrt{(N_z^2 - 1)}}{V} \quad (29)$$

where \dot{X} is expressed in radians per second. Furthermore, since airspeed is really the tangential velocity along the curved flight path, turn radius is also easily found;

$$R = \frac{V}{\dot{X}} = \frac{V^2}{g \tan \phi} = \frac{V^2}{g \sqrt{(N_z^2 - 1)}} \quad (30)$$

following substitution of equation (29) for \dot{X} in equation (30), [Hale, 1986]. The DTURNS5 program, therefore uses equations (26), (27), (28), (29), and (30) to model a maximum performance decelerating turn. Here, the state variables are X , Y , V , and \dot{X} , and the control variables are load factor, N_z , and rotor speed, Ω . Because a full 6-DOF model is not used, pilot controls are assumed to vary instantaneously with time. This is a good assumption provided that aircraft responses to pilot inputs are assumed to happen much more rapidly than the changes that occur in aircraft state variables. In other words, pilot controls are assumed to be "fast" variables and aircraft state variables considered to be "slow" variables.

The equations above are integrated within the DTURN5 model to obtain the aircraft state variables as a function of time. This is accomplished using a simple fourth-order Runge-Kutta integration scheme, [Maron, 1982]. Because of the way round-off error is handled, the Runge-Kutta integrator used in the model is generally more accurate than the modified Euler method used by Wood in his research. Comparison of the DTURN5 results with AH-1G flight test data using initial conditions found in Wood's report indicates good correlation.

5.0 THE OPTIMAL CONTROL PROBLEM

5.1 Introduction and Approach

The ideal optimum rotor speed control problem would be one that attempts to optimize a specific cost function given not only rotor speed control, but maneuvering load factor as well, since both are controls to the problem defined earlier. Ideally this would involve optimizing the type of rotor control (i.e., allowing the computer program to prescribe a family or type of control algorithms), the parameters that govern the control law's shape, and the maneuvering load factor, $N_z(t)$, to the extent that the maneuver is truly optimized. This particular problem, however, is extremely complex and the present research instead focuses on parameterization of the rotor speed controls, rather than the classical control optimization problem described above. This is accomplished by selecting several families of rotor speed control laws, *a priori*, and allowing the computer program to optimize the parameters governing the shape and character of each control such that some pre-defined cost function is minimized. It should be recognized, however, that while the solution to the parameterization problem is ideal for the rotor speed control laws defined here, it does not mean that

the family of rotor speed control laws chosen for this problem are ideal themselves - choosing the optimum control law from an infinite number of solutions remains in the domain of a classical optimal control problem.

Although parameterization of the rotor speed controls greatly simplifies the problem, the problem nevertheless remains fairly complex because of the second control, maneuvering load factor. Rather than attempting to optimize both rotor speed control parameters and maneuvering load factor, the latter control is assumed to be a prescribed function of airspeed (this is described in a later section). With this assumption, the problem reverts to an easily solved parameter optimization of one control, rather than the more complex problem involving two controls.

Because the parameterization problem requires that the control law be assumed *a priori*, the problem addressed by this research was broken down into three chronological steps in order to narrow down the almost infinite number of control laws that could be considered. The first step involved using the IBM PC-based DTURN5 program to investigate the merits of several families of control laws relative to their effects on time-to-turn 180 degrees (along with other measures of effectiveness described in the following two sections). This

initial step was not meant to be an attempt at optimization, but instead was used as a guide for the next two steps, providing a general indication of which rotor speed control laws would most likely work in decelerating the helicopter quickly. Several families of rotor speed control laws were found to work well, and variants of these were used in the remainder of the study.

The last two steps involved the actual parameterization of the chosen rotor speed control laws using the mainframe-based DT5-DNCONF optimization computer code. The first of the last two steps investigated rotor control laws as a function of airspeed while the last step investigated control laws as functions of heading angle. Since the DT5-DNCONF computer runs did not supply maneuver time histories, successful control laws were re-run on DTURN5 to provide both rotor speed control law and maneuver time histories.

5.2 DTURN5 Rotor Speed Control Laws

Rotor speed control law families considered for the initial DTURN5 problem are illustrated in Figures 10 through 16. The control laws are defined by the type and sequence of sub-functions considered (i.e., ramped or constant functions relating rotor speed to airspeed) and the placement of the airspeed "breakpoints" relative to the minimum and maximum rotor speed constraints. Minimum and maximum rotor speed limits were arbitrarily set at 90% and 120% of the nominal rotor speed (324 RPM at 100%), respectively, although maximum rotor speed breakpoints at 105% and 110% were also investigated. The following rotor speed control parameters were varied in order to investigate their effects on the helicopter's performance;

- (1) Breakpoint velocity
- (2) Breakpoint rotor speed
- (3) Number of breakpoints
- (4) Slopes of rotor speed sub-functions
(i.e., whether constant or ramped)
- (5) Pilot-commanded power level

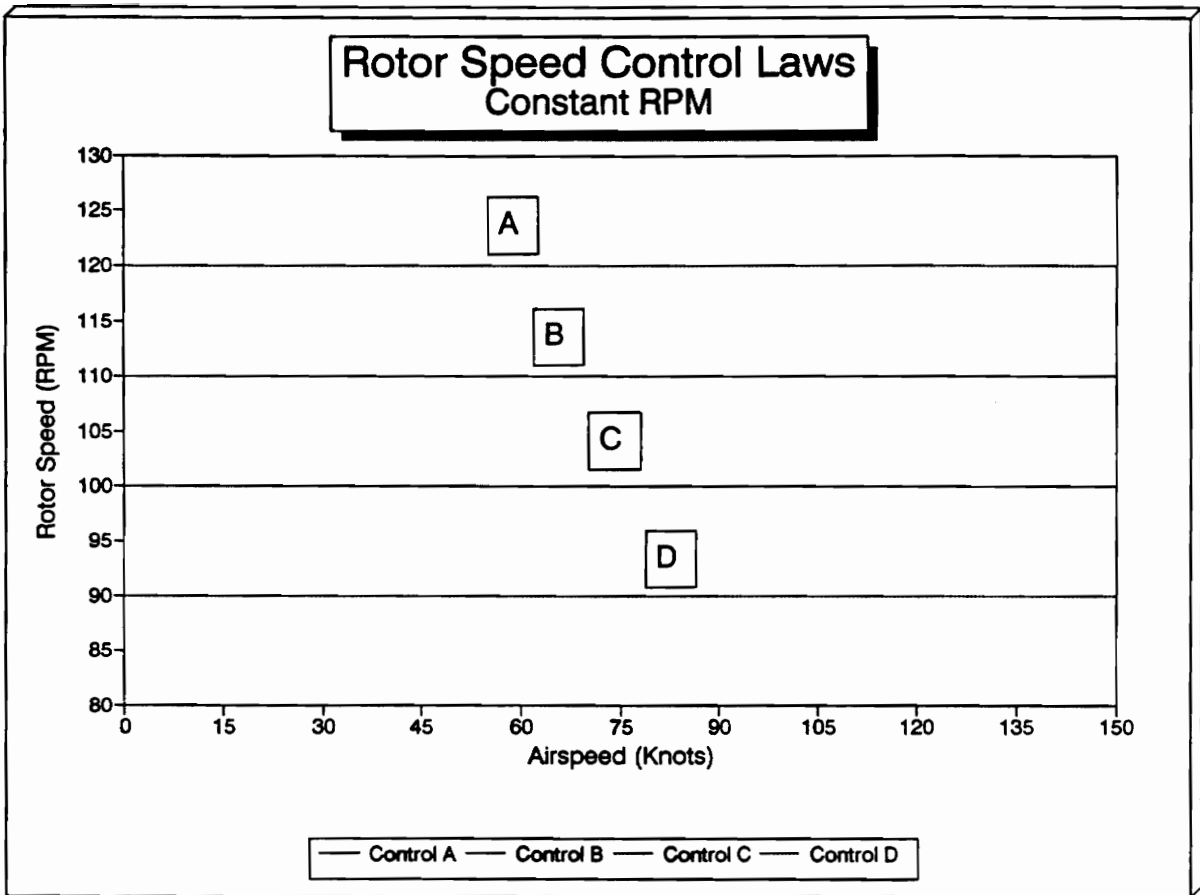


Figure 10
Proposed Rotor Speed Control Laws

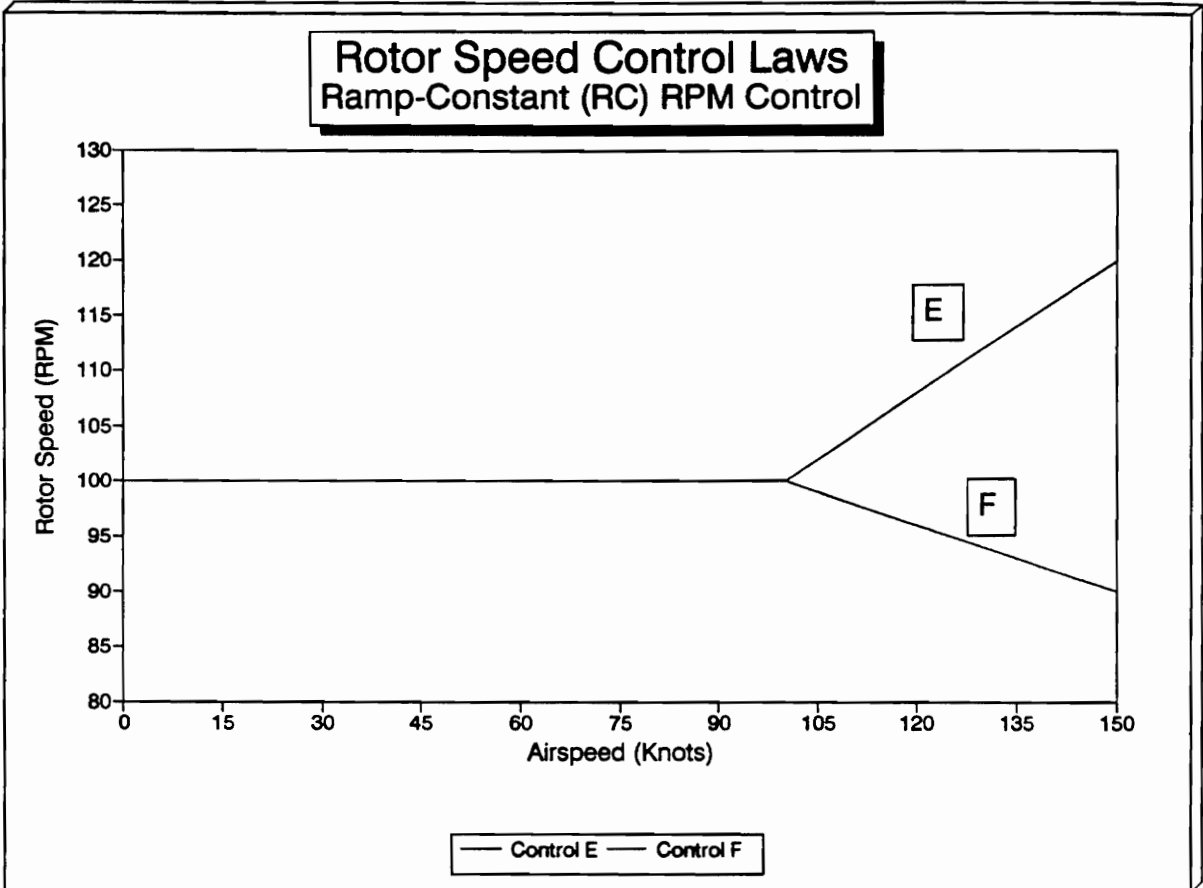


Figure 11
Proposed Rotor Speed Control Laws (continued)

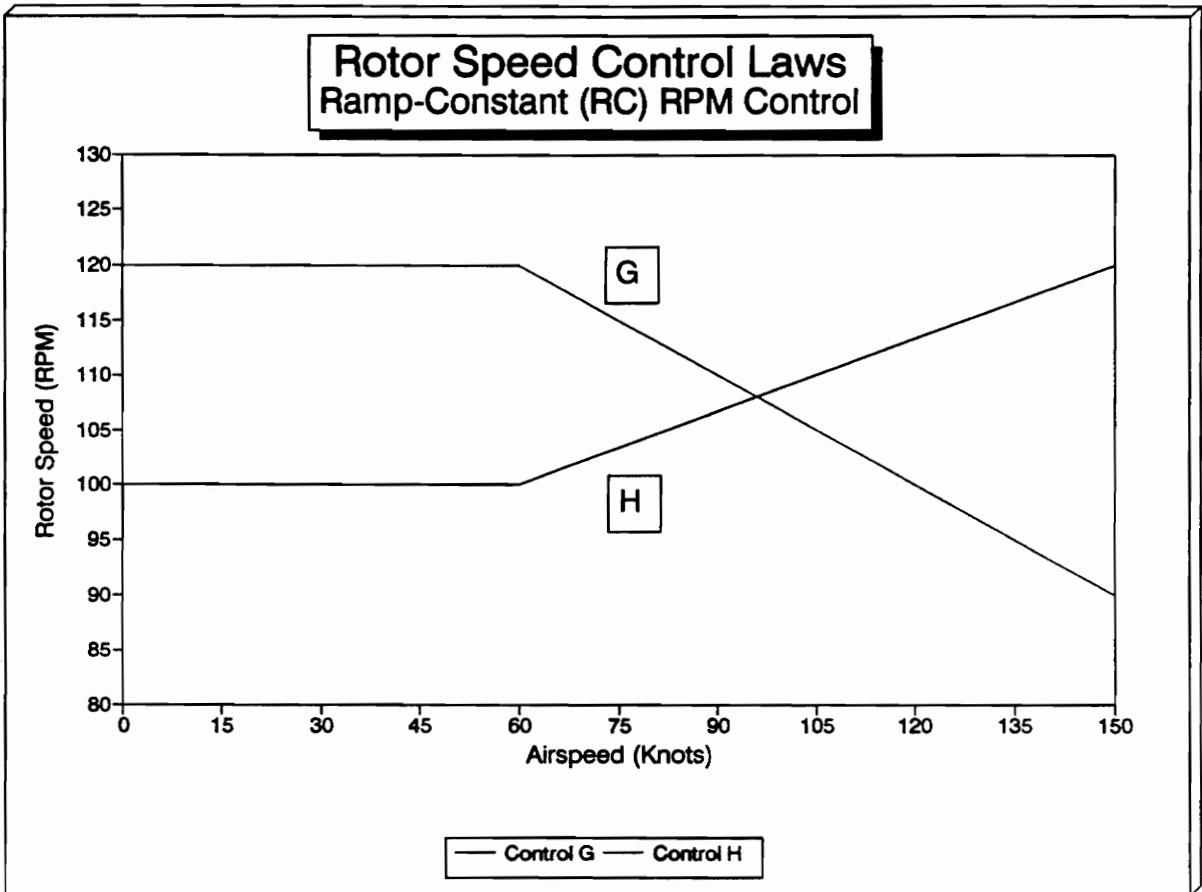


Figure 12
Proposed Rotor Speed Control Laws (continued)

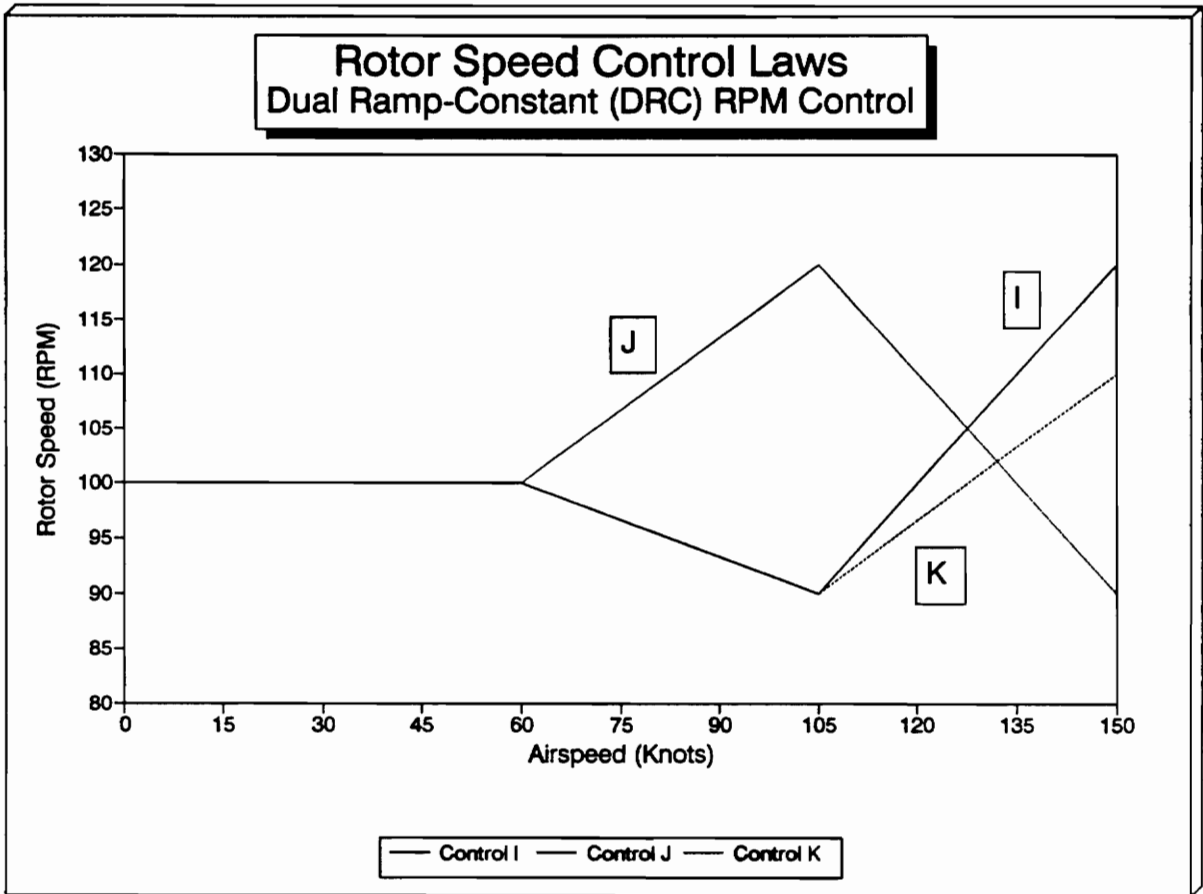


Figure 13

Proposed Rotor Speed Control Laws (continued)

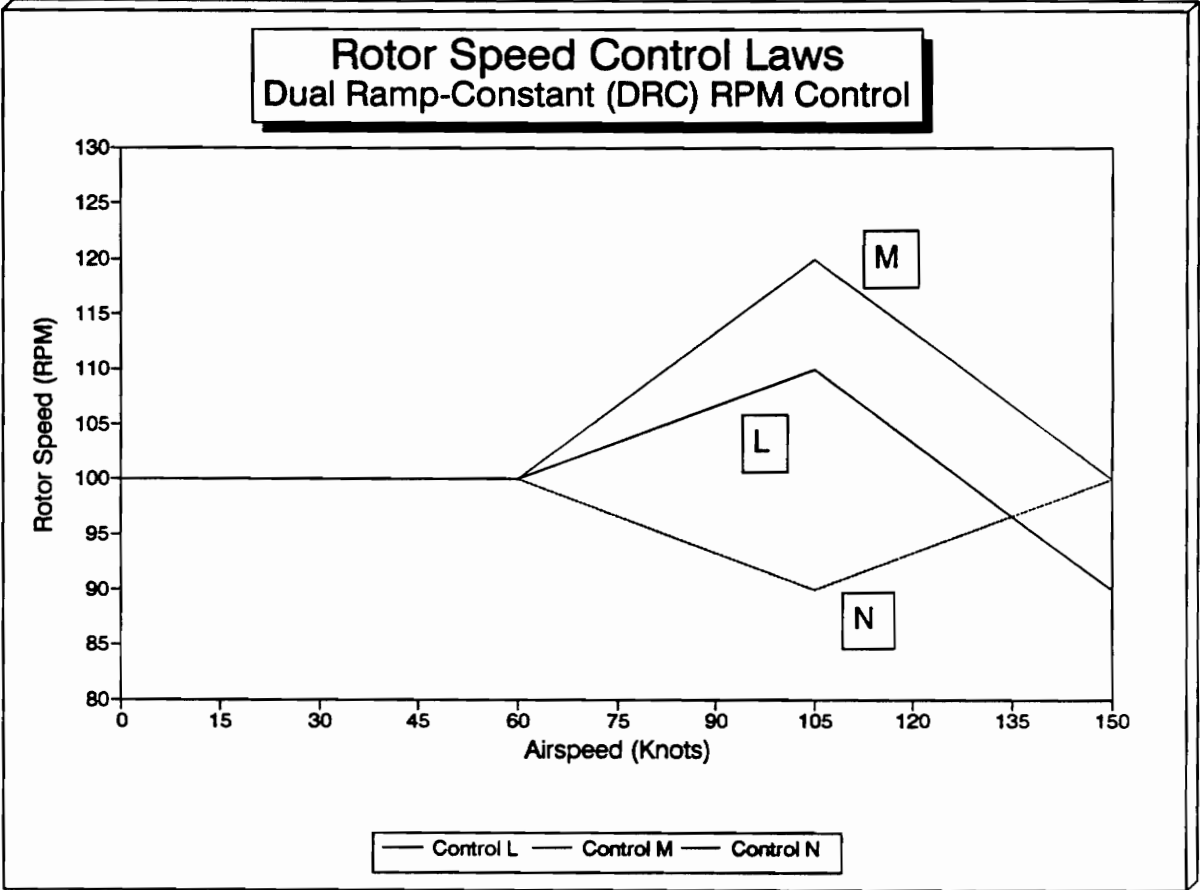


Figure 14
Proposed Rotor Speed Control Laws (continued)

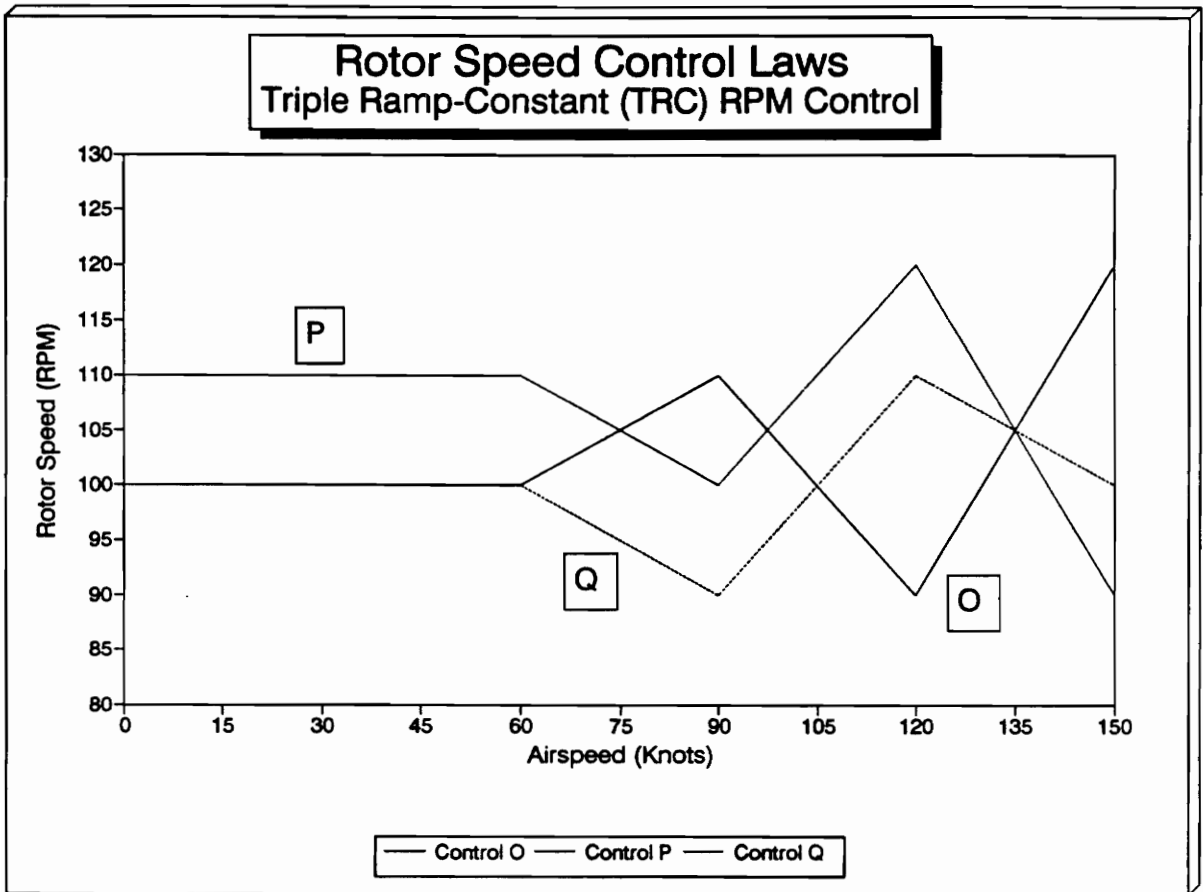


Figure 15

Proposed Rotor Speed Control Laws (continued)

Rotor Speed Control Laws
Triple Ramp-Constant (TRC) RPM Control

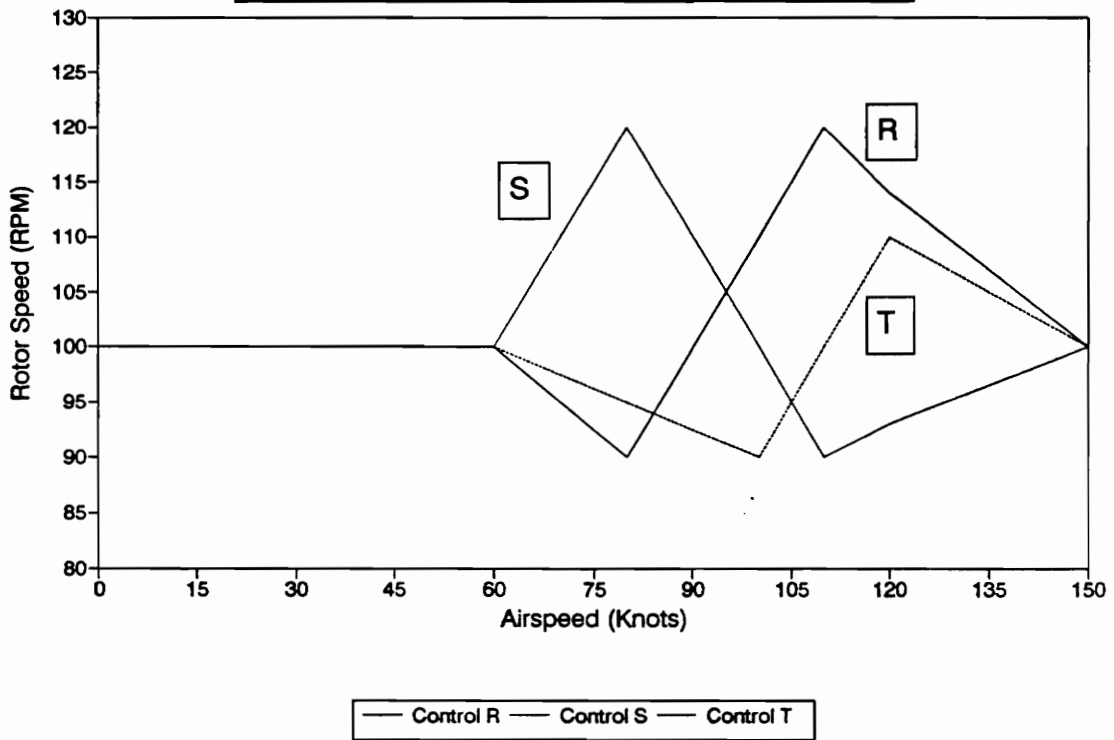


Figure 16

Proposed Rotor Speed Control Laws (continued)

Since the difference between power available and power required determines the magnitude and sign of excess power and hence deceleration time, four pilot-commanded power levels were considered. The power levels were expressed as percentages of the AH-1G main rotor transmission limit, typically 10%, 25%, 50%, and 75% of 1135 ESHP, (114, 284, 568, and 851 ESHP, respectively). In general, it was expected that an increase in the pilot-commanded power level would theoretically increase time to turn, although this was not always the case, as explained in a later section. The number and location of breakpoints, on the other hand, determined the type of rotor speed control, and in the DTURN5 model, these could be varied to tailor the particular control law of interest. The number of control laws (20) and power levels (4) resulted in a fairly large test matrix, but this was reduced somewhat, however, as preliminary results indicated that control laws that began by allowing rotor speed to decay were ineffective in their ability to slow the helicopter throughout the turn; these control laws were rejected.

5.3 DT5-DNCONF Parameterization

The rotor speed control laws used in DT5 were similar to the ones studied on the IBM PC-based DTURN5, except that placement of the breakpoints for the rotor speed controller were now parameters to be selected by the DNCONF optimization routine. Figure 17 presents the basic control law chosen for the parameterization study. The breakpoints, numbered 1 through 6, were constrained arbitrarily in the vertical (rotor speed) direction but were allowed to move horizontally (in the velocity direction), resulting in a single movement degree of freedom. Once the accuracy and consistency of DT5 was validated using previous DTURN5 data for the same initial conditions, the DT5 program was used exclusively since its speed advantage allowed a far greater number of control law parameters to be investigated.

The measures of effectiveness used in this investigation were similar to those proposed by Woods in 1985, [Woods, 1985]. It was mentioned earlier in the literature review that the Naval Air Development Center (NADC) sought to increase the versatility of the AH-1 Tactical Manual by including ground tracks of various helicopters performing maximum performance decelerating turns. From a tactical

standpoint, the ground track plots are important from the viewpoint of either the ground attack or air-to-air combat mission planner. In the former, ground tracks allow a planner to estimate time-on-target, plan for ground defense nets, and estimate various survivability, vulnerability, and lethality metrics. On the other hand, the ground tracks aid air-to-air combat scenarios and tactics planning and assist in determining weaknesses in opposition maneuverability. The ground tracks for maximum performance decelerating turns are characterized primarily by the penetration or downrange distance, the cross track or lateral separation distance between turn start and end points, and the time-to-turn to complete the 180 degree maximum performance turn. Hence, these variables are used as effectiveness measures in evaluating each rotor speed control law. Two additional measures of effectiveness, the pointing margin and turn exit velocity were also considered for their relevance and importance to air combat maneuvering. The pointing margin is defined by Tamrat as "the angle between the nose of the adversary aircraft and the line of sight joining the two fighters at the instant the friendly fighter first points its nose/weapon at the adversary's aircraft", [Tamrat, 1988]. For this study, Tamrat's definition is modified somewhat; the pointing margin is defined as the angle difference between the helicopter with rotor speed control at the instant the

180 degree turn is completed and the baseline helicopter at the same instant in time. In addition, turn exit velocity is also important to a pilot in a counter-air mission. Because the helicopter's maneuvering capability is greatest at the power bucket speed, it was desired that the simulation end with the airspeed somewhere between 50 and 80 KIAS. Exiting the turn at a lower airspeed would necessitate flying on the backside of the power curve and handing a maneuvering advantage to the adversary.

Each of the measures of effectiveness were used to evaluate each DTURN5 and DT5 run, although they were redefined in a slightly different form for the DT5 optimization program. For the DT5 computer program, the measures of effectiveness were rearranged to form a cost function which the DT5 program attempted to minimize. The cost function used is defined as follows:

$$F = W_1VF + W_2TF + W_3CT + W_4OMF \quad (31)$$

where VF is the turn exit velocity, TF is the time-to-turn, CT is the turn cross track distance, and OMF is the final

rotor speed. Penetration distance was not included in the cost function because of the difficulty in retrieving this parameter from the DT5 program and the problems inherent in keeping the program "smooth", (i.e., differentiable). (Conditional statements within a trajectory calculation complicate the process of determining the gradients of the partial derivatives of the cost function). W_1 , W_2 , W_3 , and W_4 are weighting factors taken as 10, 100, 1, and 10, respectively. The weighting factors were arbitrarily chosen such that the four variables present in the cost function would have roughly the same order of magnitude. The inequality constraints defined for the problem were established as follows;

$$CT < 1000.0, \text{ ft} \quad (32)$$

$$VF > 50.0 \text{ (84.39)}, \text{ KIAS (ft/s)} \quad (33)$$

$$TF < 10, \text{ sec} \quad (34)$$

$$90 < OMF < 120, \% \text{ RPM} \quad (35)$$

Cross track distance, CT, was arbitrarily constrained to be lower than the AH-1G flight test data. The final, or turn exit, velocity was constrained to be greater than 50 KIAS so that the helicopter would exit the turn at or near its power

bucket speed for best maneuvering advantage. The total time-to-turn was restricted to values less than 10 seconds since flight test data indicated that the basic AH-1G could complete a 180 degree turn (with an entrance velocity of 150 KIAS) in a little over 10.4 seconds. Finally, rotor speed was constrained to remain between 90% and 120% of the nominal rotor speed in order to establish realistic bounds on what was considered to be attainable with rotor speed control.

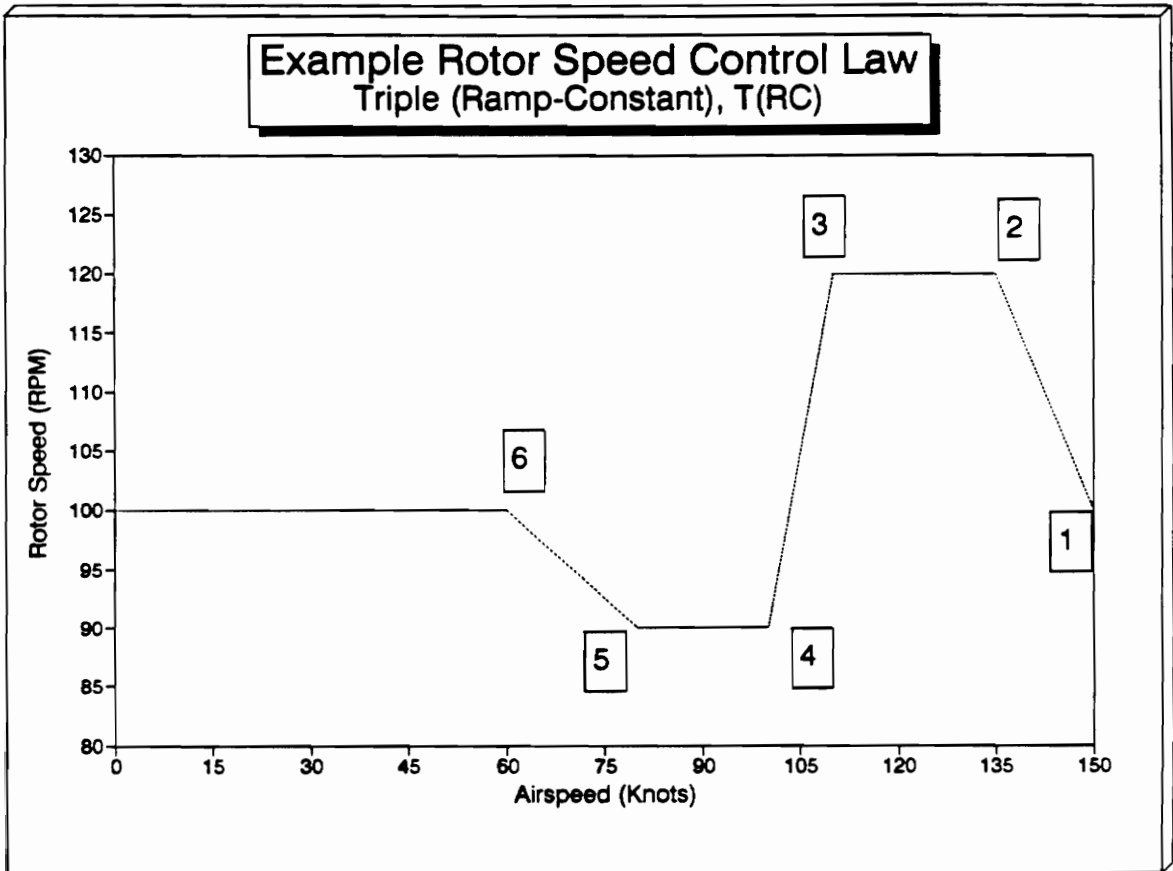


Figure 17

**Baseline Rotor Speed Control Law
Used in DT5 Parametric Optimization**

5.4 Maneuver Load Factor Control

Possibly the most difficult task in the development of the DTURN5/DT5 models was the research and verification of flight maneuver pilot control techniques, not from the stand point of technical difficulty but from the apparently contradictory information that exists with regards to AH-1G maximum maneuver capability. In essence, the maneuver controller section of the DTURN5/DT5 computer program uses a very simple flight controller to mimic, albeit indirectly, pilot control inputs in a high performance, decelerating turn. The difficulty, however, in determining the appropriate inputs lies in the difference between a fully accurate representation of pilot control with a 6-DOF model and the assumptions that must be made when using a point-mass model. But this problem can be overcome, especially since previous research has shown that a point-mass model can be used with confidence if the maximum rotor thrust capability of the helicopter is predicted accurately, [Wood et al, 1971; Woods, 1985].

In Bell Helicopter's early research of attack helicopter maneuverability and agility, the limited usefulness of the point-mass model was overcome by using a simplified analytical model to predict AH-1G maximum rotor thrust, [Wood

et al, 1971]. In this case, the maximum rotor thrust model was a simple regression analysis of data obtained from AH-1G qualification flight testing. The flight test data, however, exhibited substantial data scatter over the entire range of advance ratio's tested and the accuracy of the analytical model was subject to question, especially since comparable data acquired for other helicopters (HH-2C, CH-3C, CH-53A, and OH-6A) collapsed rather nicely to a well defined line of maximum thrust versus advance ratio. Wood attributed this discrepancy to basic differences in rotor head geometry, i.e., the teeter rotor design of the AH-1G versus the fully articulated rotor heads indigenous to the other helicopters. Nevertheless, Wood retained the rotor thrust regression model and eventually this became a standard for point-mass models used in future studies, [Woods, 1985; Wood and Waak, 1979]. Woods' model is as follows;

$$C_{T_{max}} = 0.01224 \exp^{-0.8732\mu} \quad (36)$$

where $C_{T_{\mu}}$ is defined as,

$$C_T = \frac{T}{\rho A (QR)^2} \quad (37)$$

and the advance ratio is as defined before.

Prior to Wood's research, a study of AH-1G and UH-1B maneuvering capability was published by Bell Helicopter in 1966, [Duhon, 1966]. The data presented in the report were identical to that data used by Wood in his research except that two regression lines were passed through the data rather than the one as proposed by Wood some years later. One of the regression lines passed through the upper edge of the data scatter, represented the apparent "maximum maneuver" capability of the AH-1G as limited by the onset of high vibratory loads associated with blade stall, (typical of rolling or symmetrical pullouts from diving flight). On the other hand, a line which passed roughly through the middle of the data scatter, represented "normal maneuvers" such as coordinated, sustained turns and level flight. These two lines apparently represented two different pilot techniques, with the "maximum maneuver" case representing a pure cyclic pullout (collective fixed) and the "normal maneuver" case

representing maneuvers flown mostly with collective stick inputs, (cyclic trimmed). (In reality, however, executing any maneuver requires a combination of both cyclic and collective stick inputs to maintain acceptable helicopter attitudes and rates throughout the maneuver). It seems, then, that in developing a model controller which adequately represents the maximum rotor thrust capability of the AH-1G helicopter, that the curve labeled "maximum maneuver" in Duhon's research would be the logical one to use. However, Duhon notes that

"this curve reflects the beneficial effects of rotor pitching velocity ... The pitching velocities of the rotor delay [blade] stall because the gyroscopic moments reduce the retreating blade lift. Another advantage accruing from the cyclic pullout is the increase in rotor angle of attack which reduces power required to attain a given thrust level".

This implies that maybe a full 6-DOF model would be required in order to take advantage of the added capability afforded by high aircraft pitch rates, therefore this curve does not appear to be appropriate for a simple point-mass model. Indeed, Wood's research employed a regression curve which fell somewhat between the two curves proposed by Duhon, although, possibly as a compromise, it more closely approximated the "normal maneuver" curve rather than the additional rotor thrust capability represented by the "maximum maneuver" curve.

The rotor thrust models, as proposed by Duhon, are as follows:

Maximum Maneuver Capability

$$t_{c_{\max}} = -0.508\mu + 0.4844 \quad (38)$$

Normal Maneuver Capability

$$t_{c_{\max}} = -0.531\mu + 0.40588 \quad (39)$$

where,

$$t_{c_{\max}} = \frac{2C_{T_{\max}}}{\sigma} \quad (40)$$

where σ is the rotor solidity, and t_c and C_T are two common definitions of rotor thrust coefficient as related by the

constants in equation (40), (the former is used predominantly by Bell Helicopter).

Equation (39) was chosen as the maneuver controller. Comparisons between equations (38) and (39) and the methodology proposed by Wood in 1971 indicated that equation (39) was the best compromise between the three since it agreed fairly well with flight test data, especially at the lower airspeeds where the effects of pilot technique became more pronounced.

Given the proper rotor thrust curve, calculating maximum maneuvering load factor is relatively straight forward. By definition, the maneuver load factor can be related to the rotor thrust coefficient by the following relationship,

$$N_z = \frac{t_c(1/2\rho(\Omega R)^2 b c R)}{W} \quad (41)$$

The maximum load factor which can theoretically be attained in maneuvering flight is simply found by substituting the

expression for $t_{c,max}$ into equation (41). Equation (39), therefore, gives the functional relationship between normal load factor and the helicopter airspeed through the turn. Once the normal load factor is determined, aircraft bank angle is easily determined,

$$\phi = \cos^{-1}\left(\frac{1}{N_z}\right) \quad (42)$$

Past research [Wood, 1971; Wood, 1976] has shown that maneuvering load factor is in fact a fairly complex function of aircraft attitudes and rigid body rates. However, for the point-mass simulation used in the DTURNS model, equation (42) is more than adequate, especially since the discrepancies between theory and flight test are relatively small.

6.0 RESULTS AND DISCUSSION

6.1 Power Required Model Correlation

The power required subroutine used in both the DTURN5 and DT5 models was validated using AH-1G power required flight test data for steady, level flight. The flight test data used for this validation included power required data for two extremes of the AH-1G gross weight range; light gross weight at 7500 lbs and heavy gross weight at 9500 lbs. Initial verification of the power required model, however, used only flight test data at 7500 lbs gross weight because of the difficulties associated with matching, exactly, flight test and computed power polars for both gross weights. The verification process involved determining the empirical constants (mentioned earlier in the section on simulation model development) in the power required model. These are summarized in Table II and, with a few exceptions, are very close to those derived by Wood, [Wood et al, 1971]. The biggest difference obviously occurs in the rotor efficiency factor since the DTURN5 and DT5 power required models used a less empirical expression for induced velocity derived in Prouty, [Prouty, 1986]. Because of the difference in induced power required models, slight modifications to the remainder of the constants were necessary to maintain good agreement

with flight test data. The results of the initial verification between flight test power required data and the DTURN5/DT5 power required modules are shown in Figure 18. Data is for level flight performance at sea level standard conditions with rotor speed maintained at the nominal 100% (324 RPM). As expected, agreement between the model and flight test data at 7500 lbs is very good, with only slight departures at the higher airspeeds. However, for the 9500 lb case, agreement between the model and the test data is consistently poor for much of the airspeed range, with the model over-predicting power required, except at the high airspeeds. This discrepancy was attributed to the fact that the power required model validation was only performed against low gross weight (7500 lb) flight test data. An empirical correction factor equal to the ratio between the two gross weights ($7500/9500$ for the data shown in Figures 18 and 19, but $7500/W$ for all other gross weights) was used to account for the differences associated with changes in gross weight. (The correction factor was applied only to the induced power required term. The product between the correction factor and the induced power required term resulted in the predicted induced power required for any gross weight). Although the use of this factor produced very good correlation between the model and flight test data for the gross weights considered, (see Figure 19), it is not certain why the factor works.

However, an exhaustive literature review suggests that this factor might account for differences in the rotor downwash velocities for the different helicopter gross weights. Nevertheless, this empirical factor was incorporated into the induced drag portion of the power required model and used consistently for all data runs.

TABLE II
POWER REQUIRED MODEL
EMPIRICAL CONSTANTS

<u>Constants</u>	<u>Schaefer</u>	<u>Wood</u>
Equivalent Flat Plate Area	19.33	19.50
Critical Mach Number	0.793	0.750
Blade Section Coefficients:		
Delta ₁	0.00778	0.00750
Delta ₂	0.0	0.0
Delta ₃	0.830	1.0
Rotor Efficiency Factor	0.690 (constant)	0.77 - 1.0 (variable)

6.2 Point-Mass Model Validation

Figures 20 and 21 are taken from data published by Wood comparing actual flight test data with data derived from a point-mass model of the AH-1G developed by Wood, [Wood and Wells, 1972]. Figure 20 is a ground track plot of AH-1G flight test data for a maximum performance decelerating turn initiated at 150 KIAS. Figure 21 is also a ground track plot for the AH-1G performing the same maneuver (same initial conditions), except that data is calculated by Wood. Although he does not give a technical justification for doing so, Wood's model makes two assumptions relative to the AH-1G's behavior during tight decelerating turns: that power available is zero during the maneuver, and that rotor overspeed occurs due to the high rotor inflow velocities characteristic of maximum performance turns. To compensate for the latter assumption, Wood reduced (arbitrarily) specific excess power by 20% in the point-mass model he used for his research, [Wood and Livingston, 1971]. In contrast to Wood's assumption, discussions with several U.S. Marine Corps AH-1 helicopter pilots indicate that their goal is to maintain nearly constant rotor speed at approximately 25 - 50% power level throughout the duration of the turn. (Again, Wood makes no mention of the pilot technique used to produce the flight test data in his research, so it was assumed that the pilot technique was

identical to that discussed above).

Wood's point-mass model of the AH-1G generally over-estimates the helicopter flight trajectory except at the terminal area of the maneuver where his model predicts tighter turn radii than exist for the flight test data. Figures 22, 23, and 24 show the maneuver time history and ground track of the AH-1G calculated by DTURN5 using Wood's assumptions for excess power required mentioned above. Unfortunately, when compared against flight test data, Figure 24 indicates that penetration distance is under-estimated by 8% while cross track distance is over-predicted by nearly 20%. Since it was believed that this error existed due to Wood's assumptions regarding rotor overspeed during tight turns, a new run of DTURN5 was made using the pilot technique described to the author by the U.S. Marine Corps pilots (i.e., rotor speed held constant at 100% and power level set at 50%). Unfortunately, the results showed only a slight improvement when contrasted with the flight test data. Although predicted penetration distance remained unchanged at 8 - 9% lower than flight test data, predicted cross track distance still remained higher, but at 15% vice the 20% obtained using Wood's methodology. The discrepancies are difficult to resolve, but it is most likely that, given the difficulties in establishing proper maneuver control techniques and the inaccuracies inherent in

any point-mass model, that these may be the cause of the disparities between test and model data. The DTURN5 model nevertheless was adopted as representative and the evaluation of the rotor speed control laws continued using Wood's methodology as a baseline for maneuver comparisons.

6.3 Sub-Optimal Control Laws and Data Presentation

Table III presents a maneuver summary of several rotor speed control laws considered to be optimum with regards to enhancing one or more of the measures of effectiveness discussed earlier. The maneuver summary does, however, contain rotor speed control laws which do not satisfy all the constraints established for the problem considered here, but they were nevertheless included to illustrate several peculiarities discovered during the course of the research. In addition, two baseline runs are included that present the results of the two data runs discussed in the last section. Only one of these, that based on Wood's methodology, is used as the baseline for data comparison, as this methodology has been fairly standard for data comparisons in past research.

Each rotor speed control law presented in Table III represents the optimum rotor control law for that particular family. Although each of the sub-optimal control laws minimizes the cost function and satisfies the constraints placed on the problem, maneuver time histories indicate that different rotor speed control laws augment different measures of effectiveness (if taken separately rather than combining into a single cost function), indicating that rotor speed control laws ideal for the air combat mission may be different from those required for the ground attack mission. For example, a rotor speed control algorithm could be chosen such that turn penetration and cross track distances were minimized and exit speed maximized, but at the expense of minimum time-to-turn. The opposite was also true, that is that time-to-turn could be driven down, but at the expense of turn exit airspeed and, sometimes, penetration and cross track distances.

The results of the DT5 data runs indicated that both the rotor speed control law parameters and the pilot-commanded power levels had profound effects on the outcome of each maneuver. In general, increasing the power level for the maneuver increased all but one (pointing margin, which decreased) of the measures of effectiveness, leading to larger

ground track radii, increased time-to-turn, and increased velocity at the turn exit. Increasing peak rotor speed (110%, 115%, or 120%), on the other hand, decreased time-to-turn, turn radius, and exit velocity, but increased pointing margin. The velocity "breakpoints" also had an effect on the outcome of the maneuver -- the longer the rotor speed remained above the nominal rotor speed, the quicker the time to turn and the lower the exit velocity and turn radii.

The ramp-constant-double ramp (RCDR) type of control algorithm seemed ideally suited to optimizing, separately, each measure of effectiveness. (This rotor speed control law is not illustrated in Figures 10 - 16 since this control was a result of searches performed by DT5. The time histories of these rotor speed control laws are given in the figures noted below). Of the maneuvers listed in Table III, the RCDR control law, characterized by high rotor speed, high power, and widely spaced velocity breakpoints, seemed especially suited to decreasing turn penetration distance and maximizing turn exit velocities. Using the RCDR control with a maximum rotor speed of 115%, 851 ESHP (power level 4), and velocity breakpoints at 140, 100, and 80 KIAS, the AH-1G was capable of exiting the turn at 69.7 KIAS, the highest exit airspeed measured. The maneuver time histories and ground tracks are illustrated in Figures 25, 26, and 27. Referencing the

maneuver time histories, the AH-1G began the decelerating turn at 150 KIAS, wings level ($N_z = 1.0$), at zero penetration distance, cross track distance, and heading angle. As the helicopter decelerates, the RCDR control rapidly (in less than 0.6 seconds) advances rotor speed until it reaches the peak rotor speed at 140 KIAS. Rotor speed remains at a constant 115% for approximately 2 seconds, then begins to decline to 90%, reaching this point at 80 KIAS. For the terminal phase of the maneuver, the rotor speed again increases, not quite making 100% upon completion of the maneuver. Normal load factor rises very quickly at the beginning of the maneuver, reaching a peak of 2.7 g's about 30% through the turn. As rotor speed decreases, rotor thrust capability decreases also and this is reflected in the load factor time history. At the terminal phase (> 6.5 seconds), however, load factor begins to build once more, reaching 2.0 g's at maneuver termination. The specific excess power time history is nearly a mirror image of the load factor trace and reflects its dependence on power required and hence rotor thrust. The negative value of P_s reflects the dominance of horsepower required over horsepower available, hence the deceleration of the AH-1G helicopter. Both the negative value of P_s and its relationship to the load factor trace is consistent for all rotor control laws investigated. As the load factor builds

during the first third of this maneuver, the aircraft decelerates rapidly, and non-linearly, until rotor speed begins to fall at a constant rate after 2.5 seconds, where airspeed decay decreases linearly until the last second of the maneuver. (It should be kept in mind that the rotor speed algorithm is really controlling the nature of the rotor thrust time history -- the pilot can only command the maximum rotor thrust level based on the instantaneous velocity and blade thrust coefficient allowable at each particular point in time. It is interesting to note here, however, that while the maximum thrust coefficient increases linearly (see equations (38) and (39)) with decreasing airspeed (it is a function of blade characteristics and rotor geometry), the load factor during the maneuver varies in a highly non-linear fashion. Again, this is the direct result of the time varying rotor speed). It is also interesting to note that while the RCDR control law decreases time-to-turn by only 2 seconds (a 22% reduction over the baseline, but nearly a full second longer than the best control algorithm tested), the penetration distance was nearly halved over the baseline and represented the best improvement.

The best, or minimum, time-to-turn could be achieved using a different rotor speed control law, ramped-constant-ramped (RCR), also optimized by DT5, (see Figures 28, 29, and

30). Using a power corresponding to 851 ESHP with velocity breakpoints at 140 and 100 KIAS, the time needed to execute a complete 180 degree turn was only 7.2 seconds. This represents a 31% improvement over the baseline rotor speed control. Inspection of the time history for this maneuver shows rotor speed and load factor increasing rapidly for the first second of the maneuver followed by 3 seconds at a constant 110% RPM. During the constant rotor speed portion of the maneuver, load factor increases linearly toward its peak value of about 2.5 g's then declines gradually until the terminal portion of the maneuver when this parameter again begins to rise. Airspeed decreases fairly constantly for the entire maneuver. Of the maneuvers that met all the maneuver constraints, this particular rotor speed control algorithm produced the best cross track or lateral distance at 690.6 ft.

The maneuver which minimized penetration or downrange distance was again of the RCDR type, but with a maximum rotor speed of 110% at a power level corresponding to 568 ESHP, (Figures 31, 32, and 33). Velocity breakpoints for the rotor speed control were 140, 100, and 80 KIAS. Inspection of the time history trace reveals data trends similar to the other forms of RCDR control except that load factor increases sharply during the terminal phase of the maneuver. During the

last 1.5 seconds, N_z increases nearly 0.8 g's. This increase is reflected in the velocity trace, indicating that deceleration increases sharply with the increase in maneuvering load factor.

It was mentioned earlier that, in general, increases in power level increased time-to-turn, penetration and cross track distances, and exit velocity. Such was not the case, however, for the DT5-optimized triple ramp-constant (TRC) control law illustrated in Figures 34 through 39. Although this maneuver did not meet the constraints placed on the problem, it did indicate, at least for this control law, that a power increase actually produced a decrease in all measures of effectiveness (except pointing-margin). Comparisons between Figures 34 and 37 indicates that the power level actually affects the time at which the velocity breakpoints occur; in this case, increasing power level delayed the peak rotor speed (and hence load factor) by 0.2 seconds. Although this delay was small, it meant that the helicopter remained at the higher load factor for a greater period of time, allowing for a different deceleration schedule. Examination of Figure 34 indicates that airspeed rapidly decays during the terminal phase of the maneuver regardless of the increased power available. It is interesting to note that for this TRC

control, doubling the power level produced nearly a 10% reduction in time-to-turn. Of all the rotor speed control laws investigated, this was the only one that displayed this phenomenon.

An interesting phenomenon occurred in a DT5 data run that, again, was not present for any other control law. The rotor speed control law for this maneuver was actually an unsuccessful attempt to satisfy the cost function and problem constraints and normally would have been ignored except for the interesting time history trace discussed below. (A cursory inspection of the data (Figures 40, 41, and 42) indicates that one constraint was not met, i.e., exit airspeed was less than 50 KIAS). However, the rotor speed control algorithm breakpoints chosen by the computer program actually caused the helicopter to accelerate through a small portion of the maneuver. This occurred as a direct result of the rapid reduction in rotor speed between 3 and 3.5 seconds. Equation (28) indicates that if specific excess power is only slightly negative, and the rotor speed is decreasing rapidly, that a sign reversal will occur in equation (28), causing the aircraft to accelerate. Although this phenomenon was isolated to this particular maneuver only, it is likely that the control law parameters could be tailored to "draw out" the acceleration to the point where exit velocity would increase

above the 50 KIAS constraint.

Upon inspection of this maneuver time history, it is apparent that this maneuver is particularly violent, with decelerations on the order of 4.5 - 5.0 g's. The effect of this maneuver on the pilot(s) cannot be evaluated, however, since the point-mass model makes it impossible to determine the resultant vector of acceleration and the direction in which it acts. Two components of acceleration exist for all maneuvers investigated in this study, the downward component of normal load factor and the forward acting deceleration vector. Superposition principles would put the resultant vector acting somewhere through the helicopters gun turret (i.e., a vector pointing nearly through the pilot's knees), although this would depend on the aircraft attitude and the relative magnitudes of the vectors themselves.

Finally, Figures 43 through 48 present data runs of other RCDR control laws found to produce good, but not optimum results. These time histories are presented for comparison only and clearly indicate the effects of velocity breakpoint placement on the AH-1G's turn performance. These figures are best contrasted with the data shown in Figures 25 - 27 and Figures 31 - 33.

6.4 Operational Feasibility

It is very easy, in any feasibility study, to tout new technology as the panacea for all ills. However, reality dictates that the true operational feasibility of such a system be considered, even during the preliminary design stages of the system life cycle where such considerations have historically been neglected. Operational feasibility studies must address specific issues as reliability, maintainability, human factors or manability, and other concerns relative to the total engineering design effort, [Blandchard and Fabrycky, 1990].

It is uncertain to a quantitative degree what effect continuous, variable rotor speed control will have on reliability and maintainability. Any such considerations must in fact be addressed relative to assumed or specified operating conditions, existing maintenance capabilities, and existing or assumed logistics support. It is expected, however, that the technology proposed in this report will impact reliability and maintainability of existing helicopters to such a degree as to be nearly infeasible without drastic redesign of various components and airframe structure. Certainly from the standpoint of required changes in flight

control and FADEC software, firmware, and hardware, current technologies will allow fairly high expectations with regards to reliability and maintainability in these systems. However, the effect of rotor speed control on existing airframe structure, rotor/engine dynamic components, and transmissions is likely to be more dramatic, perhaps to the point where structural fatigue lives could be reduced substantially, requiring major redesign and retrofit of these components or, at the minimum, severely taxing existing logistics support and maintenance personnel. In addition, increased maintenance downtime and reduced aircraft availability is likely if no consideration is given to these aspects during the design. This study, however, is part of the system requirements definition process and reliability and maintainability would most likely not be addressed until conceptual or preliminary design, at the earliest. But without a doubt, this research has wide ranging implications on all aspects of the aircraft and total system life cycle.

The results of the research indicated that adaptive or continuous, variable rotor speed control can, at least for rapidly decelerating helicopters, induce decelerations on the order of 5 g's. Although it is uncertain what effects negative accelerations have on pilot workload and reserve capacity, previous research has indicated that pilots can

sustain decelerations on the order of 15 g's for periods not exceeding 6 seconds, [Sanders and McCormick, 1987]. The same research indicated that the pilot can tolerate 5 g decelerations for approximately 10 minutes before voluntary tolerance levels fall below acceptable norms. Therefore, it is unlikely that the decelerations of the magnitudes predicted by the model presented here would cause any adverse effects on pilot performance or situational awareness.

TABLE III

Control Algorithm	Exit Velocity (ft/s)	Time to Turn (sec)	Penetration Distance (ft)	Cross Track Distance (ft)	Pointing Margin (deg)
Baseline (Wood)	68.1	10.4	1050.0	1200.0	--
T(RC), 120% Pwr 3	43.1	6.5	--	501.7	93.5
RCDR, 110 Pwr 3 125,105,80	57.9	8.7	756.9	862.4	47.4
RCDR, 115 Pwr 4 140,100,80	69.7	8.1	557.9	746.8	61.4
RCDR, 115 Pwr 3 125,105,80	49.0	7.8	652.0	744.25	67.7
RCDR, 110 Pwr 3 140,100,80	50.0	7.8	647.6	759.1	67.7
RCR, 110% Pwr 4 140,100	51.8	7.2	702.6	690.6	78.1
TRC, 120% Pwr 1 120,80	19.3	7.4	623.0	723.0	79.9
TRC, 120% Pwr 2 120,80	18.01	6.7	601.0	629.0	89.8

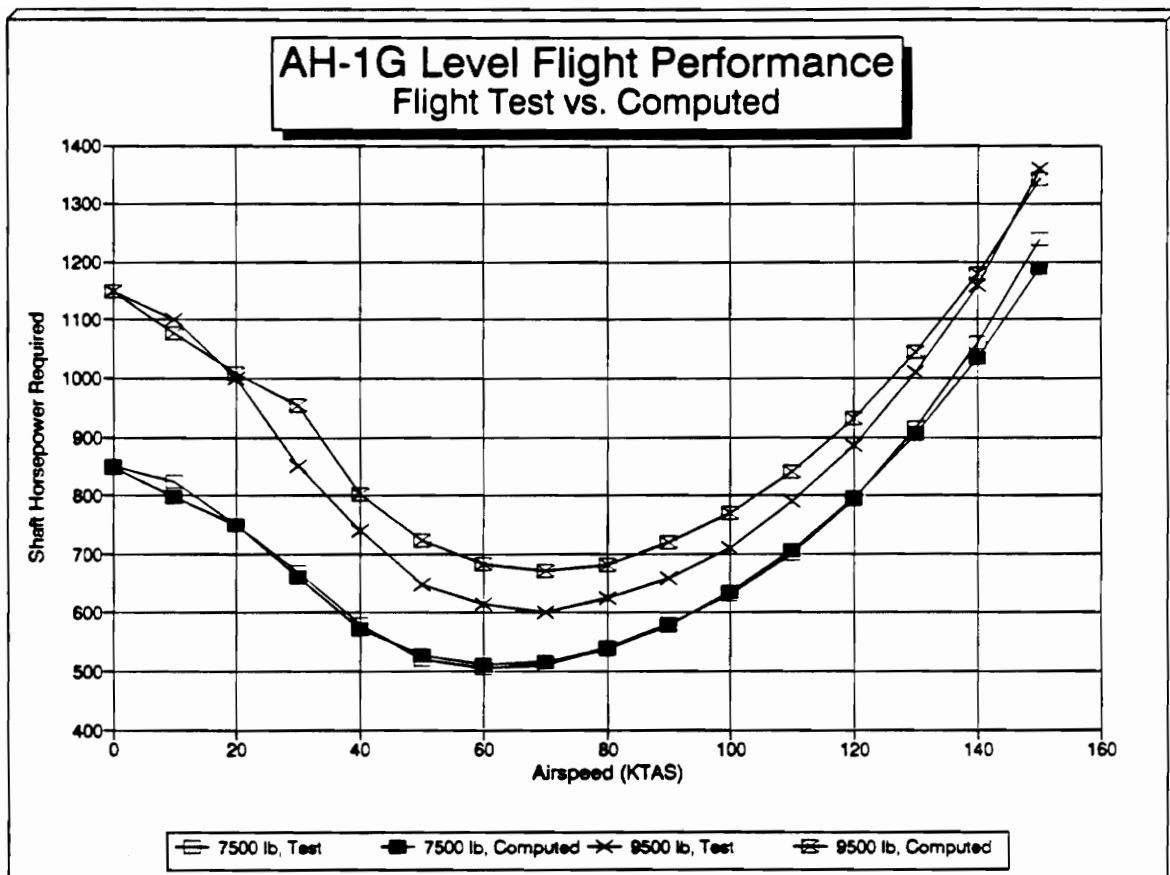


Figure 18

AH-1G Level Flight Performance
(Calculated vs. Flight Test)

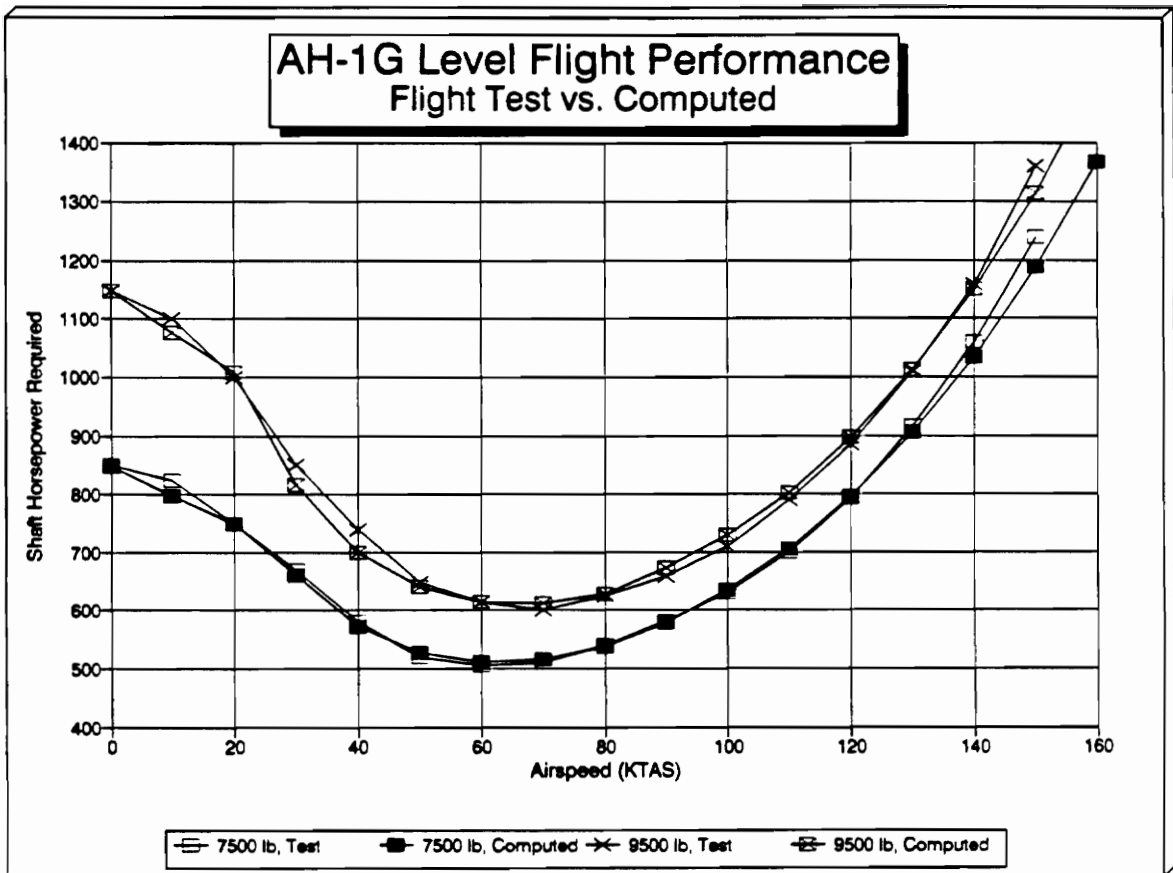


Figure 19

Corrected AH-1G Level Flight Performance
(Calculated vs. Flight Test)

AH-1G Turn Performance Flight Test

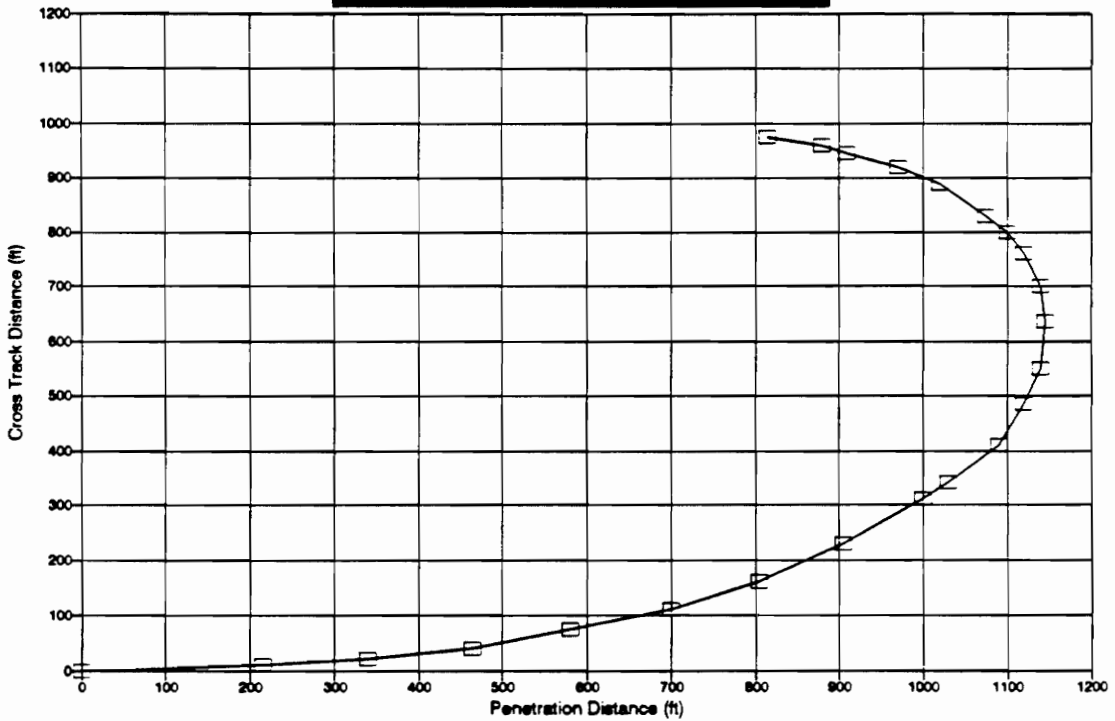


Figure 20

AH-1G Turn Performance
Flight Test

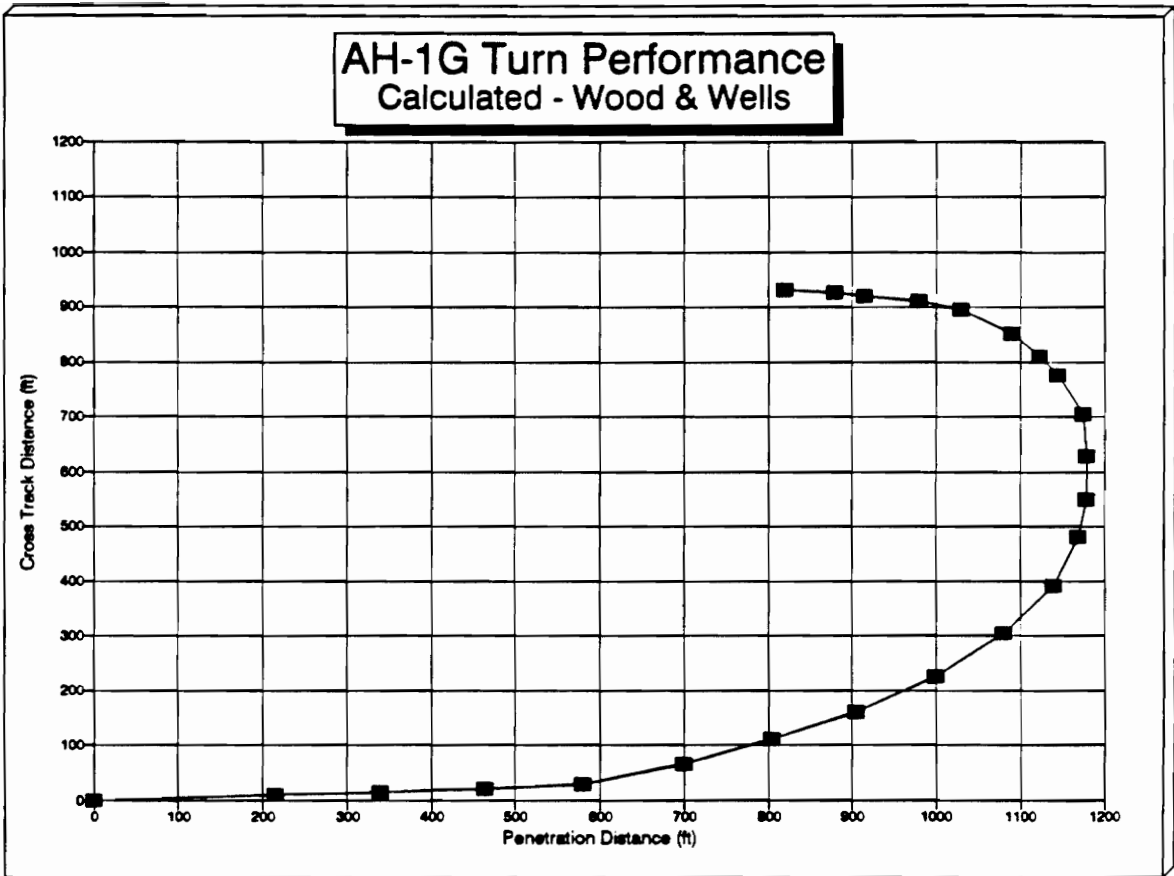


Figure 21

**AH-1G Turn Performance
Calculated (Wood and Wells)**

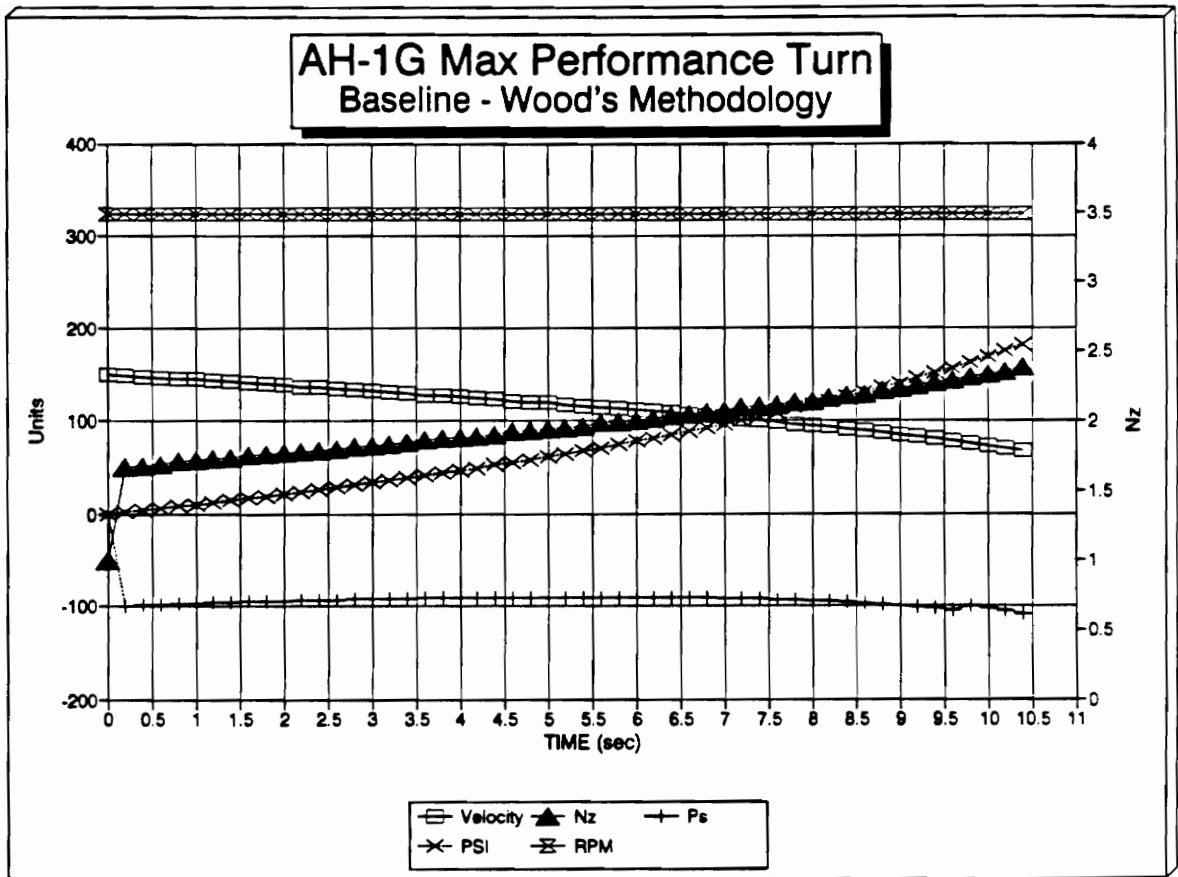


Figure 22

**AH-1G Max Performance Turn
Wood's Methodology**

**AH-1G Max Performance Turn
Baseline - Wood's Methodology**

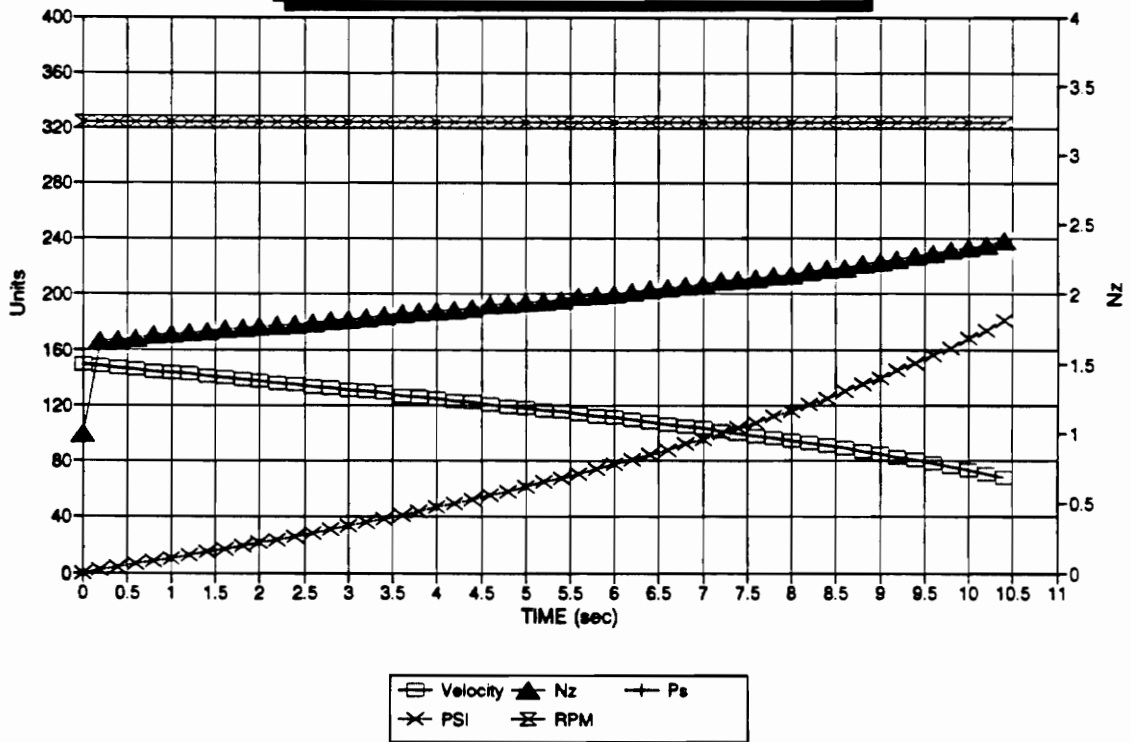


Figure 23

**AH-1G Max Performance Turn
Wood's Methodology**

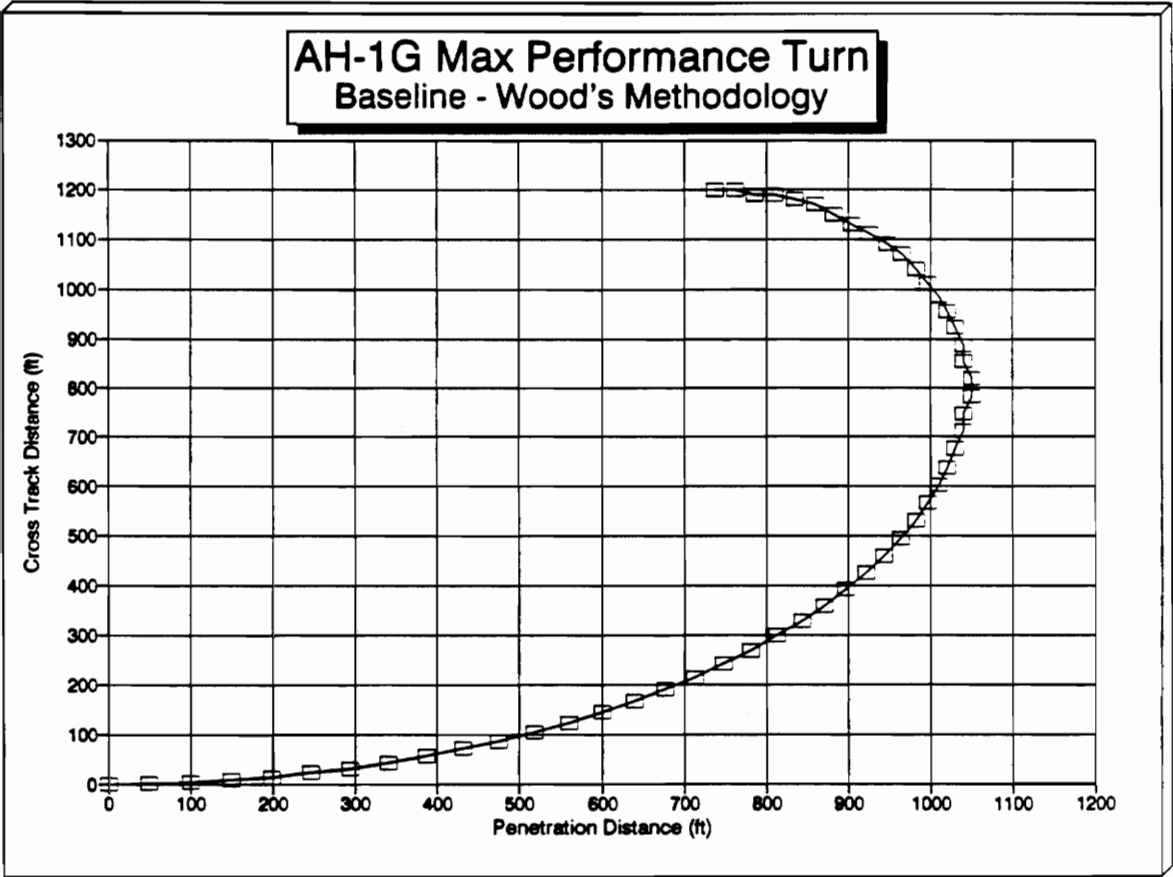


Figure 24

**AH-1G Max Performance Turn
Wood's Methodology**

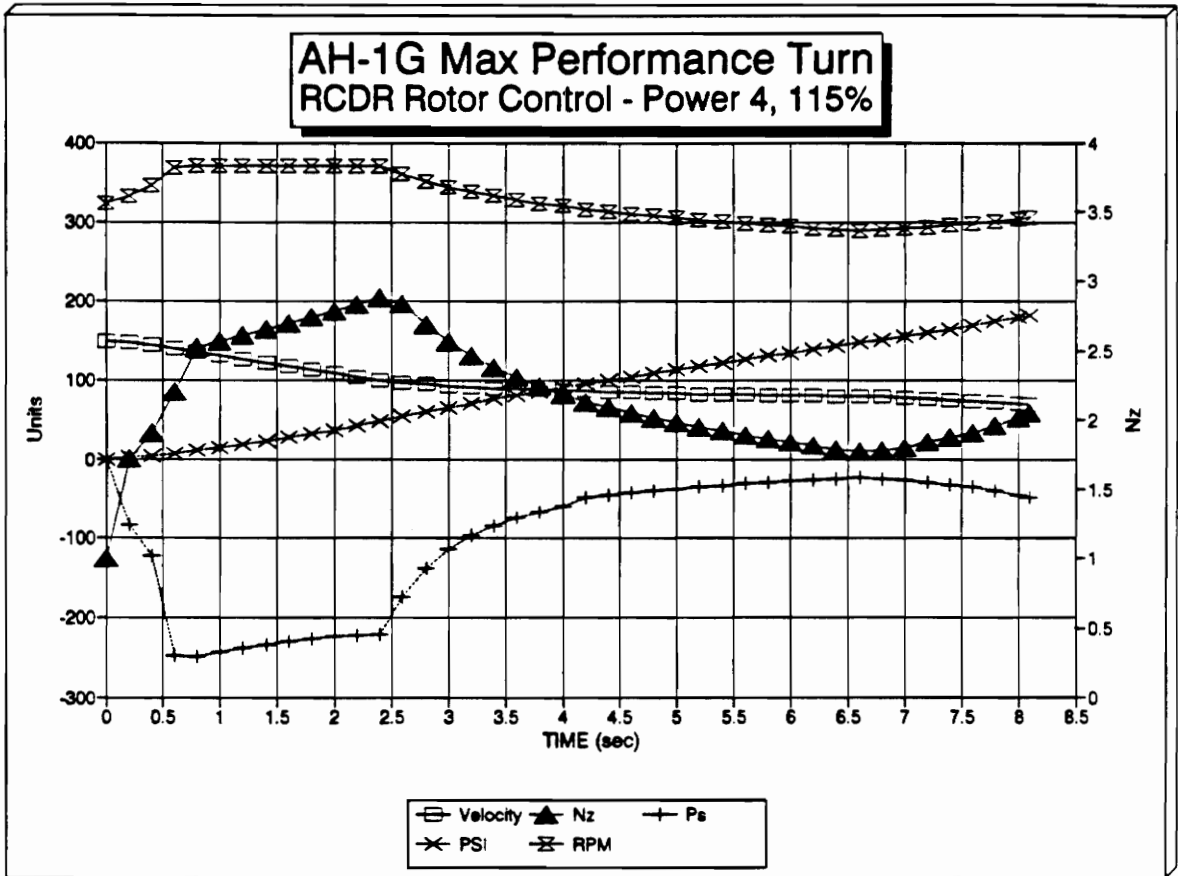


Figure 25

**AH-1G Max Performance Turn
RCDR Control, Power 4, 115% RPM**

**AH-1G Max Performance Turn
RCDR Rotor Control - Power 4, 115%**

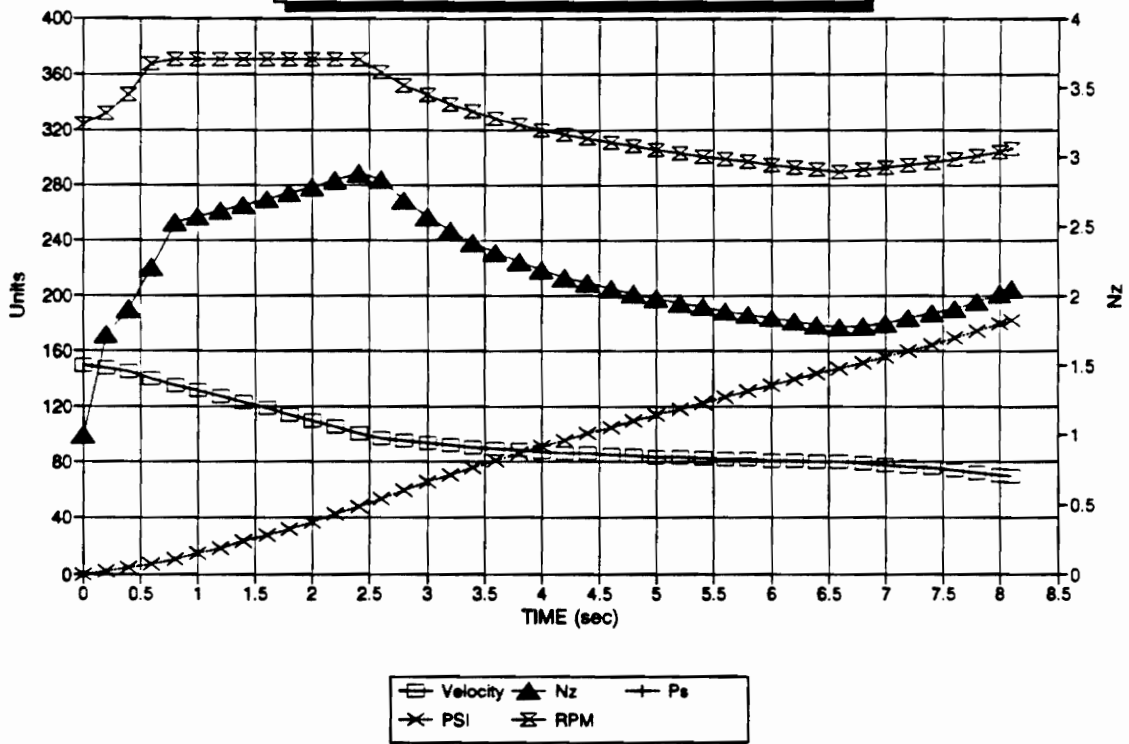


Figure 26

**AH-1G Max Performance Turn
RCDR Control, Power 4, 115% RPM**

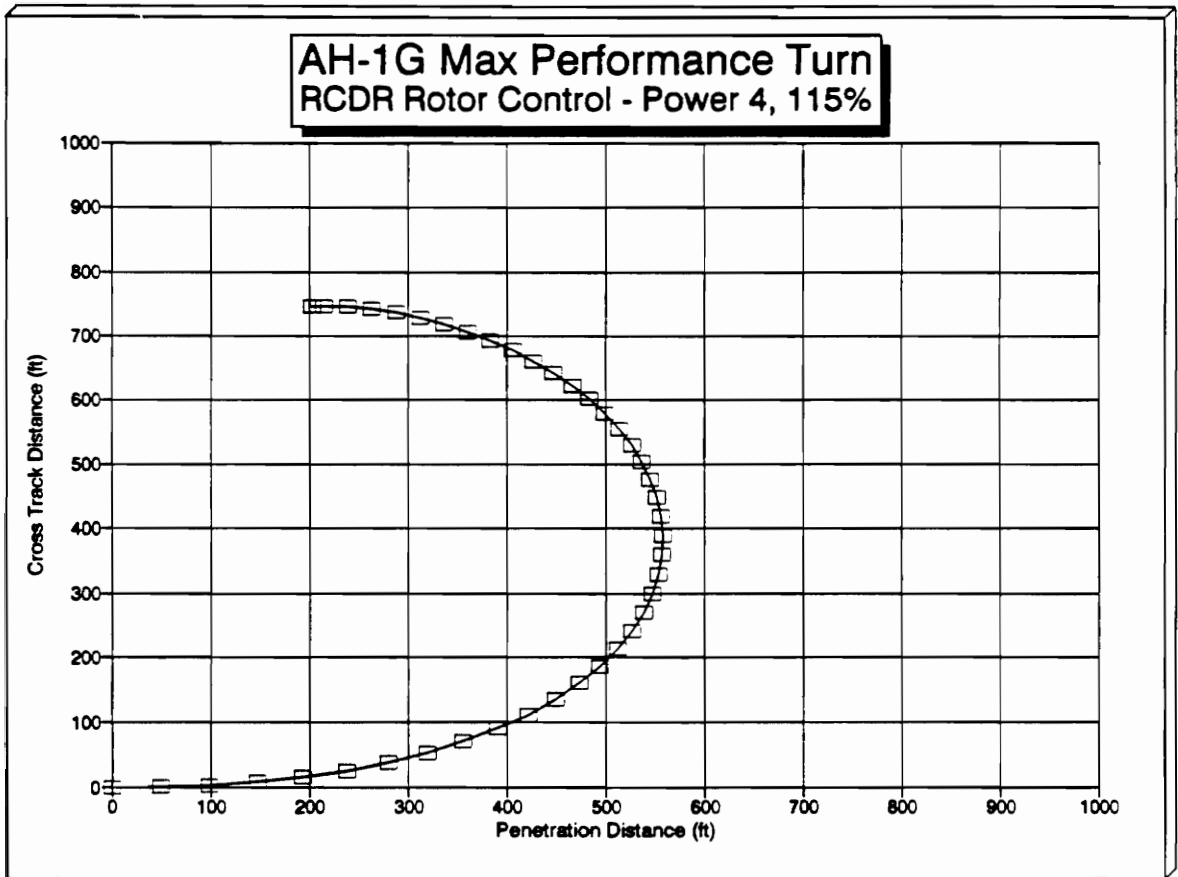


Figure 27

**AH-1G Max Performance Turn
 RCDR Control, Power 4, 115%**

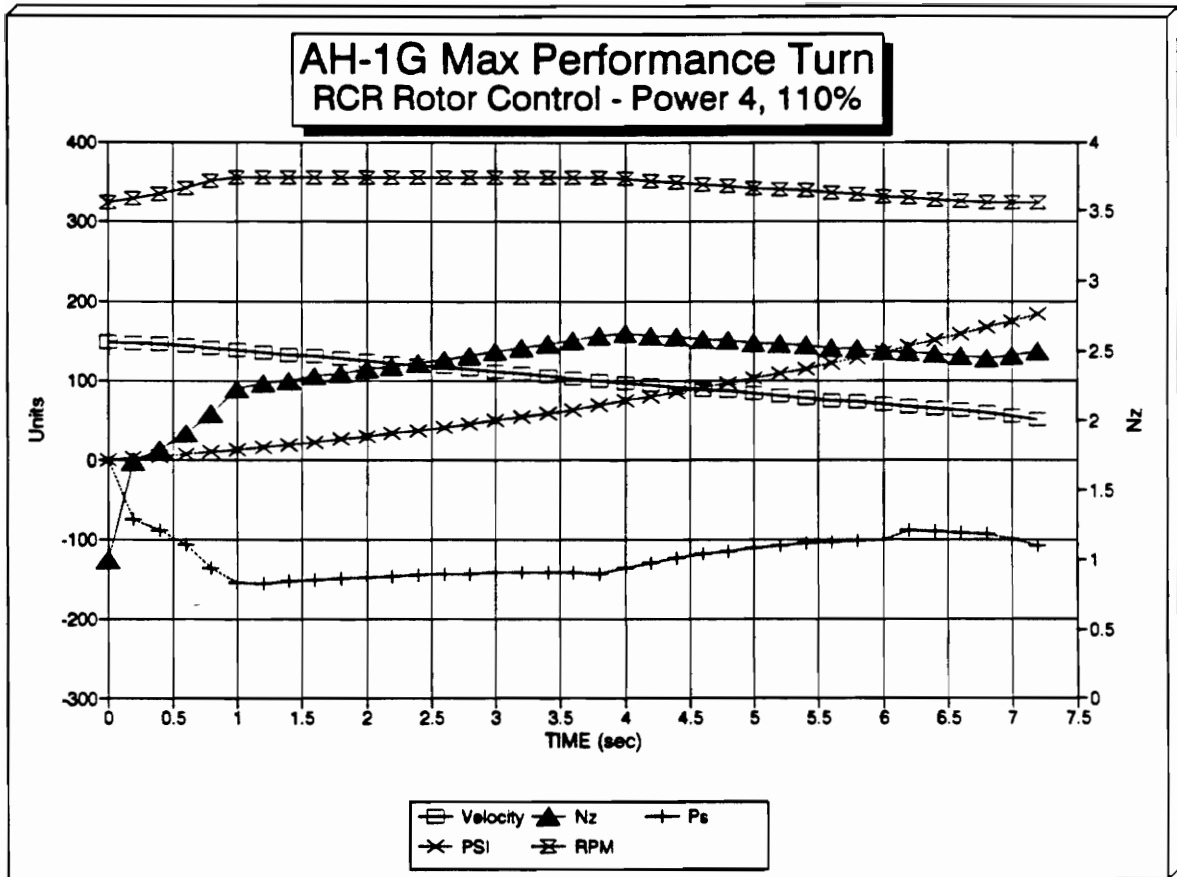


Figure 28

**AH-1G Max Performance Turn
RCR Control, Power 4, 110% RPM**

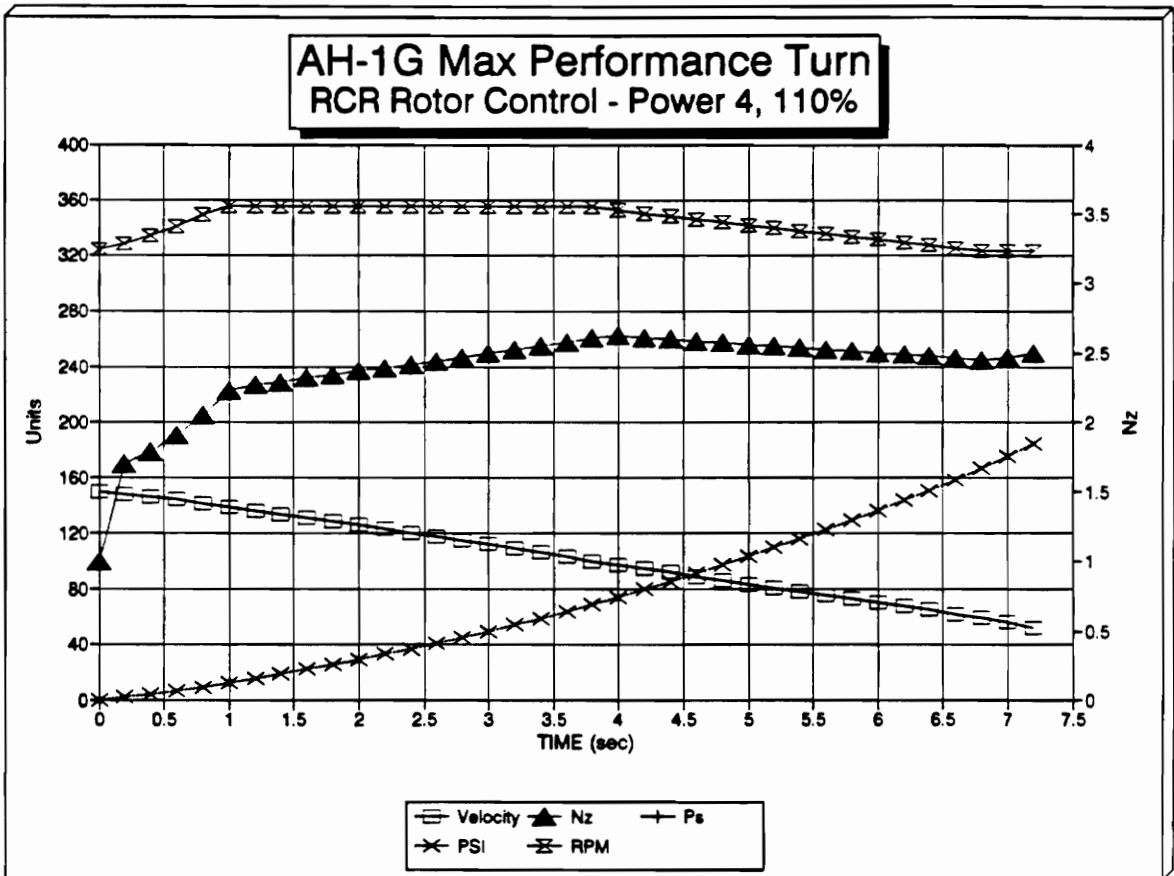


Figure 29

**AH-1G Max Performance Turn
RCR Control, Power 4, 110% RPM**

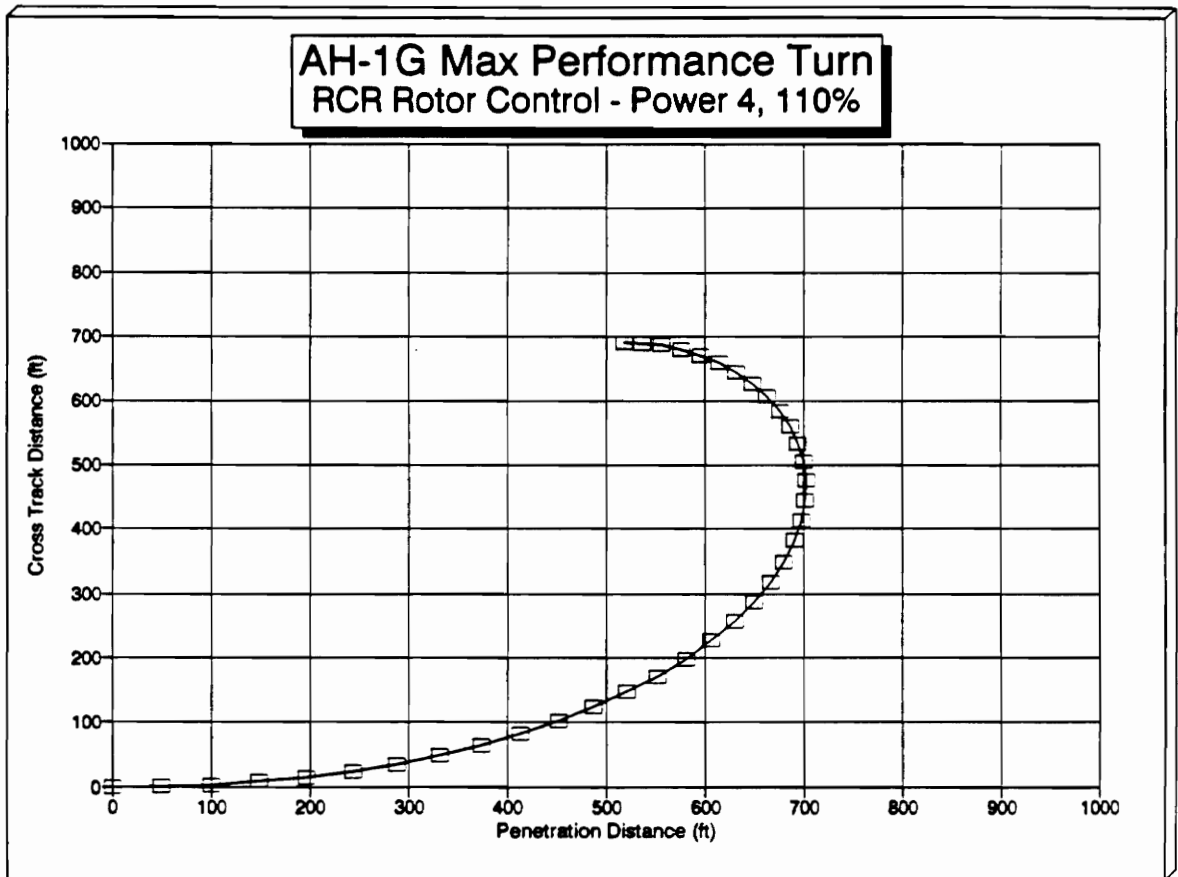


Figure 30

**AH-1G Max Performance Turn
RCR Control, Power 4, 110% RPM**

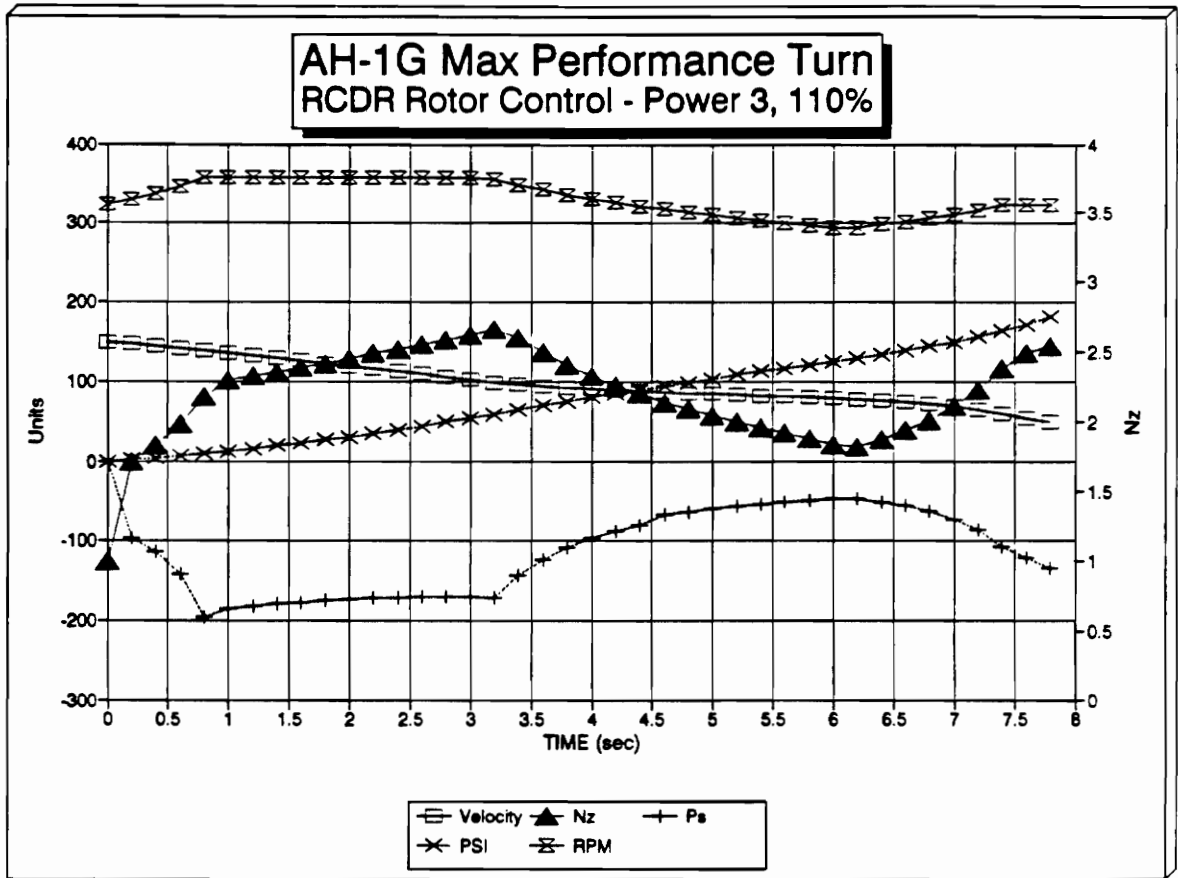


Figure 31

**AH-1G Max Performance Turn
RCDR Control, Power 3, 110% RPM**

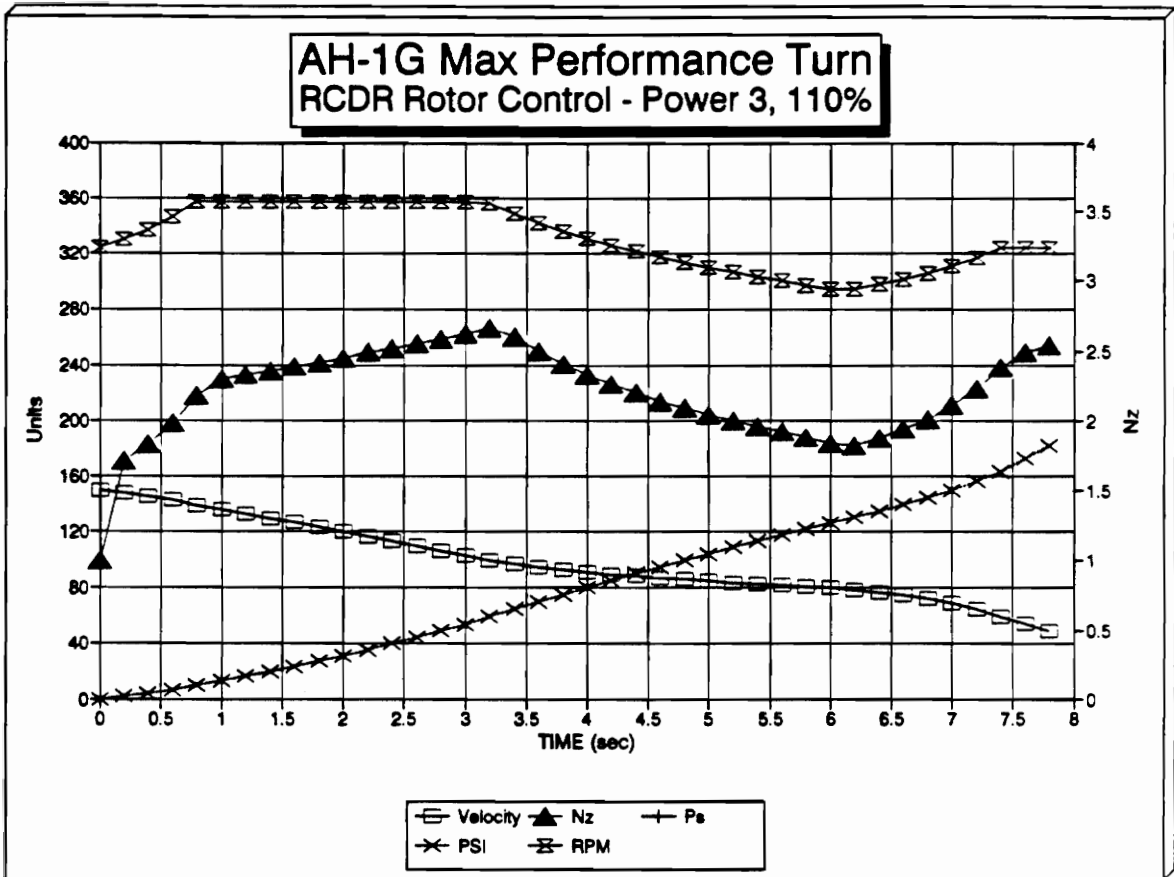


Figure 32

**AH-1G Max Performance Turn
RCDR Control, Power 3, 110% RPM**

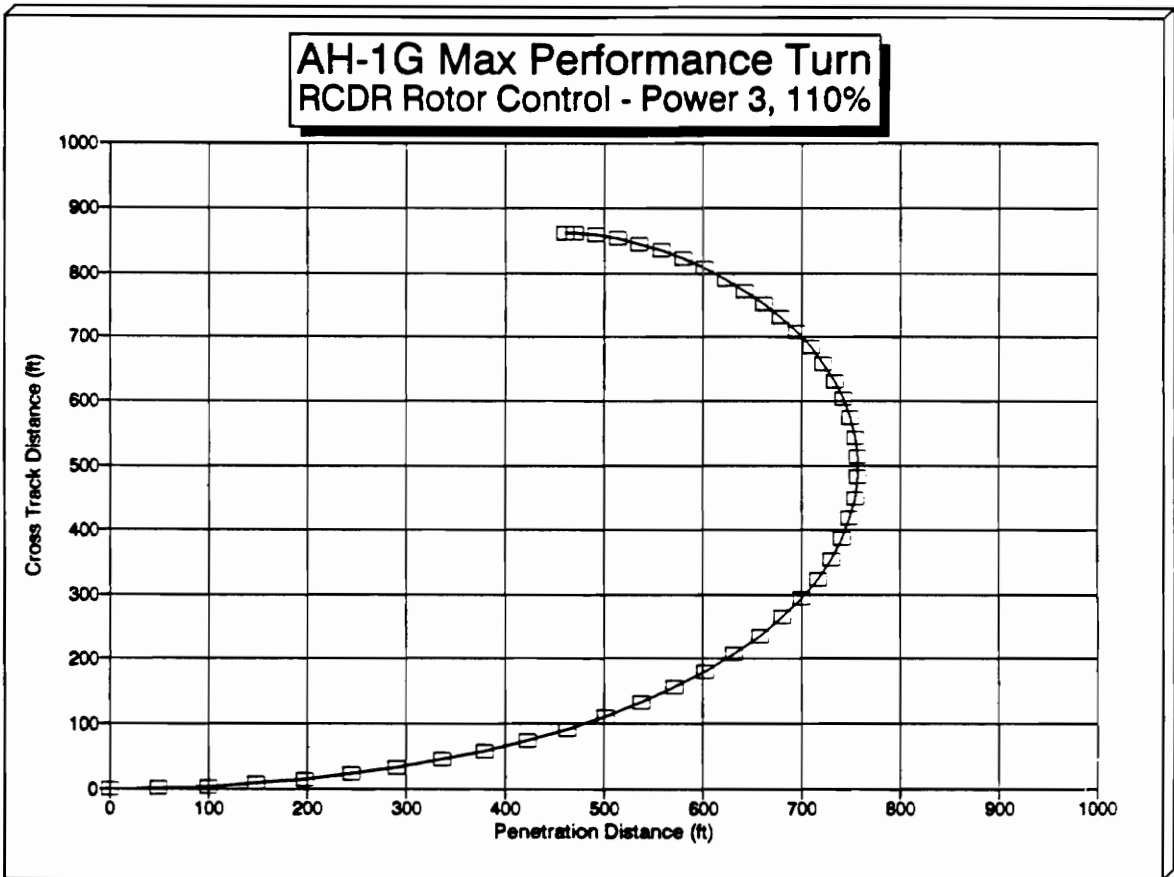


Figure 33

AH-1G Max Performance Turn
RCDR Control, Power 3, 110% RPM

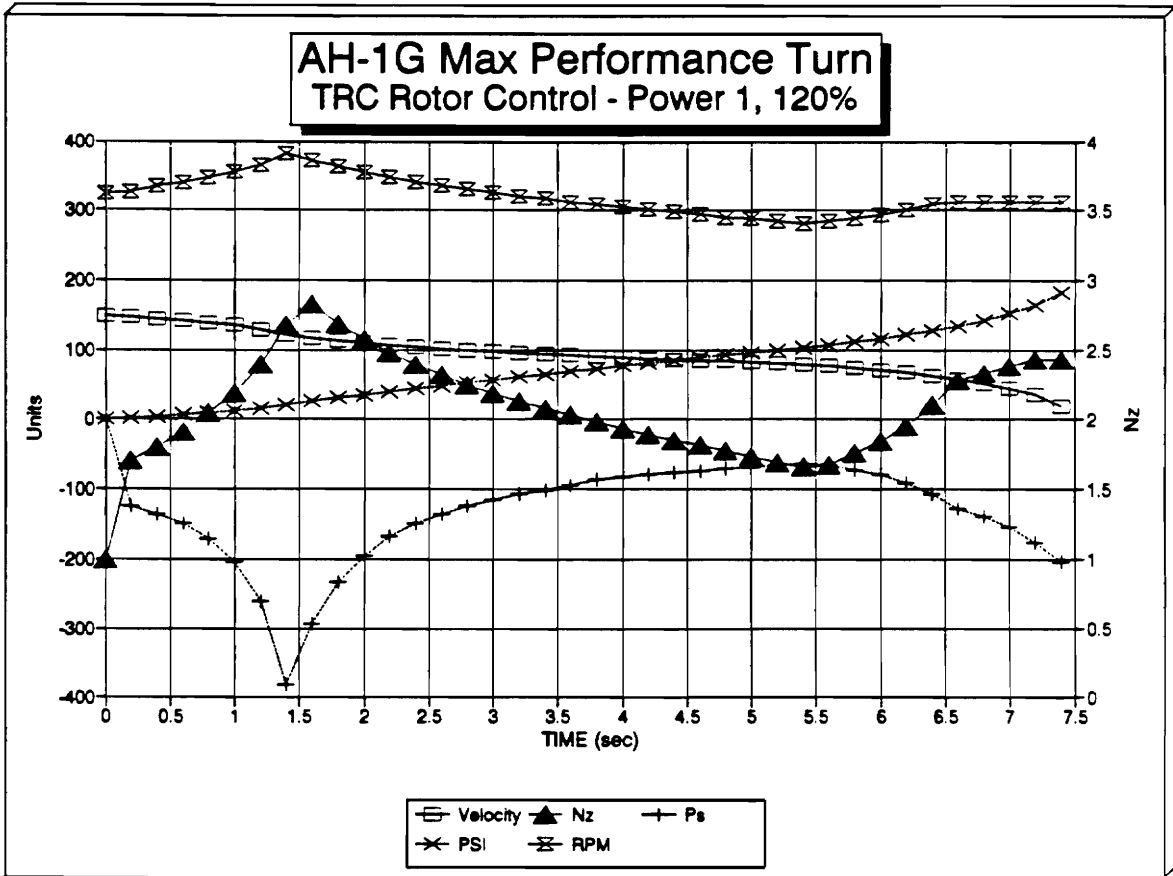


Figure 34

**AH-1G Max Performance Turn
TRC Control, Power 1, 120% RPM**

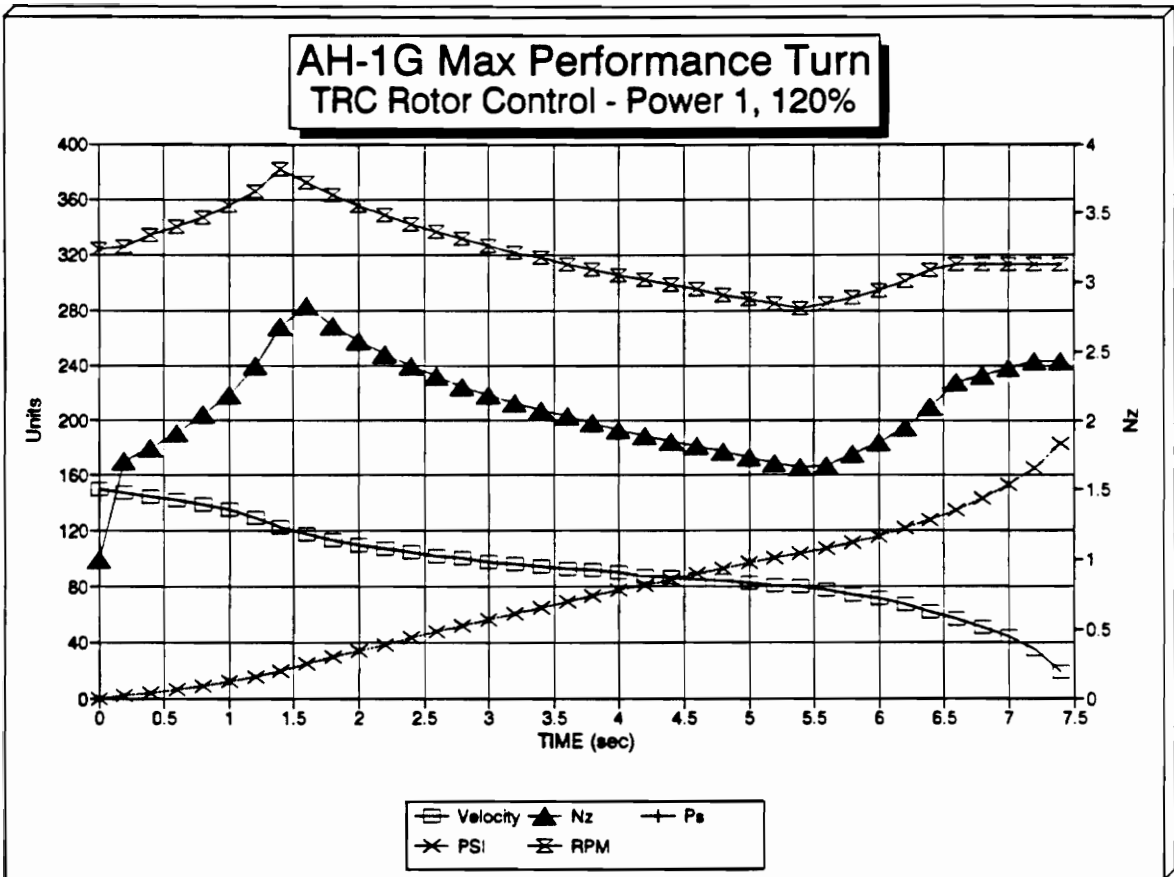


Figure 35

**AH-1G Max Performance Turn
TRC Control, Power 1, 120% RPM**

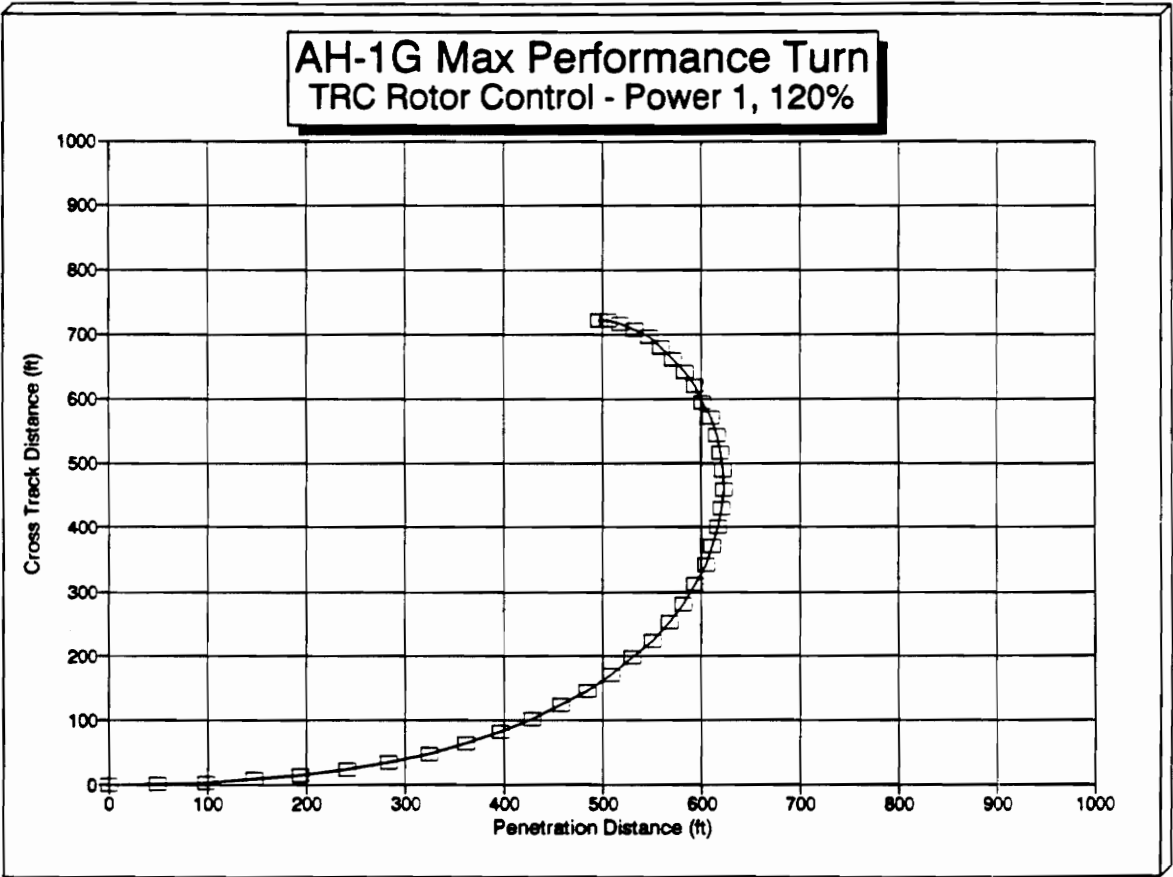


Figure 36

**AH-1G Max Performance Turn
 TRC Control, Power 1, 120% RPM**

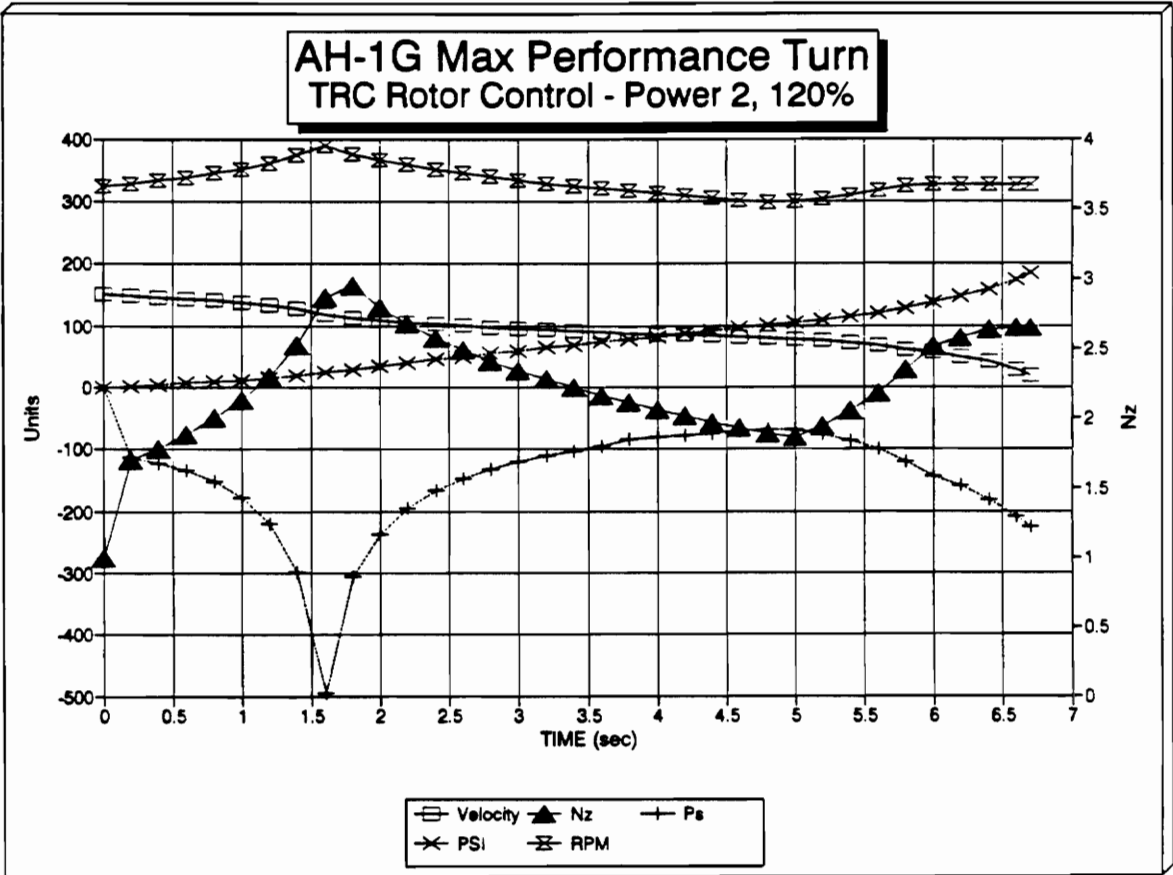


Figure 37

**AH-1G Max Performance Turn
TRC Control, Power 2, 120% RPM**

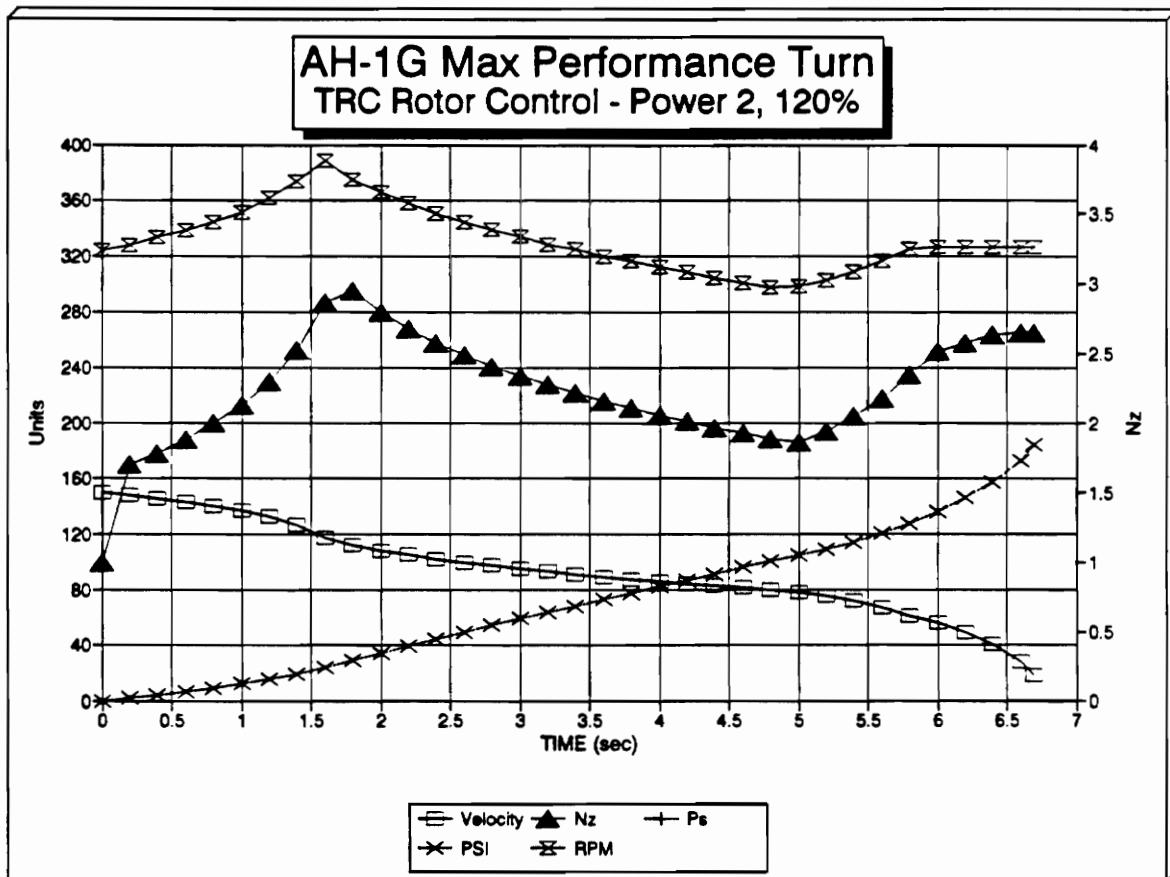


Figure 38

**AH-1G Max Performance Turn
TRC Control, Power 2, 120% RPM**

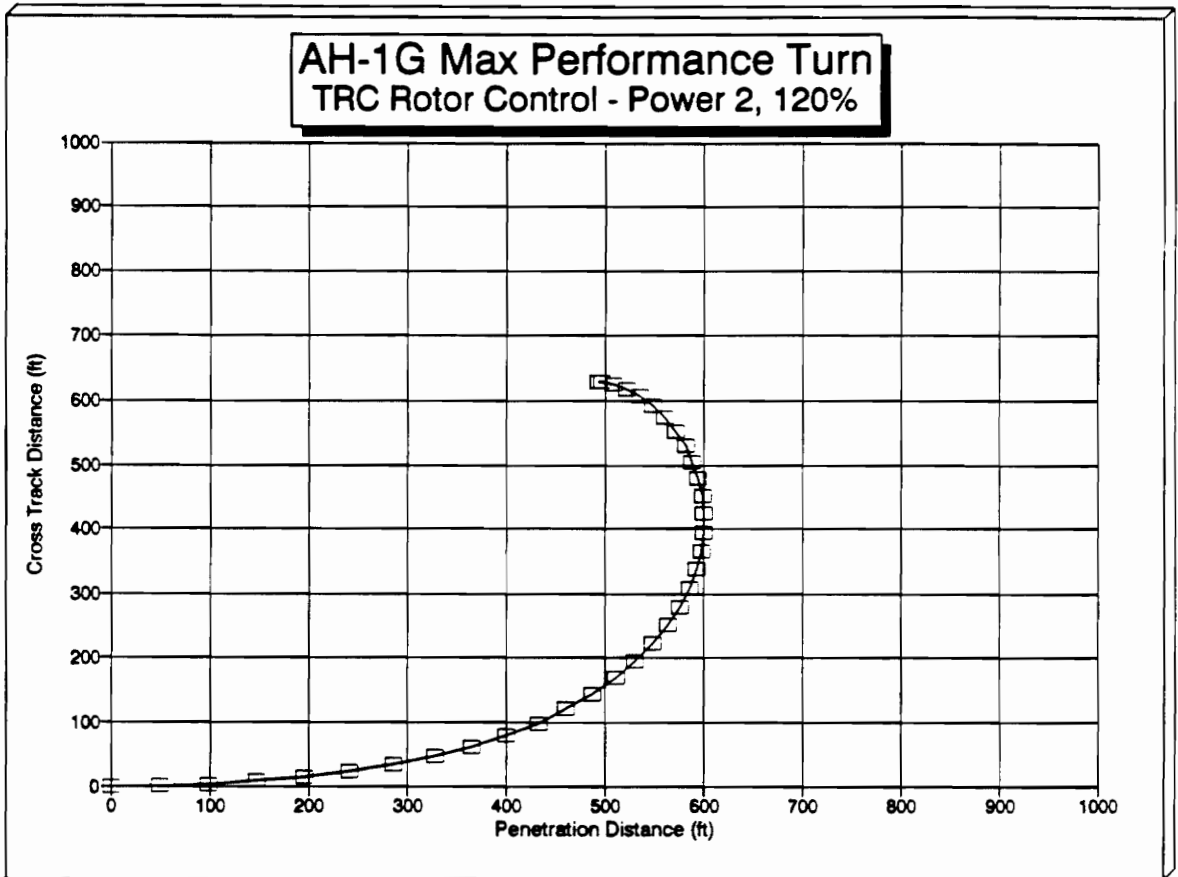


Figure 39

**AH-1G Max Performance Turn
TRC Control, Power 2, 120% RPM**

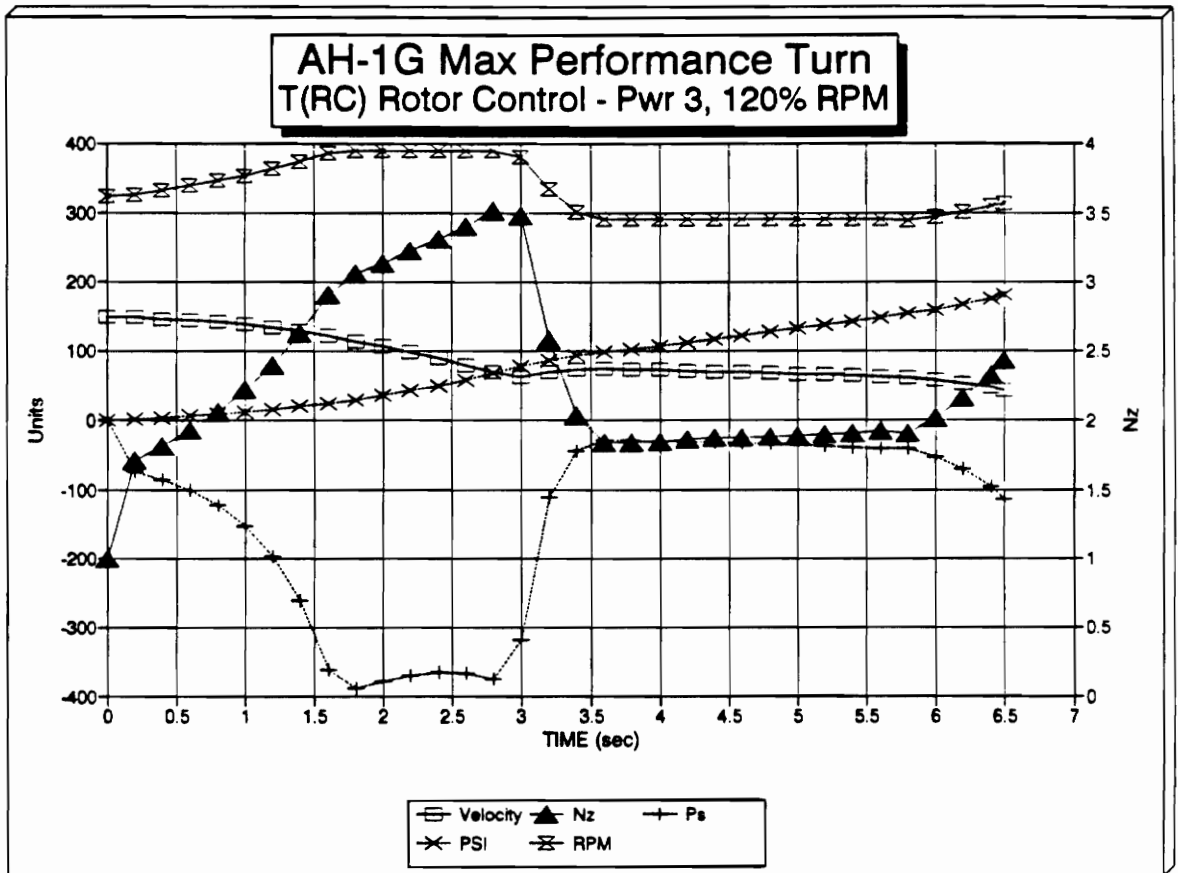


Figure 40

**AH-1G Max Performance Turn
T(RC) Control, Power 4, 120% RPM**

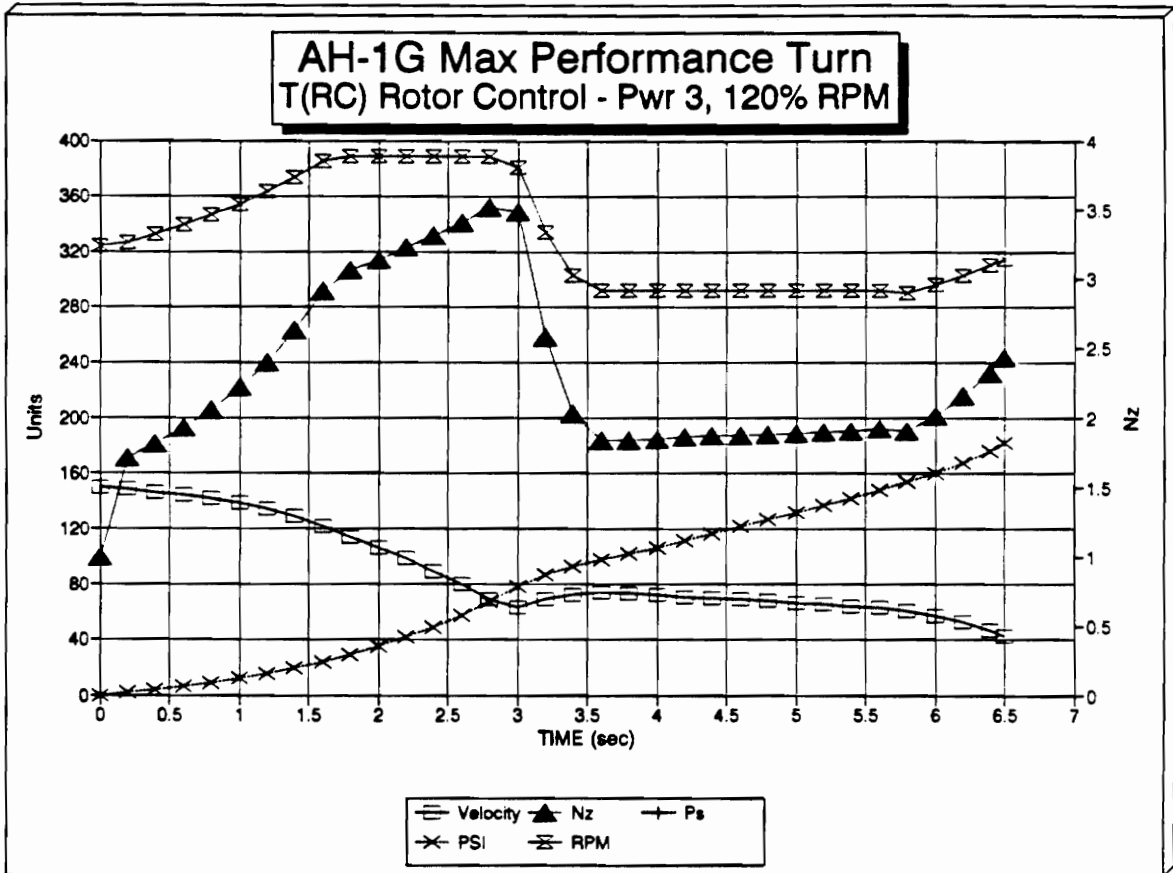


Figure 41

AH-1G Max Performance Turn
T(RC) Control, Power 4, 120% RPM

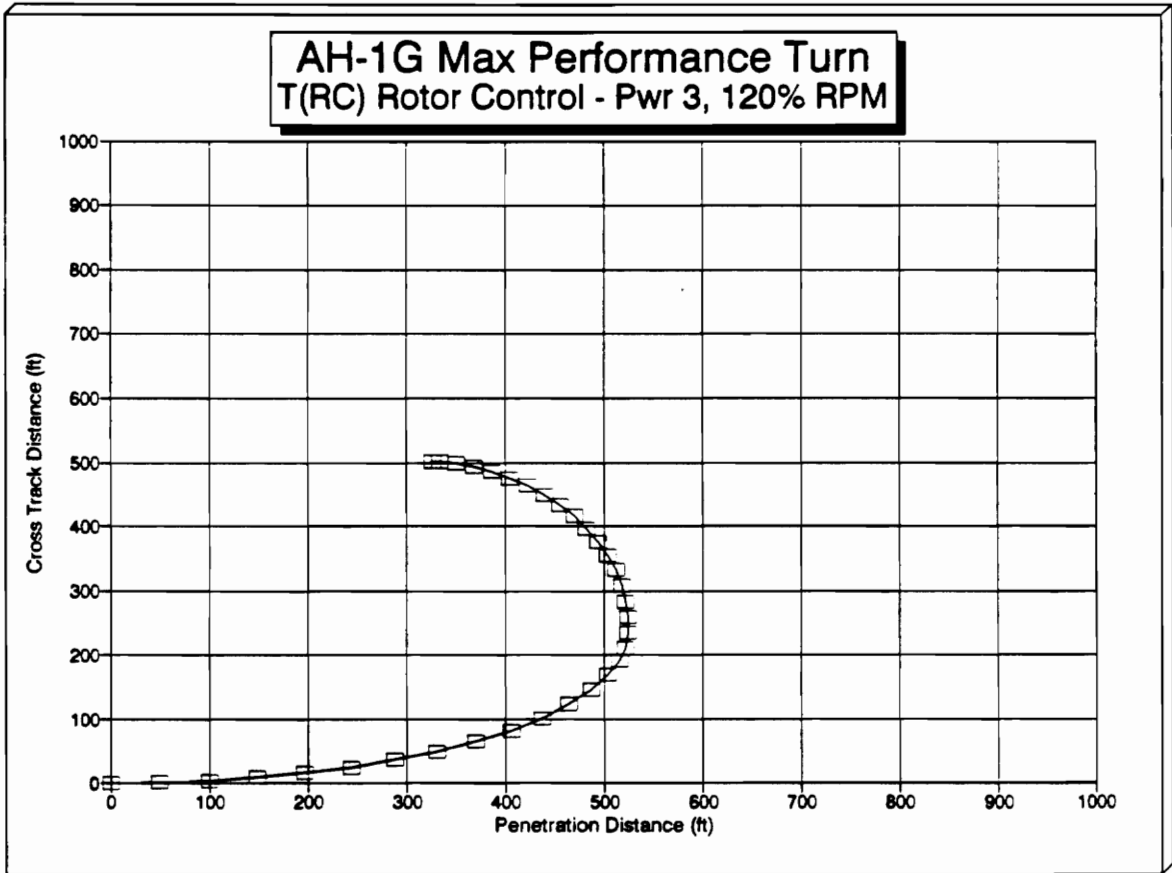


Figure 42

**AH-1G Max Performance Turn
T(RC) Control, Power 4, 120% RPM**

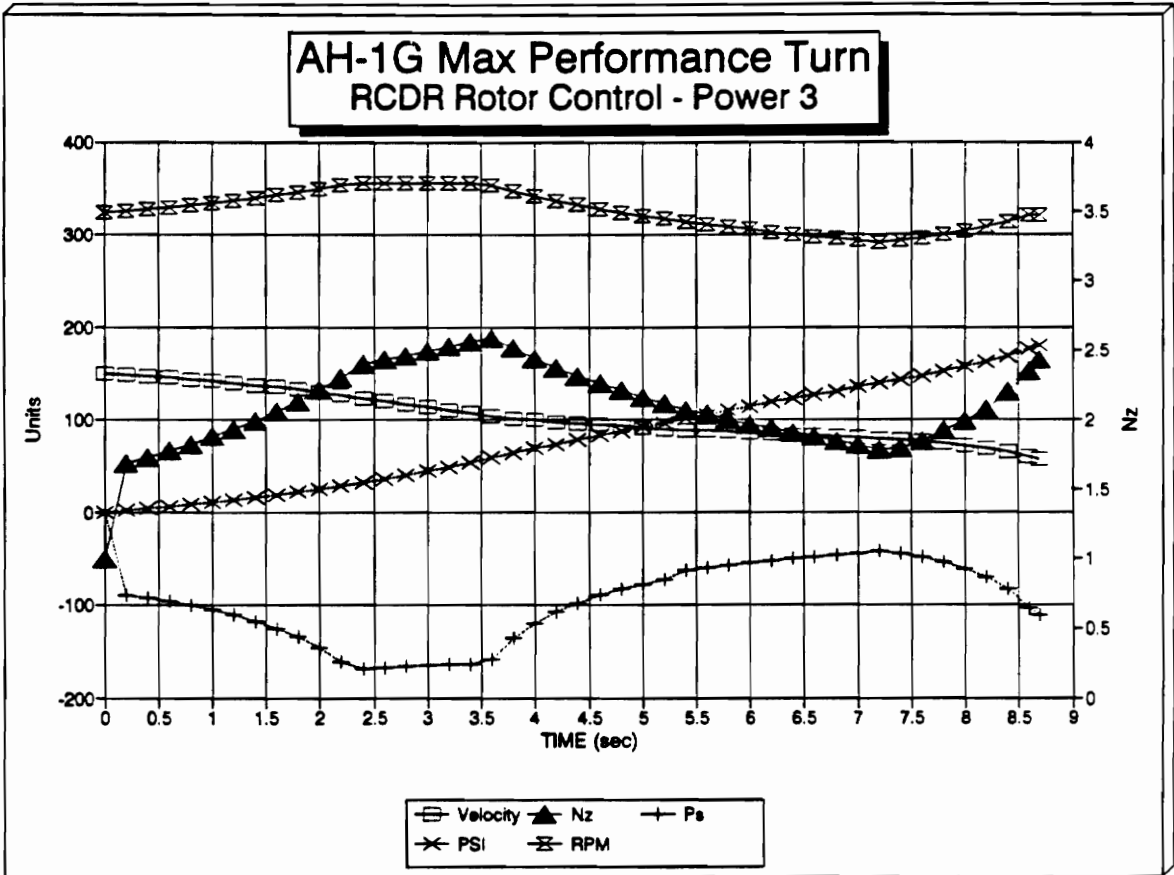


Figure 43

**AH-1G Max Performance Turn
RCDR Control, Power 3, 110% RPM
125, 105, 80 Velocity Breakpoints**

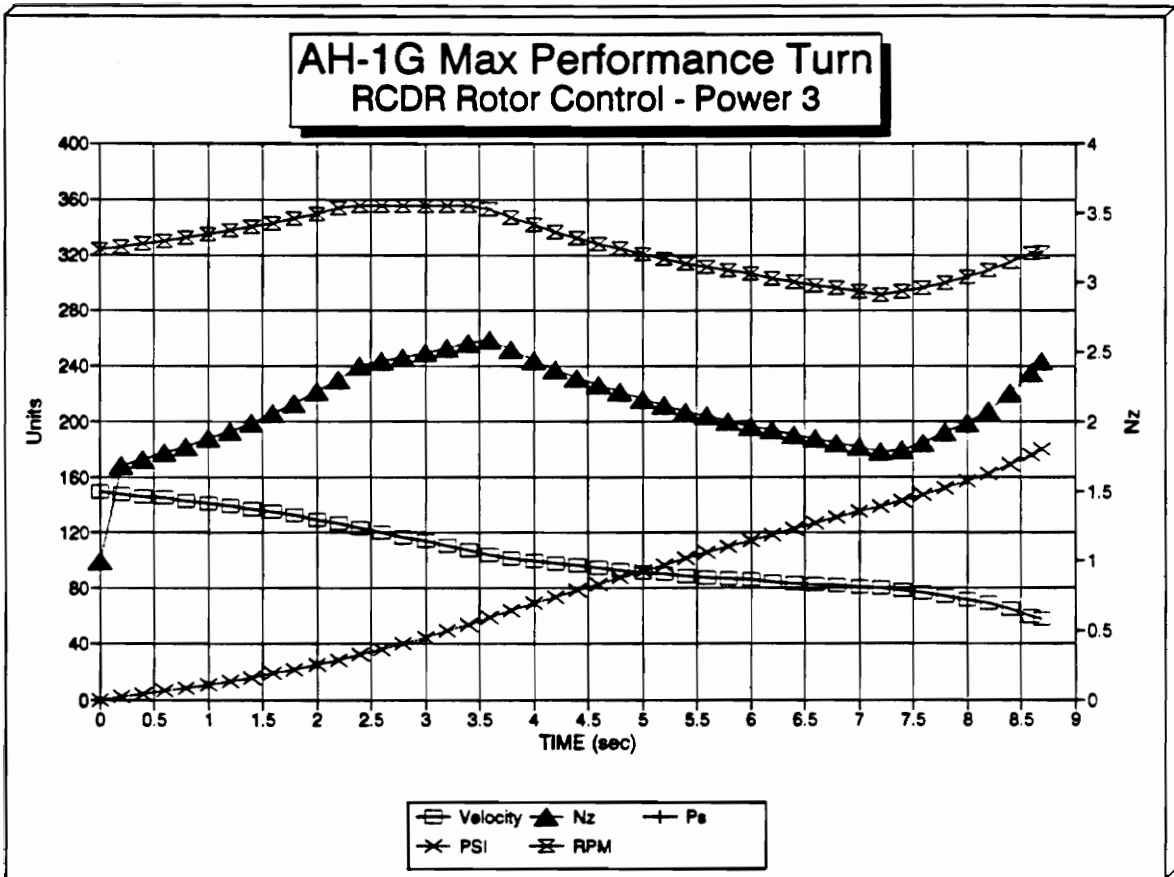


Figure 44

**AH-1G Max Performance Turn
RCDR Control, Power 3, 110% RPM
125, 105, 80 Velocity Breakpoints**

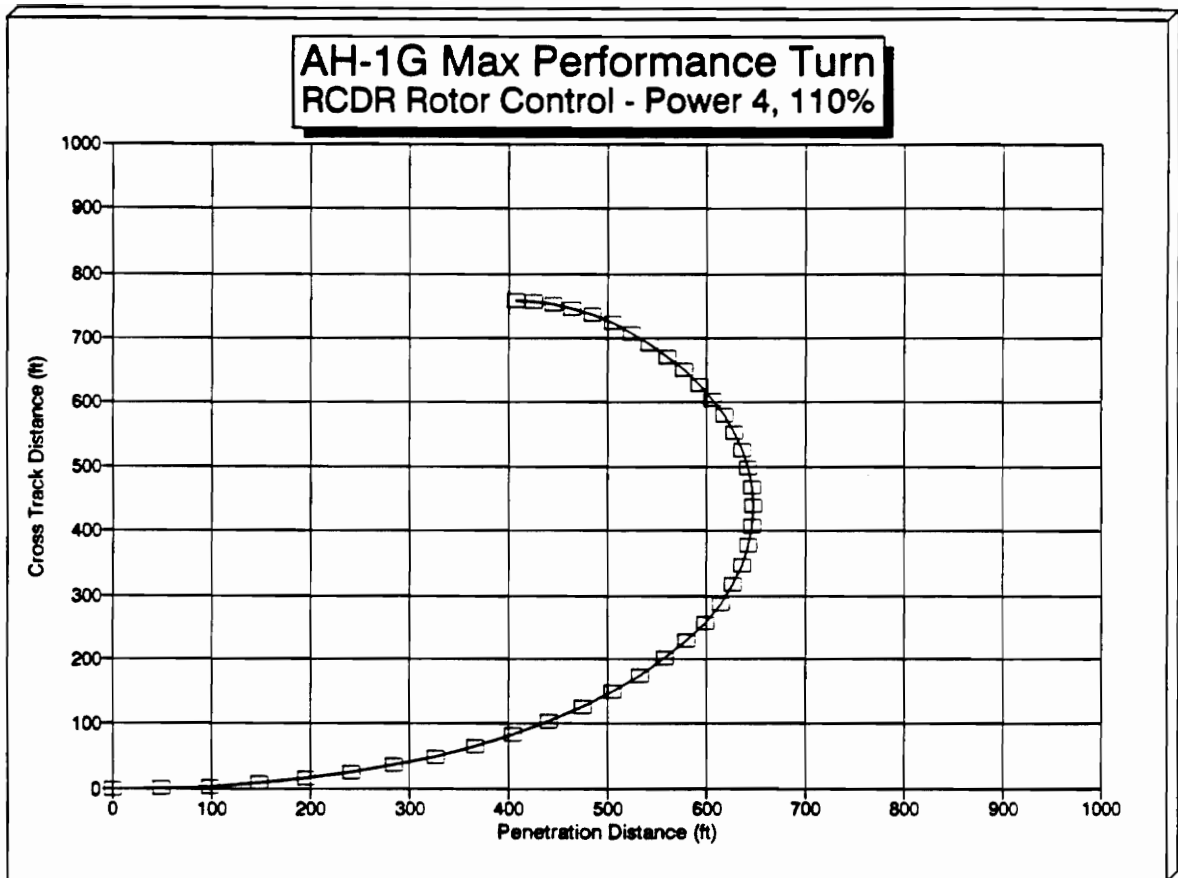


Figure 45

AH-1G Max Performance Turn
RCDR Control, Power 3, 110% RPM
125, 105, 80 Velocity Breakpoints

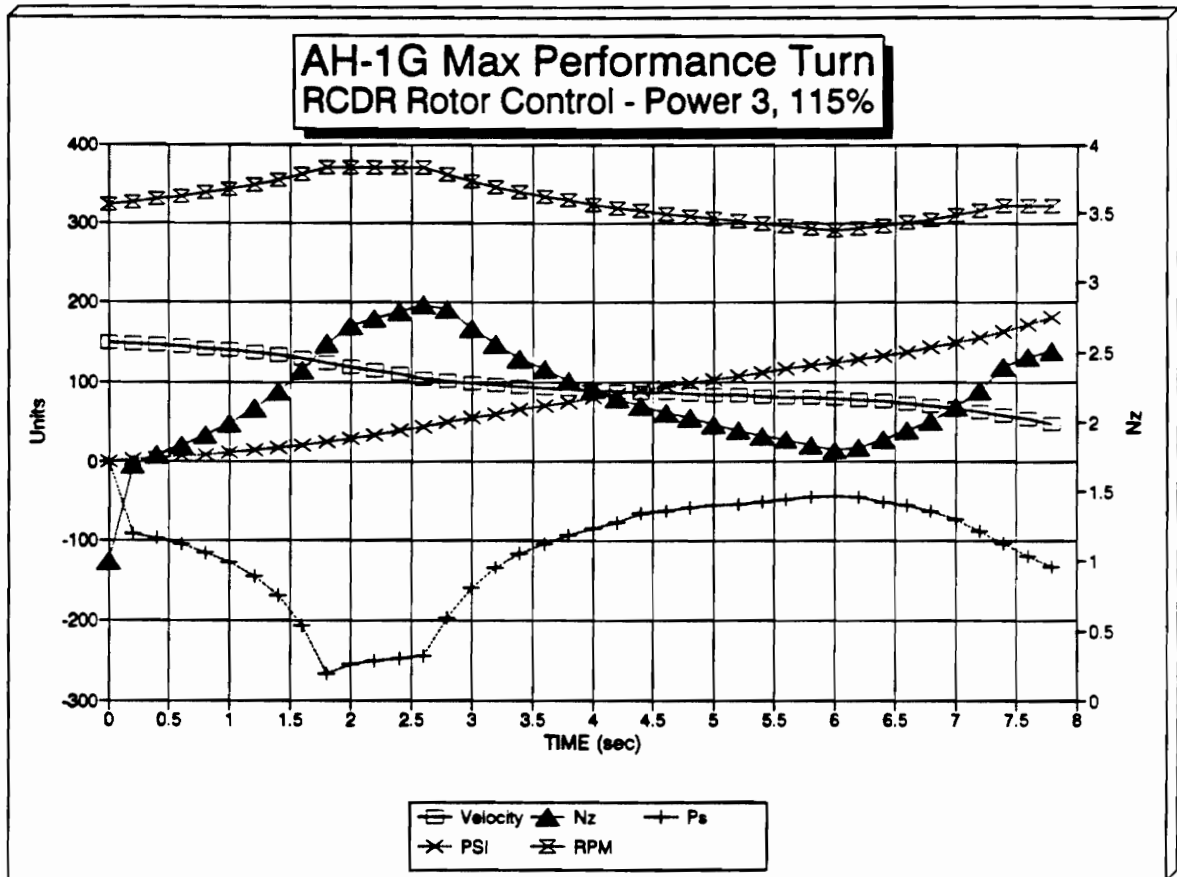


Figure 46

AH-1G Max Performance Turn
RCDR Control, Power 3, 115% RPM
125, 105, 80 Velocity Breakpoints

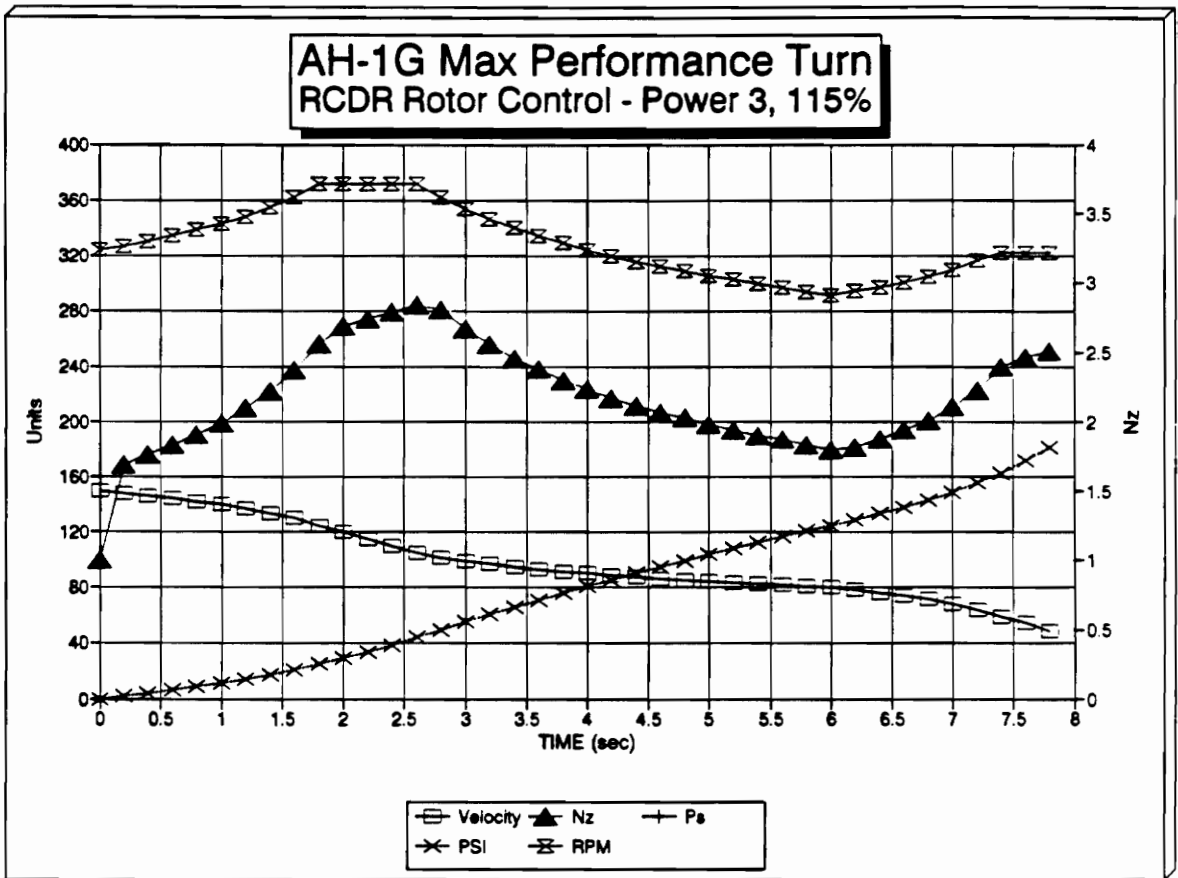


Figure 47

**AH-1G Max Performance Turn
RCDR Control, Power 3, 115% RPM
125, 105, 80 Velocity Breakpoints**

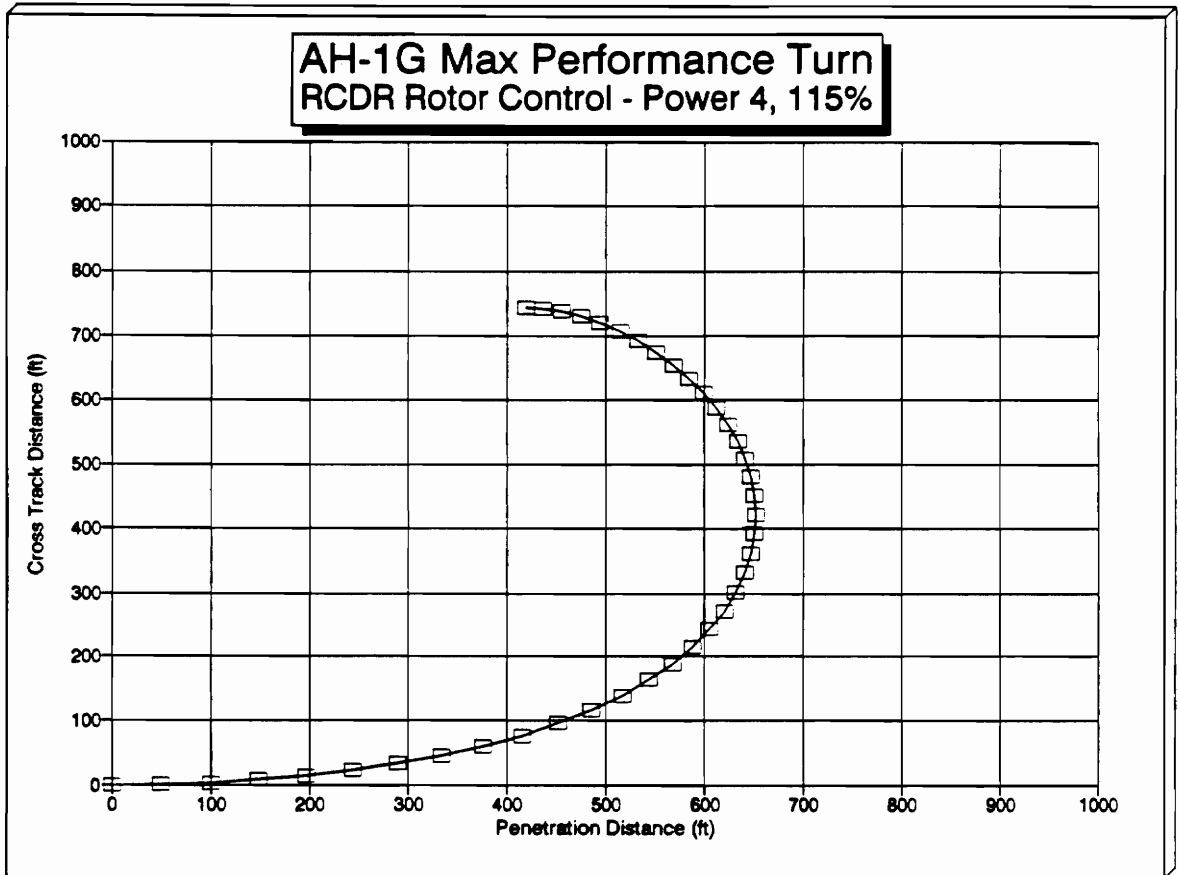


Figure 48

**AH-1G Max Performance Turn
RCDR Control, Power 3, 115% RPM
125, 105, 80 Velocity Breakpoints**

7.0 RECOMMENDATIONS FOR FUTURE RESEARCH

The research reported in the preceding chapters was purposely limited in its scope, first because of the sheer complexity of the complete problem and second to remain fundamentally at the root of the problem in order to understand the cause and effect relationships between the rotor speed control laws and their effects on helicopter maneuverability. Obviously, any recommendations for future research would include increasing the scope of the problem and eliminating many of the assumptions contained herein. The following recommendations can be made:

- (1) Increase the complexity of the simulation model from a point-mass representation of the helicopter to a full 6-DOF model.
- (2) Re-state the problem as an ideal optimum control problem rather than a parameter optimization study. The new problem should attempt to optimize rotor speed control laws, maneuvering load factor, and any other controls introduced by the

6-DOF model.

- (3) This research concentrated only on enhancing decelerating turn performance, but the results seem to indicate that any maneuver within the mission spectrum dependent on accelerated flight can be improved by optimal rotor speed control.
- (4) The tactical implications of this research are very clear. An important next step would be to investigate optimum rotor speed control laws using an M-on-N air combat simulation program in order to measure improvements in combat effectiveness against threat helicopters and to develop tactics using this new control.
- (5) Some of the maneuver time histories indicated that rotor speed control can be violent, with accelerations approaching -5 g's acting in the longitudinal plane. A 6-DOF model can be used to not only verify the direction and magnitude of

this acceleration vector, but to also investigate the effects of these accelerations on pilot physiology, their mission performance, and their workload.

- (6) Variable rotor speed control is certain to have an effect on dynamic component fatigue lives and airframe strength. Future helicopter designs using variable rotor speed control will need to be more robust in these areas or else the increased mission capability of the helicopter using variable rotor speed control will be offset by decreased mission availability.
- (7) Finally, the current FADEC engine control technology may not be adequate for variable rotor speed control. An investigation should be made relative to the small time constants required to vary the rotor speed and the increased torque demands placed on the engine and transmission.

8.0 CONCLUSIONS

The results of this research indicate that continuous, variable rotor speed control is a viable solution to increased helicopter maneuverability and agility. Of the rotor speed control laws investigated, the RCDR and T(RC) types seem the most promising. In particular, these control laws demonstrated a 31% improvement in time-to-turn 180 degrees, a 38% improvement in turn penetration distance, a 42% improvement in turn cross track distance, and a pointing margin advantage of nearly 94 degrees. In addition, the rotor speed control law parameters could be optimized such that the helicopter exited a maximum performance decelerating turn at or above its power bucket speed, affording the helicopter a distinct maneuvering advantage. It was also shown that different rotor speed control laws would most likely be required for the air combat and ground attack mission scenarios.

The author feels that successful variable rotor speed control can be achieved through an appropriate marriage of FADEC engine control and high performance flight control systems. But numerous questions remain relative to the successful integration of this technology to existing and/or

future helicopter designs, (addressed in the Recommendations for Future Research section). Nevertheless, this technology shows considerable promise and it is hoped that this study will be a stepping stone to future investigations in this area.

9.0 BIBLIOGRAPHY

- Anonymous, "Helicopter Design Handbook, Helicopter Engineering: Part One, Preliminary Design", AMCP 706-201, Headquarters, U.S. Army Materiel Command, August 1974.
- Anonymous, "Helicopter ACM Guide", United States Marine Aviation Weapons and Tactics Squadron One, S-3D dated 25 August 1986.
- Bailey, F.J., Jr., "A Simplified Theoretical Method of Determining the Characteristics of a Lifting Rotor in Forward Flight", NACA Report 716, 1941.
- Belov, M., Quote taken from Soviet Military Review as reprinted in the U.S. Army Aviation Digest, October 1981.
- Bennet, J.A.J., "Rotary Wing Aircraft", Aircraft Engineering, a series published from January 1940 through August 1940.
- Blanchard, B.S., and Fabrycky, W.J., Systems Engineering and Analysis, 2nd Edition, Prentice Hall International Series in Industrial and Systems Engineering, Englewood Cliffs, New Jersey, 1990.
- Bodansky, Yossef, "Return of the Red Baron", Defense Helicopter World, Aug/Sept 1989.
- Bramwell, A.R.S., Helicopter Dynamics, Edward Arnold Publishers, London, England, 1976.
- Chen, Robert T.N., "Flight Dynamics of Rotorcraft in Steep High-g Turns", Journal of Aircraft, Vol. 21, No. 1, Jan 1984.
- Colucci, Frank, "Fighter Helicopter Conference", Defense Helicopter World, Feb/Mar 1990.
- Cunningham, Randy, Fox Two - The Story of America's First Ace in Vietnam, Warner Books, Inc., New York, 1984.

- Cuppernull, Michael J., "Helicopter Maneuverability and Agility Design Sensitivity Analysis - Volume III, Weight Methodology", Sikorsky Aircraft Division, United Technologies Corporation, U.S. Army Aviation Systems Command RPT USAAVSCOM TR-87-D-6C, Contract DAAK51-84-C-0018, Jan 1989.
- Drummond, Sharon L., "Air-to-Air Combat Test - IV (AACT-IV); Volume I - AH-64A Mission Effectiveness Analysis", McDonnell Douglas Helicopter Company, U.S. Army Aviation Systems Command RPT USAAVSCOM TR-88-D-18A, Contract DAAJ02-86-C-0035, Dec 1988.
- Finnestead, Rodger L., Pelikan, Ralph J., Wray, Donald P., and Buss, Marvin W., "Engineering Flight Test, AH-1G Helicopter (HueyCobra), Final Report", USAASTA Project No., 66-06, U.S. Army Aviation Systems Test Activity, Edwards Air Force Base, CA., Dec 1970.
- Greenberg, Charles E., "Adaptive Electronic Fuel Control Test Test Techniques", Presented at the 45th Annual Forum of the American Helicopter Society, May 1989.
- Hale, Francis J., Aircraft Performance, Selection and Design, John Wiley and Sons, New York, 1984.
- Heffley, Robert K., et al, "A Compilation and Analysis of Helicopter Handling Qualities Data, Volume One: Data Compilation", Systems Technology, Inc., NASA Contractor Report 3144, Contract NAS2-9344, 1979.
- Howlett, J.J., Morrison, T., Zagranski, R.D., "Adaptive Fuel Control for Helicopter Applications", Journal of the American Helicopter Society, Oct 1984.
- Johnson, Wayne, Helicopter Theory, Princeton University Press, Princeton, N.J., 1980.
- Lamb, J.R., and Trainer, T.N., "Structural Lessons Learned from Flight Tests of Sikorsky Helicopters in Air Combat Roles", American Helicopter Society, Rotorcraft Test Technologies Conference, March 1988.
- Lappos, Nicholas D., "Insights into Helicopter Air Combat Maneuverability", Presented at the 40th Annual Forum of the American Helicopter Society, Paper No., A-84-40-11-4000, May 1984.

- Layton, Donald M., Helicopter Performance, Matrix Publishers, Inc., Beaverton, OR, 1984.
- Lindsey, J., Mosher, M., and Raley, P., "AH-1W Air Combat Maneuvering Flight Loads Survey", Naval Air Test Center, Rotary Wing Aircraft Test Directorate Report RW-151R-88, Naval Air Systems Command Contract A511-5115/053-2/8276-000-755, Final Report, March 1989.
- Maron, Melvin J., Numerical Analysis: A Practical Approach, Macmillan Publishing Co., Inc., New York, 1982.
- McCue, J.J., Scott, Leslie E. CW4 USA, and Casler, James G. MAJ USMC, "Testing Helicopters for the Air-to-Air Combat Role", United States Naval Test Pilot School, Patuxent River, MD, Report B-84-SE-26-6000, File Copy on Reserve at the Technical Information and Reference Center, Naval Air Systems Command, Washington, D.C., 1984.
- Occhiato, John J., Kaplita, Thaddeus T., and Olsen, John R., "Helicopter Maneuverability and Agility Design Sensitivity Analysis - Volume I Design Guidelines", Sikorsky Aircraft Division, United Technologies Corporation, U.S. Army Aviation Systems Command, USAAVSCOM TR-87-D-6A, Final Report, Jan 1989.
- Parlier, Charles A. (Cap), "Go For the Throat", Defense Helicopter World, page 4-6, June/July 1989.
- Prouty, Raymond W., Helicopter Performance, Stability, and Control, PWS Publishers, Boston, MA, 1986.
- Rotor and Wing International, "Soviet Military Review Reveals Hokum", page 46, Dec 1989.
- Sanders, M.S., and McCormick, E.J., Human Factors in Engineering and Design, 6th Edition, McGraw-Hill Book Company, New York, 1987.
- Schaefer, Jr., Carl G., "The Effects of Air Combat on Helicopter Structural Integrity", Presented at the 45th Annual Forum of the American Helicopter Society, May 1989.
- Schneider, Garret L., and Watt, George W., "Minimum-Time Turns Using Vectored Thrust", Journal of Guidance and Control, Vol 12, No. 6, Nov-Dec 1989.

Shaw, Robert L., Fighter Combat - Tactics and Maneuvering, United States Naval Institute Press, Annapolis, MD, 1985.

Sweet, David H., "Flight Testing of the Chandler Evans Adaptive Fuel Control on the S-76A Helicopter", Presented at the 45th Annual Forum of the American Helicopter Society, May 1989.

Tamrat, B.F., "Fighter Aircraft Agility Assessment Concepts and Their Applications to Future Agile Fighter Design", AIAA/AHS/ASEE Aircraft Design, Systems and Operations Meeting, Sept 7-9, 1988, AIAA Paper No. AIAA-88-4400.

Thomas, J., Capt USAF, "Energy Maneuverability for the Helicopter Pilot", Marine Aviation Weapons and Tactics Squadron One (MAWTS-1), Assault Support Division, Proceedings of Conference on Air-to-Air Combat Involving Helicopters, 15-19 June 1987, Vol. 1 (UNCLASSIFIED).

Walsh, David M., "Adaptive Electronic Fuel Control Test Techniques", Presented at the 45th Annual Forum of the American Helicopter Society, May 1989.

Wolfrom, Joseph A., "Findings From Fixed-Gun Air-to-Air Combat Tests Involving Both Foreign and U.S. Helicopters", Aviation Applied Technology Directorate, U.S. Army Aviation Systems Command, USAAVSCOM TR-86-D-24 AST-1340X015-86, Dec 1986.

Wolfrom, Joseph A., and Fisher, Chris E., "Data Presentation from Air-to-Air Combat Maneuvering Between an S-76 and a UH-60A", Aviation Applied Technology Directorate, RPT USAAVSCOM TR-85-D-17, Sept 1985.

Woods, S.A., "DECEL, A Helicopter Decelerating Turn Performance Computer Program", Naval Air Development Center Technical Memorandum, ACSTD-TM-2266, Jan 1985.

Wood, T.L., "High Energy Rotor System", Presented at the 32nd Annual Forum of the American Helicopter Society, May 1976.

Wood, T.L., Ford, D.G., and Brigman, G.H., "Maneuver Criteria Evaluation Program", Bell Helicopter Textron, Research under U.S. Army Aviation Systems Command Contract DAAJ02-73-C-0015, Report No. USAAMRDL-TR-74-32, May 1974.

- Wood, T.L., and Livingston, C.L., "An Energy Method for Prediction of Helicopter Maneuverability", Bell Helicopter Technical Report 299-099-557, Air Force Studies Analysis Contract F33615-70-C-1052, Dec 1971.
- Wood, T.L., and Waak, T., "Improved Maneuver Criteria Evaluation Program", Bell Helicopter Textron; Research under U.S. Army Aviation Systems Command Contract DAAJ02-76-C-0064, Report No. USARTL-TR-79-20, Nov 1979.
- Wood, T.L., and Wells, C.D., "Maneuverability - Theory and Application", Presented at the 28th Annual Forum of the American Helicopter Society, May 1972.

10.0 APPENDICES

10.1 POWER3 Program Listing

POWER3

Specific Excess Power Program

Carl G. Schaefer, Jr.
Systems Engineering
Virginia Tech
March 1990

```
CLS
PRINT "                Specific Excess Power Program"
PRINT : PRINT
INPUT "Altitude - "; H
INPUT "Density Ratio - "; SIG
INPUT "Speed of Sound - "; VS
VS = VS * 1.6878
INPUT "Rotor RPM - "; RPM
INPUT "Normal Load Factor - "; NZ
INPUT "Equivalent Flat Plate Drag, f - "; F
INPUT "Gross Weight - "; GW
INPUT "Critical Mach Number - "; MCR
INPUT "Vertical Velocity - "; VV
INPUT "Available Power - "; AVAIL
LPRINT : LPRINT : LPRINT : LPRINT
LPRINT "Altitude = "; H; " ft"; "      RPM = "; RPM; "      Nz = "; NZ
LPRINT : LPRINT : LPRINT
LPRINT "Airspeed      Ps          Esh          HP (req)"
DEN = SIG * (.002378)
OMEGA = RPM * (.10472): ' IN RAD/SEC
R = 22!: ' IN FT.
ASLOPE = 6.283185: ' LIFT CURVE SLOPE, NACA 0012
DELO = .0077
DEL1 = 0!
DEL2 = .83
NOB = 2: ' # OF BLADES
BI = 2842: ' BLADE INERTIA
CHD = 2.25: ' BLADE CHORD
A = 3.141593 * R ^ 2: ' DISC AREA
TC = (NZ * GW) / (.5 * DEN * (OMEGA * R) ^ 2 * (NOB * CHD * R))
CT = (NZ * GW) / (DEN * A * (OMEGA * R) ^ 2)
ALF = 3.5 * TC / ASLOPE: ' MEAN ANGLE OF ATTACK
FOR VEL = 0 TO 180 STEP 5
V = VEL * 1.6878
MU = V / (OMEGA * R)
```

```

***** Power to Overcome Flat Plate Drag *****
HPF = (.5 * DEN * F * V ^ 3) / 550!

***** Rotor-Induced Power *****

K4 = .69
K3 = .37
K33 = 1.95
IF V > 35 THEN GOTO 5
HPI = (NZ * GW) ^ 1.5 / (550 * (2 * DEN * A) ^ .5)
HPI = HPI * (1! + K3 * (1 - K33 * MU / .14))
GOTO 7
5 HPI = (NZ * GW) ^ 2 / (1100 * DEN * A * V)
HPI = (HPI / K4) * (7500! / GW)

***** Blade Profile Power *****

7 SUB1 = ((DELO + DEL1 * ALF + DEL2 * ALF ^ 2) * NOB * CHD * R) / 8!
SUB2 = DEN * (1 + 4.5 * MU ^ 2)
SUB3 = ((OMEGA * R) ^ 3) / 550!
HPP = SUB1 * SUB2 * SUB3

***** Compressibility Power *****

MTEST = (OMEGA * R * (1 + MU)) / VS
IF MTEST < MCR THEN DELM = 0 ELSE GOTO 10
GOTO 20
10 DELM = MTEST - MCR + .75 * TC
20 S1 = DEN * A * SUB3
S2 = DELM ^ 3 * (.0033 - DELM * (.022 - .11 * DELM))
HPC = S1 * S2

***** Stall Power *****

TCDIV = .1 + (.2 / ((1 + 50 * MU ^ 2) ^ .5))
TCDIFF = TC - TCDIV
IF TCDIFF < 0 THEN GOTO 40 ELSE GOTO 30
30 HPS = (3410! * (TC - TCDIV)) ^ 1.5
GOTO 50
40 HPS = 0

***** Vertical Velocity Power *****

50 IF VV > 0 THEN ETA = .85
IF VV = 0 THEN ETA = 1!
IF VV < 0 THEN ETA = .8
HPV = (VV * GW) / (550 * ETA)

***** Total Power Required *****

HPREQ = HPF + HPI + HPP + HPC + HPS + HPV
PS = ((AVAIL - HPREQ) * 550!) / GW
IF PS < 0 THEN PS = .8 * PS
ES = H
ESH = ES - (V ^ 2 / (2 * 32.17)) - (BI * OMEGA ^ 2 / (2 * GW))
LPRINT VEL; " "; PS; " "; ESH; " "; HPREQ
NEXT VEL
GOTO 1
END

```

10.2 DTURN5 Program Listing

```

      DTURN5

      MAXIMUM TURN PERFORMANCE PROGRAM
      AH-1G ATTACK HELICOPTER

      Carl G. Schaefer, Jr.
      Systems Engineering
      Virginia Tech
      March 1990

This program uses the energy method to calculate point
mass performance for high-g decelerating turns

***** DEFINE CONSTANTS *****
***** AND HELICOPTER DATA *****

OPTION BASE 1
DEFINT I-J
DIM Y(5), YP(5), Q(5), A(4), B(4), C(4)

Where:
Y(1)=V, Y(2)=PSI, Y(3)=X, Y(4)=Y, Y(5)=OMEGA, YP(1)=VDOT, YP(2)=PSIDOT
YP(3)=XDOT, YP(4)=YDOT, YP(5)=OMEGADOT

CLS
READ T, TMAX, STP, NEQ, FP0, FP1, FP2, FP3, FP6
READ H, F, GW, MCR, VV, G
  FOR I = 1 TO NEQ
    READ Y(I)
  NEXT
Y(1) = Y(1) * 1.6878
Y(5) = .10472 * Y(5)
  FOR I = 1 TO NEQ
    Q(I) = FP0
  NEXT
DATA 0., 20., 0.1, 5, 0, 1., 2., 3., 6.
DATA 2400., 19.33, 8250., 0.793, 32.17
DATA 150., 0., 0., 0., 324.

***** HEADER INFORMATION *****

LPRINT "          Maximum Turn Performance"
LPRINT "          AH-1G Attack Helicopter"
LPRINT : LPRINT
LPRINT "          RAMP-CONSTANT-DOUBLE RAMP, 110%"
LPRINT "          POWER 4"
LPRINT "          MIDRANGE BREAKPOINT 1 = 125 KNOTS"
LPRINT "          MIDRANGE BREAKPOINT 2 = 105 KNOTS"
LPRINT "          MIDRANGE BREAKPOINT 3 = 80 KNOTS"
LPRINT : LPRINT : LPRINT
LPRINT "  VEL          PSI          X          Y          RPM"
LPRINT "-----"
LPRINT "  VDOT        PSIDOT        XDOT        YDOT        RPMDOT"
LPRINT : LPRINT : LPRINT
```

```

' ***** AH-1G Constants & Characteristics *****
'
R = 22!: ' IN FT.
ASLOPE = 6.283185: ' LIFT CURVE SLOPE, NACA 0012
DEL0 = .00778
DEL1 = 0!
DEL2 = .83
NOB = 2: ' # OF BLADES
BI = 2842!: ' BLADE INERTIA
CHD = 2.25: ' BLADE CHORD
A = 3.141593 * R ^ 2: ' DISC AREA
'
' ***** Initialization of Integration Constants *****
' ***** Fourth-Order Runge-Kutta (Gill) *****
'
A(1) = FP1 / FP2
SQ2 = SQR(FP2)
A(2) = (FP2 - SQ2) / FP2
C(2) = A(2)
A(3) = (FP2 + SQ2) / FP2
C(1) = A(1)
C(4) = A(1)
C(3) = A(3)
A(4) = FP1 / FP6
B(1) = FP2
B(4) = FP2
B(2) = FP1
B(3) = FP1
IFLAG = 1
'
' ***** Density Calculation *****
' ***** (as a function of altitude) *****
' ***** straight line fit gives accuracy up to 0.5% *****
10 SIG = -2.46854E-05 * H + .98921
DEN = SIG * (.002378)
VS = -2.33142E-03 * H + 661.609: 'speed of sound calculation
VS = VS * 1.6878
'
15 TCSUB = (.5 * DEN * (Y(5) * R) ^ 2 * (NOB * CHD * R))
CTSUB = (DEN * A * (Y(5) * R) ^ 2)
'
' ***** HORSEPOWER AVAILABLE *****
' ***** AH-1G DATA *****
'
IF H <= 3300! THEN GOTO 20
AVAIL = -.03535 * H + 1198.32: ' at 20 deg C.
GOTO 100
20 AVAIL = 1135!

```

```

***** START MAIN PROGRAM *****
100 MU = Y(1) / (Y(5) * R)
      ***** CALCULATION OF MAX THRUST *****
      ***** AH-1G DATA *****
      ***** MAX THRUST - COLLECTIVE ONLY *****
IF MU <= .1 GOTO 105
TCMAX = -.531 * MU + .40588
      ***** MAX THRUST - CYCLIC ONLY *****
      ***** ACCOUNTS FOR PITCH RATE ALLEVIATION ON STALL *****
IF MU <= .26 GOTO 105
TCMAX = -.508 * MU + .4844
GOTO 106
105 TCMAX = .353
106 NZMAX = TCMAX * TCSUB / GW
NZ = NZMAX
TC = TCMAX
ALF = 3.5 * TC / ASLOPE: ' MEAN ANGLE OF ATTACK
      ***** Start of RK4 Call Routine *****
JRK = 0
120 JRK = JRK + 1
J = JRK
GOSUB 400
GOSUB 10000
FOR I = 1 TO NEQ
TEMP = A(J) * (YP(I) - B(J) * Q(I))
Y(I) = Y(I) + STP * TEMP
Q(I) = Q(I) + FP3 * TEMP - C(J) * YP(I)
NEXT
IF (JRK = 2) THEN GOTO 120
IF (JRK = 4) THEN GOTO 150
T = T + STP / FP2
GOTO 120
150 LPRINT "
LPRINT "T = "; : LPRINT USING "###.#"; T;
LPRINT " Ps = "; : LPRINT USING "####.#"; PS;
LPRINT " Nz = "; : LPRINT USING "###.###"; NZ
FOR K = 1 TO NEQ
LPRINT USING "###.#####^_____ "; Y(K); :
NEXT
LPRINT CHR$(13);
FOR K = 1 TO NEQ
LPRINT USING "###.#####^_____ "; YP(K); :
NEXT
IF (T > TMAX) OR (Y(1) <= 20!) OR (Y(2) > 3.14) GOTO 11000 ELSE GOTO 15

```

```

,
,
,
***** Power to Overcome Flat Plate Drag *****
400 HPF = (DEN * F * Y(1) ^ 3) / 1100!
,
***** Rotor-Induced Power *****
,
K4 = .69
UT = (NZ * GW) / (2! * DEN * A)
VM = Y(1) ^ 2 / 2!
V1 = SQR(-VM + SQR(VM ^ 2 + UT ^ 2))
DIND = (NZ * GW * V1) / Y(1)
HPI = (DIND * Y(1)) / 550!
HPI = (HPI / K4) * (7500! / GW)
,
***** Blade Profile Power *****
700 SUB1 = ((DELO + DEL1 * ALF + DEL2 * ALF ^ 2) * NOB * CHD * R) / 8!
SUB2 = DEN * (1 + 4.6 * MU ^ 2)
SUB3 = ((Y(5) * R) ^ 3) / 550!
HPP = SUB1 * SUB2 * SUB3
,
***** Compressibility Power *****
,
MTEST = (Y(5) * R * (1 + MU)) / VS
IF MTEST < MCR THEN DELM = 0 ELSE GOTO 1000
GOTO 2000
1000 DELM = MTEST - MCR + .75 * TC
2000 S1 = DEN * A * SUB3
S2 = DELM ^ 3 * (.0033 - DELM * (.022 - .11 * DELM))
HPC = S1 * S2
,
***** Stall Power *****
,
TCCRT = .1 + (.2 / (SQR(1! + 50! * MU ^ 2)))
IF (MU > .26) THEN TCCRT = -.2 + (.8279 / (SQR(1! + 50! * MU ^ 2)))
HPS = 0!
TCDIFF = TC - TCCRT
IF TCDIFF < 0 THEN GOTO 5000
HPS = (3410! * (TCDIFF)) ^ 1.5
,
***** Vertical Velocity Power *****
5000 IF VV > 0 THEN ETA = .85
IF VV = 0 THEN ETA = 1!
IF VV < 0 THEN ETA = .8
HPV = (VV * GW) / (550 * ETA)
,
***** Total Power Required *****
,
HPREQ = HPF + HPI + HPP + HPC + HPS + HPV
AVAIL = .75 * AVAIL
PS = ((AVAIL - HPREQ) * 550!) / GW
ES = H
ESH = ES - (Y(1) ^ 2 / (2 * 32.17)) - (BI * Y(5) ^ 2 / (2 * GW))
RETURN

```

```

'      **** State, Control, Kinematic, and Trajectory Eqns      ****
'
10000  ETA = 1!
'
'      **** Rotor Speed Control Algorithm      ***
'
      IF (Y(1) < 254) AND (Y(1) >= 210.975) GOTO 10100
      IF (Y(1) < 210.975) AND (Y(1) >= 177.219) GOTO 10200
      IF (Y(1) < 177.219) AND (Y(1) >= 135.024) GOTO 10300
      IF (Y(1) < 135.024) AND (Y(1) >= 101.268) GOTO 10350
      IF (Y(1) < 101.268) GOTO 10400
10100  YP(5) = -.08041 * YP(1)
      GOTO 10700
10200  YP(5) = 0!
      GOTO 10700
10300  YP(5) = .16082 * YP(1)
      GOTO 10700
10350  YP(5) = -.10051 * YP(1)
      GOTO 10700
10400  YP(5) = 0!
'
'
10700  YP(1) = ETA * ((G / Y(1)) * (PS - (BI * Y(5) * YP(5) / GW)))
      RADIUS = (Y(1) ^ 2) / (G * SQR(NZ ^ 2 - 1))
      YP(2) = Y(1) / RADIUS
      YP(3) = Y(1) * COS(Y(2))
      YP(4) = Y(1) * SIN(Y(2))
      RETURN
11000  END

```

10.3 DT5 Program Listing

```
INTEGER IBTYPE, IPRINT, M, MAXITN, ME, N
PARAMETER (IBTYPE=0, IPRINT=0, M=3, MAXITN=100, ME=0, N=4)
REAL FVALUE, X(N), XGUESS(N), XLB(N), XSCALE(N), XUB(N)
EXTERNAL FCN, DNCONF
DATA XGUESS/0.404, 1.27, 1.65, 2.56/
DATA XSCALE/1.0EO, 1.0EO, 1.0EO, 1.0EO/
DATA XLB/ 0.0EOEO, 0.8EOEO, 1.0EOEO, 2.0EO/
DATA XUB/1.0EO, 1.8EO, 2.5EO, 3.0EO/
CALL DNCONF(FCN, M, ME, N, XGUESS, IBTYPE, XLB, XUB, XSCALE, IPRINT,
*MAXITN, X, FVALUE)
WRITE(6, 10) X(1), X(2), X(3), X(4)
10 FORMAT(1X, 'X(1)= ', E12.4, 'X(2)= ', E12.4, 'X(3)= ', E12.4,
* 'X(4)= ', E12.4)
WRITE(6, 20) FVALUE
20 FORMAT(1X, 'FVALUE = ', E12.4)
END

C
SUBROUTINE FCN(M, ME, N, X, ACTIVE, F, G)
INTEGER M, ME, N
REAL X(4), F, G(3), CT, VF, TF
LOGICAL ACTIVE(3)
CALL DTURN(X, VF, TF, CT)
WRITE(6, *) 'X, VF = ', X, VF
WRITE(6, *) 'TF, CT = ', TF, CT

C
F=10*VF+100*TF+CT

C
IF (ACTIVE(1)) G(1)=1000-CT
IF (ACTIVE(2)) G(2)=VF-84.39
IF (ACTIVE(3)) G(3)=10-TF
RETURN
END

C
C
SUBROUTINE DTURN(X, VF, TF, CT)
REAL MCR, NZ, NZMAX, K4, MTEST, X(4)
DIMENSION Y(4), YP(4), Q(4), A(4), B(4), C(4)
PSI5=0.
PSI5=3.14159
SL01=6.78586/X(1)
SL23=-10.17878/(X(3)-X(2))
SL45=3.39293/(PSI5-X(4))
INTER23=40.71514-SL23*X(2)
INTER45=30.53635-SL45*X(4)
T=0.
TMAX=20.
STP=.1
Y(1)=150.
Y(1)=Y(1)*1.6878
Y(2)=0.
Y(3)=0.
Y(4)=0.
NEQ=4
FPO=0.
FP1=1.
FP2=2.
FP3=3.
FP6=6.
H=2400.
F=19.33
GW=8250.
```

```

5 CONTINUE
  R=22.
  ASLOPE=6.283185
  DELO=0.00778
  DEL1=0.
  DEL2=0.83
  NOB=2
  BI=2842.
  CHD=2.25
  AR=3.141593*R**2
  A(1)=FP1/FP2
  SQ2=SQRT(FP2)
  A(2)=(FP2-SQ2)/FP2
  C(2)=A(2)
  A(3)=(FP2+SQ2)/FP2
  C(1)=A(1)
  C(4)=A(1)
  C(3)=A(3)
  A(4)=FP1/FP6
  B(1)=FP2
  B(4)=FP2
  B(2)=FP1
  B(3)=FP1
50 SIG=-2.46854E-05*H+.98921
  DEN=SIG*0.002378
  VS=-2.33142E-03*H+661.609
  VS=VS+1.6878
60 IF (Y(2).LE.X(1)) GOTO 61
  IF ((Y(2).GT.X(1)).AND.(Y(2).LE.X(2))) GOTO 62
  IF ((Y(2).GT.X(2)).AND.(Y(2).LE.X(3))) GOTO 63
  IF ((Y(2).GT.X(3)).AND.(Y(2).LE.X(4))) GOTO 64
  IF ((Y(2).GT.X(4)).AND.(Y(2).LE.PSIS)) GOTO 65
  IF (Y(2).GT.PSIS) GOTO 66
61 OM=SL01*Y(2)+33.92928
  OMDOT=SL01*YP(2)
  GOTO 69
62 OM=40.71514
  OMDOT=0.0
  GOTO 69
63 OM=SL23*Y(2)+INTER23
  OMDOT=SL23*YP(2)
  GOTO 69
64 OM=30.53635
  OMDOT=0.0
  GOTO 69
65 OM=SL45*Y(2)+INTER45
  OMDOT=SL45*YP(2)
  GOTO 69
66 OM=33.92928
  OMDOT=0.0
  GOTO 69
C   WRITE(6,*)' X =',X
C   WRITE(6,*)' OM, OMDOT=',OM, OMDOT
69 TCSUB=(.5*DEN*(OM*R)**2*(NOB*CHD*R))
  CTSUB=(DEN*AR*(OM*R)**2)
  IF (H.LE.3300.) GOTO 70
  AVAIL=-.03535*H+1198.32
  GOTO 100
70 AVAIL=1135.
100 XMU=Y(1)/(OM*R)
  IF (XMU.LE.0.1) GOTO 105

```

```

105 TCMAX=.353
106 NZMAX=TCMAX*TCSUB/GW
    NZ=NZMAX
    TC=TCMAX
    ALF=3.5*TC/ASLOPE
    JRK=0
120 JRK=JRK+1
    J=JRK
    CALL POWER(DEN, F, Y, NZ, GW, AR, DELO, DEL1, ALF, DEL2, NOB,
+CHD, R, XMU, OM, VS, MCR, TC, VV, H, BI, G, PS)
    CALL RHS(Y, OM, G, PS, BI, OMDOT, GW, NZ, YP)
    DO 130 I=1, NEQ
    TEMP=A(J)*(YP(I)-B(J)*Q(I))
    Y(I)=Y(I)+STP*TEMP
    Q(I)=Q(I)+FP3*TEMP-C(J)*YP(I)
130 CONTINUE
    IF (JRK.EQ.2) GOTO 120
    IF (JRK.EQ.4) GOTO 150
    T=T+STP/FP2
    GOTO 120
150 IF ((Y(1).LE.25.).OR.(Y(2).GE.3.14)) THEN
    GOTO 200
    ELSE
    GOTO 60
    ENDIF
200 VF=Y(1)
    TF=T
    CT=Y(4)
210 RETURN
    END
C
C
    SUBROUTINE POWER(DEN, F, Y, NZ, GW, AR, DELO, DEL1, ALF, DEL2, NOB,
+CHD, R, XMU, OM, VS, MCR, TC, VV, H, BI, G, PS)
    REAL K4, MTEST, MCR, NZ
    DIMENSION Y(4)
C
C    POWER TO OVERCOME FLAT PLATE DRAG
C
    HPF=(DEN*F*Y(1)**3)/1100.
C
C    ROTOR-INDUCED POWER
C
    K4=.69
    UT=(NZ*GW)/(2.*DEN*AR)
    VM=Y(1)**2/2.
    V1=SQRT(-VM+SQRT(VM**2+UT**2))
    DIND=(NZ*GW*V1)/Y(1)
    HPI=(DIND*Y(1))/550.
    HPI=(HPI/K4)*(7500./GW)
C
C    BLADE PROFILE POWER
C
    SUB1=((DELO-DEL1*ALF+DEL2*ALF**2)*NOB*CHD*R)/8.
    SUB2=DEN*(1+4.6*XMU**2)
    SUB3=((OM*R)**3)/550.
    HPP=SUB1*SUB2*SUB3
C
C    COMPRESSIBILITY POWER
C
    MTEST=(OM*R*(1+XMU))/VS
    IF (MTEST.LT.MCR) THEN
    DELM=0.
    ELSE

```

```

        GOTO 1000
      ENDIF
      GOTO 2000
1000  DELM=HTEST-MCR+.75*TC
2000  S1=DEN*AR*SUB3
      S2=(DELM**3)*(0.0033-DELM*(0.022-0.11*DELM))
      HPC=S1*S2
C
C      STALL POWER
C
      HPS=0.
C
C      VERTICAL VELOCITY POWER
C
      HPV=0.
C
C      TOTAL POWER REQUIRED
C
      HPREQ=HPF+HPI+HPP+HPC+HPS+HPV
      AVAIL=851.
      PS=((AVAIL-HPREQ)*550.)/GW
      ES=H
      ESH=ES-(Y(1)**2/(2*G))-(BI*OM**2/(2*GW))
      RETURN
      END
C
C
      SUBROUTINE RHS(Y, OM, G, PS, BI, OMDOT, GW, NZ, YP)
      REAL NZ
      DIMENSION Y(4), YP(4)
      ETA=1.
      YP(1)=ETA*((G/Y(1))*(PS-(BI*OM*OMDOT/GW)))
      RADIUS=(Y(1)**2)/(G*SQRT(NZ**2-1.))
      YP(2)=Y(1)/RADIUS
      YP(3)=Y(1)*COS(Y(2))
      YP(4)=Y(1)*SIN(Y(2))
      RETURN
      END

```